UNIVERSIDADE DE SÃO PAULO

INSTITUTO DE QUÍMICA

Programa de Pós-Graduação em Química

GUSTAVO THALMER DE MEDEIROS SILVA

Hybrid pigments from fibrous clays and chromophores inspired by the color of fruits, flowers and wine

Versão original da Tese defendida

São Paulo

Data do Depósito na SPG:

14/05/2019

GUSTAVO THALMER DE MEDEIROS SILVA

Pigmentos híbridos a partir de argilas fibrosas e cromóforos inspirados nas cores de frutas, flores e vinhos

Tese apresentada ao Instituto de Química da Universidade de São Paulo para obtenção do Título de Doutor em Ciências (Química)

Orientador: Prof. Dr. Frank Herbert Quina

São Paulo

2019

Ficha Catalográfica elaborada eletronicamente pelo autor, utilizando o programa desenvolvido pela Seção Técnica de Informática do ICMC/USP e adaptado para a Divisão de Biblioteca e Documentação do Conjunto das Químicas da USP

Bibliotecária responsável pela orientação de catalogação da publicação:
Marlene Aparecida Vieira - CRB - 8/5562

S586h

Silva, Gustavo Thalmer de Medeiros
Hybrid pigments from fibrous clays and chromophores inspired by the color of fruits, flowers and wine / Gustavo Thalmer de Medeiros Silva. - São Paulo, 2019.
118 p.

Tese (doutorado) - Instituto de Química da Universidade de São Paulo. Departamento de Química Fundamental.
Orientador: Quina, Frank Herbert

1. Photophysics. 2. Fluorescence. 3. Anthocyanins. 4. Clays. 5. Hybrid materials. I. T. II. Quina, Frank Herbert, orientador.

À minha família

Página mantida intencionalmente em branco

AGRADECIMENTOS

Agradeço especialmente ao professor **Frank** pela amizade, orientações, conselhos e confiança.

Agradeço à **minha família** pelo apoio, colaboração e incentivo. À minha esposa **Mayara**, pela paciência e por sempre me aconselhar visando o meu bem acadêmico.

Ao **Cassio** por termos formado uma parceria de sucesso no laboratório, resultando em diversas publicações, e à **Karen** por ter me ajudado muito nos experimentos no último ano de doutorado.

Ao professor **Marcelo Gehlen**, professora **Cornelia Bohne, Jessy Oake** e **Ana Clara** pelas colaborações e contribuições no desenvolvimento deste trabalho.

Aos **técnicos e professores do Instituto de Química (IQ)** pela ajuda prestada, em especial os amigos e técnicos **Joaquim** e **Jair**, os quais me ajudaram e contribuíram bastante.

Ao **Josué** e **Thiago** pela contribuição nas análises de BET e DRX. Ao **Jan**, **Larissa** e **Rafaela** por terem me ajudado em alguns experimentos, que embora não estejam presentes neste trabalho, foram de grande importância para minha formação. Ao **Paulo Firmino** e **Rafael Macedo** pela grande ajuda nos primeiros experimentos, que serviu bastante como aprendizado.

Aos **colegas e amigos do laboratório e da república estudantil** pela convivência harmoniosa e amizade.

À **CAPES** pelo financiamento concedido.

Enfim, agradeço a todos que contribuíram de forma direta ou indireta para o desenvolvimento deste trabalho.

Página mantida intencionalmente em branco

RESUMO

Silva, G.T.M. Pigmentos híbridos a partir de argilas fibrosas e cromóforos inspirados nas cores de frutas, flores e vinhos. 2019. 118p. Tese (doutorado) – Programa de Pós-Graduação em Química. Instituto de Química, Universidade de São Paulo, São Paulo – Brasil.

Características como cor, brilho, fluorescência e estabilidade são extremamente importantes em aplicações de pigmentos. As antocianinas, os pigmentos naturais responsáveis pela maioria das cores púrpura, azul e vermelha das flores e frutas, têm grande potencial para aplicações práticas como corantes ou antioxidantes. No entanto, estas aplicações são limitadas pela sua reatividade química, que é afetada por diversos fatores, incluindo o pH, temperatura, luz e oxigênio, entre outros. Os materiais híbridos inspirados no antigo pigmento Maya Blue são uma alternativa promissora para melhorar as propriedades e a aplicabilidade dos corantes naturais e sintéticos. Os cátions flavílios servem como modelos para a reatividade química e fotoquímica das antocianinas. Da mesma forma, os cátions piranoflavílios servem como modelos do cromóforo fundamental das piranoantocianinas, moléculas que podem se formar a partir de reações das antocianinas das uvas em vinhos tintos durante sua maturação. Argilas fibrosas, constituintes responsáveis pela excelente estabilidade do pigmento Azul Maia, possuem canais que podem potencialmente permitir a inserção parcial ou total dessas moléculas corantes. Portanto, na presente tese, pigmentos híbridos foram preparados pela adsorção de uma série de cátions flavílio e piranoflavílio sintéticos nas argilas fibrosas paligorsquita e sepiolita e suas propriedades fotofísicas e estabilidade foram avaliadas. A observação de decaimentos biexponenciais de fluorescência é condizente com a emissão

de moléculas do corante adsorvidas em dois sítios distintos nas argilas fibrosas. As propriedades de fluorescência das moléculas de corante podem ser melhoradas, dependendo da quantidade de corante adsorvida na argila, aos híbridos do tipo corante/argila. A cor das moléculas de corante adsorvidas foi um pouco mais resistente a alterações no pH externo, a estabilidade fotoquímica foi mantida e a labilidade térmica foi marcadamente melhorada. Além do desenvolvimento de novos híbridos de cátions flavílios/argilas fibrosas, obtivemos avanços na estabilização dessas moléculas corantes, principalmente no que diz respeito aos equilíbrios dependentes do pH e ao tratamento térmico. Ao mesmo tempo, o presente trabalho representa o primeiro estudo sistemático de materiais híbridos preparados a partir de cátions piranoflavílios. Portanto, os resultados aqui obtidos apontam definitivamente para cátions flavílios e cátions piranoflavílios como cromóforos promissores e argilas fibrosas como substratos promissores para o desenvolvimento de novos pigmentos híbridos altamente fluorescentes com cores atrativas e estabilidade química e térmica marcante.

Palavras-chave: cátions flavílios, cátions piranoflavílios, corantes, argilas, paligorsquita, sepiolita, pigmentos híbridos.

ABSTRACT

Silva, G.T.M. Hybrid pigments from fibrous clays and chromophores inspired by the color of fruits, flowers and wine. 2019. 118p. PhD Thesis – Graduate Program in Chemistry. Institute of Chemistry, Universidade de São Paulo, São Paulo – Brazil.

Features such as color, brightness, fluorescence and stability are extremely important in applications of pigments. Anthocyanins, the natural pigment responsible for most of the purple, blue and red colors of flowers and fruits, have great potential for practical applications as dyes or antioxidants. However, these applications are limited by their chemical reactivity, which is affected by several factors, including pH, temperature, light, and oxygen, among others. Hybrid materials inspired by the ancient Maya Blue pigment are a promising alternative to improve the properties and applicability of natural and synthetic dyes. Flavylium cations serve as models for the chemical and photochemical reactivity of anthocyanins. Likewise, pyranoflavylium cations serve as models of the fundamental chromophoric moiety of pyranoanthocyanins, molecules that can form from reactions of the grape anthocyanins in red wines during their maturation. Fibrous clays, constituents responsible by the excellent stability of Maya blue pigment, have channels that can potentially allow partial or full insertion of these dyes molecules. Therefore, in the present thesis, hybrid pigments were prepared by the adsorption of a series of synthetic flavylium cations and synthetic pyranoflavylium cations on the fibrous clays palygorskite and sepiolite and their photophysical properties and stability were evaluated. The observation of biexponential fluorescence decays is consistent with emission from dye molecules adsorbed at two distinct sites on the fibrous clays. The fluorescence properties of dye molecules can be improved, depending on the amount of dyes adsorbed on the clay, by the formation of dye/clay hybrids. The color of the adsorbed dye molecules was

somewhat more resistant to changes in external pH, photochemical stability was maintained and the thermal lability was markedly improved. Besides the development of novel hybrid flavylium cation/fibrous clay, we have achieved advances in the stabilization of these dye molecules, with regard mainly to the pH-dependent equilibrium and thermal treatment. In addition, the present work represents the first systematic study of hybrid materials prepared from pyranoflavylium cations. Therefore, the results obtained here definitively point to flavylium cations and pyranoflavylium cations as promising chromophores and fibrous clays as promising substrates for the development of novel, highly fluorescent hybrid pigments with attractive colors and marked chemical and thermal stability.

Keywords: flavylium cations, pyranoflavylium cations, dyes, clays, palygorskite, sepiolite, hybrid pigments.

CONTENTS

CHAPTER 1

Theoretical framework

In this chapter, the main theoretical aspects necessary for the development of this thesis are presented. Based on several works available in the literature, the theoretical basis that resulted in the main idea for the development of the studies presented in the next chapters is outlined, together with the importance and significance of these studies.

1.1 Anthocyanins

Anthocyanins (from the Greek words for flower, *anthos*, and blue, *kyanos*) are naturally occurring plant pigments responsible for most of the blue, red and purple colors of the plant kingdom (examples in Figure 1.1) (Quina et al., 2009). Among the natural pigments of fruits and flowers and water-soluble natural pigments, the anthocyanins are particularly noteworthy from the standpoint of their widespread occurrence and the range of colors that they are capable of producing in nature as the result of changes in their chemistry, conferring attractive shades and bright colors to many flowers, fruits, vegetables and plant leaves (Quina and Bastos, 2018).

Figure 1.1 – Examples of pigmentation of anthocyanins in nature.

The basic chromophore of anthocyanins is the 7-hydroxyflavylium cation (Figure 1.2). However, naturally occurring anthocyanins usually have additional hydroxyl groups

at positions 5 (sometimes glycosylated, Gly) and 3 (always glycosylated, apparently necessary for thermal stability), and the 2-phenyl- or B-ring has one or more hydroxy or methoxy substituents, as shown in Figure 1.3 for the six basic anthocyanidin (or deglycosylated anthocyanin) structures. Therefore, the structural diferences between a given anthocyanidin and the corresponding anthocyanin are due to the nature and extent of glycosylation and to the presence or absence of additional acyl groups attached to the sugars (Quina et al., 2009; Silva et al., 2016).

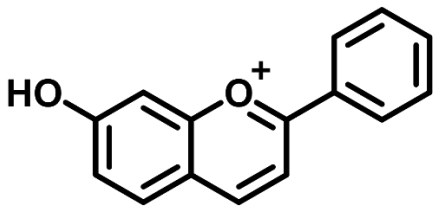

Figure 1.2 – The basic chromophore of anthocyanins, the 7-hydroxyflavylium cation.

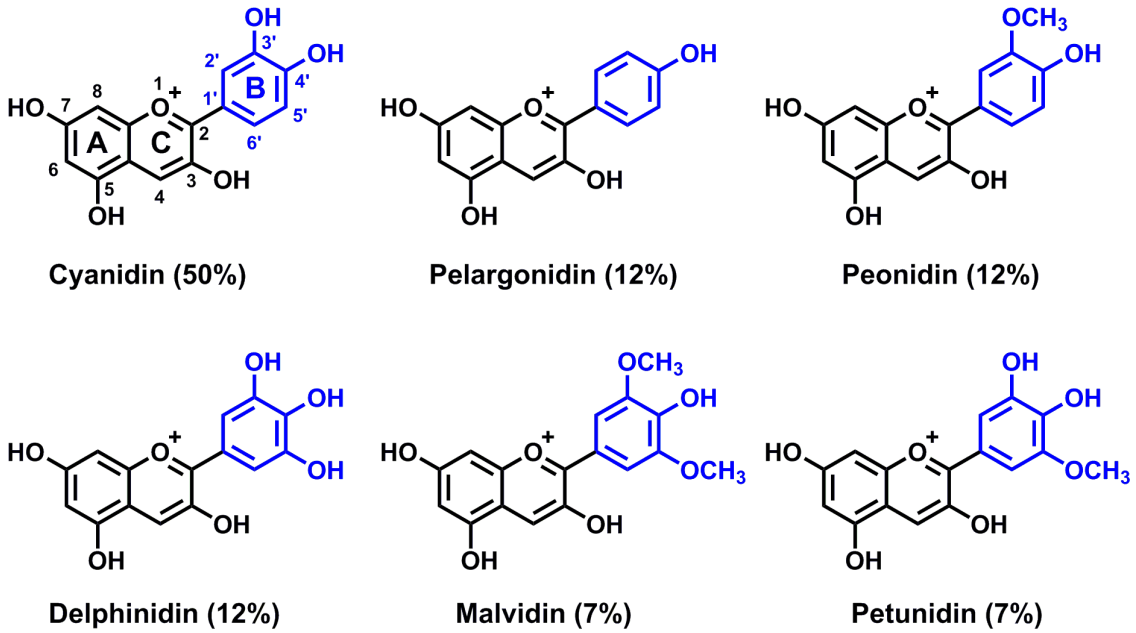

Figure 1.3 – The six most common basic anthocyanin chromophoric structures, represented as anthocyanindins, with the approximate relative percentages found in nature indicated in parentheses.

Anthocyanins are of great interest to the food, pharmaceutical, and cosmetic industries. Due to their antioxidant and color properties, they possess several health benefits (acting in the prevention and reduction of chronic diseases, such as diabetes, cancer, cardiovascular and metabolic diseases) and great potential for practical applications as dyes, for example as alternatives to substitute toxic synthetic food dyes as food additives in jams, confectionaries and beverages (Castañeda-Ovando et al., 2009; Khoo et al., 2017). In addition, they are non-toxic and have affinity for aqueous media, which makes them interesting for use as natural water-soluble liquid colorants, for example for shampoos, hair conditioner, liquid soaps and lotions, among others. However, these applications are limited by their chemical reactivity, which is affected by several factors including pH, temperature, light, oxygen, among others (Castañeda-Ovando et al., 2009; Cavalcanti et al., 2011; Ferreira Da Silva et al., 2005; Quina et al., 2009; Silva et al., 2016).

Taking as an example the predominant pH conditions in plants, food and in the digestive system (pH range 1-8) (Fernandes et al., 2015), anthocyanins undergo transformations in their structure and consequently changes or loss of color due to acid-base reactions, hydration and isomerization. Figure 1.4 shows the pH-dependent multiequilibria of anthocyanins in aqueous solution. Below pH 3, the dominant form of anthocyanins is the red or red-purple flavylium cation form (AH^+), which undergoes attack of water at the 2-position above about pH 3 to form the colorless or pale yellow hemiacetal (B), followed by ring-opening tautomerization to form the (E)-chalcone (EC) and then slow isomerization to the (Z)-chalcone (ZC), which are also colorless or pale yellow. At short times and slightly higher pH, the hydroxyl group of AH^+ undergoes deprotonation, resulting in the conjugate base (A), which exhibits a different color (usually a bluish color) in relation to AH^+ (Quina and Bastos, 2018; Silva et al., 2016).

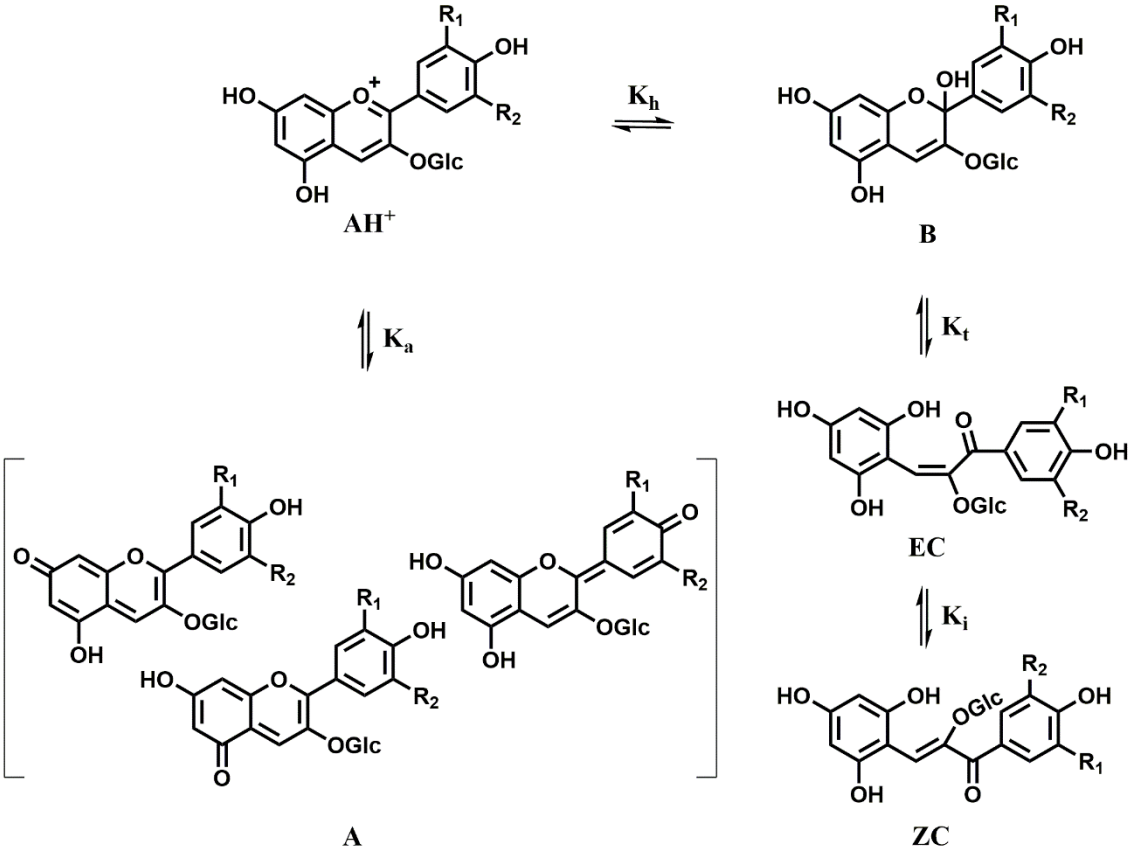

Figure 1.4 - pH-dependent multiequilibria of anthocyanins in aqueous solution, including deprotonation (K_a) to form the conjugate bases (A), hydration (K_h) to form the hemiketal (B) and subsequent ring-opening tautomerization (K_t) to form the (E)-chalcone (EC) and isomerization (K_i) to the (Z)-chalcone (ZC).

In order to prevent the hydration-dependent loss of color of anthocyanins, as well as improve photo and thermal stabilities, researchers have tried to isolate or encapsulate the anthocyanins in an environment that prevents external contacts. Indeed, the inclusion of synthetic analogues of anthocyanins (flavylium cations) in inorganic matrices such as mesoporous materials (Kohno et al., 2011), zeolites (Kohno et al., 2008) and clays (Kohno et al., 2010, 2009, 2007), as well as in supramolecular and colloidal systems, such as cucurbiturils (Held et al., 2016) and anionic micelles (Lima et al., 2002), represent promising alternatives for preventing the undesirable chemistry of these dye molecules.

1.1.1 Flavylium cations

Isolating anthocyanins from nature is not an easy task, since they are present as mixtures of different basic structures with different degrees of glycosylation. In addition, when purified or in solution, they decompose easily. Such factors represent a barrier to systematic studies of the chemistry of natural anthocyanins (Quina and Bastos, 2018). Fortunately, the chemical and photochemical features of synthetic flavylium cations mimic many of those of natural anthocyanins (Pina et al., 2012).

Flavylium cations are synthetic analogues that contain the chromophore of anthocyanins and have the advantage of the facility and versatility of modifying and varying systematically the positions and nature of the substituents on the flavylium chromophore in order to develop structure-property and structure-reactivity correlations. Consequently, the reactivity can be manipulated, as for example in the 3',4',7-trimethoxy-flavylium cation (FL1), in which only hydration occurs, the 7-hydroxy-4-methyl-flavylium cation (FL4), in which the acid-base equilibrium is preserved but hydration is blocked, and the 7-methoxy-4-methyl-flavylium cation, in which none of the multiequilibria occur (see structures in the next chapter, Scheme 2.1).

1.2 Pyranoanthocyanins

Pyranoanthocyanins are one of the most important classes of anthocyanin derivatives. They are formed during the storage and aging of red wines (Casassa and Harbertson, 2014; Heras-Roger et al., 2016; Tang et al., 2017), from chemical reactions of grape anthocyanins with yeast metabolites, colorless copigments or other additives

present in the wine (Brouillard et al., 2003; Figueiredo-González et al., 2014; Fulcrand et al., 2006; Marquez et al., 2013; Oliveira et al., 2014; Schwarz et al., 2003). Figure 1.5 shows a representation of pyranoanthocyanins formation from anthocyanins.

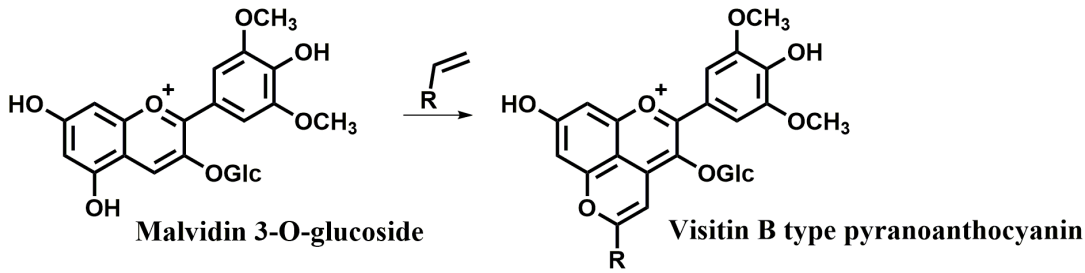

Figure 1.5 – Formation of pyranoanthocyanins during the maturation of red wine from anthocyanins reactions (example mavidin 3-O-glucoside).

Among the products formed during the maturation process of red wine, pyranoanthocyanins contribute to the coloration of the wine, because they have greater color intensity and stability at wine pH (de Freitas and Mateus, 2011). In addition, they have the potential for contributing to the taste (e.g., astringency) (García-Estévez et al., 2017), antioxidant capacity (Azevedo et al., 2014; Tománková et al., 2016) and the health benefits (Oliveira et al., 2016) of moderate consumption of red wines.

The origin of the higher colour intensity and chemical stability of pyranoanthocyanins compared with their anthocyanin precursors is associated with the structural features of the pyranoanthocyanins, which consist of an additional pyran ring formed between the OH group at position C-5 and C-4 (de Freitas and Mateus, 2011; Freitas et al., 2018). This prevents the hydration reaction that would lead to the loss of color. However, pyranoanthocyanins can still to undergo deprotonation leading to the formation of the neutral quinoidal base or anionic base (depending on the substituents). As reported recently by us, synthetic pyranoflavylium cations are weak acids in the

ground state, with pK_a values between 3.5 - 4.5, similar to flavylium cations and anthocyanins, which have pK_a values around 4 – 5 (Freitas et al., 2018).

1.2.1 Pyranoflavylium cations

Just as flavylium cations are analogs of anthocyanins, pyranoflavylium cations are analogs of pyranoanthocyanins, i.e., pyranoflavylium cations are synthetic analogues containing the basic chromophore of pyranoanthocyanins. Pyranoflavylium cations have the advantage of relatively facile and versatile modification of the substituents and, consequently, the reactivity and properties of the chromophore. Therefore, studies of synthetic pyranoflavylium cations should contribute to a better understanding of the properties and reactivity of the much more complex, but analogous pyranoanthocyanins. Indeed, recently we have reported ground and excited state properties of pyranoflavylium cations, with regard to acidity, triplet excited states, and singlet oxygen formation (Freitas et al., 2018; Siddique et al., 2019; Silva et al., 2019).

1.3 Clays

The joint nomenclature committes (JNCs) of the Association Internationale pour l'Etude des Argiles (AIPEA) and the Clay Minerals Society (CMS) defined clay as: "a naturally occurring material composed primarily of fine-grained minerals, which is generally plastic at appropriate water contents and will harden with (sic) dried or fired", and clay minerals as: "phyllosilicate minerals and minerals which impart plasticity to clay and which harden upon drying or firing''. Unlike clay, which by definition cannot be

synthetic, the origin of clay minerals is not part of the definition; therefore, clay minerals can also be synthetic materials (Bergaya and Lagaly, 2006).

Studies of clays and clay minerals have a multidisciplinary nature, so that it is common to find scientists from diverse backgrounds with diverse interests in this field, for example chemists, geologists, materials engineers, physicists and biologists. Although we have worked in this thesis with clay minerals, we have used the term clay in order to simplify and facilitate for the reader. It is important to emphasize that, although there are distinctions between clay and clay minerals, there is no uniform nomenclature and, in the literature, the treatment of both as clay is accepted.

Clays have high availability (mainly due to natural occurrence), are inexpensive, and environmentally friendly. In addition, they have desirable properties, such as ion-exchange capacity, adsorbent capacity and chemical, thermal and mechanical stabilities, which make them a good inorganic substrate to host or adsorb ions or molecules, important for the production of hybrid materials.

Clays can be classified as lamellar or fibrous clays (Oliveira et al., 2013), besides other types of classifications such as 2:1 or 1:1 tetrahedral and octahedral layers associated with the structure (Brigatti et al., 2006). Several studies of the association of flavylium cations and anthocyanins with clays or other inorganic substrates have been reported in the literature, as indicated in section 1.1. However, no study involving flavylium cations and fibrous clays was found prior to our first publication, which is described in Chapter 2. Background about the two known types of fibrous clays used in this work, palygorskite and sepiolite, is outlined below.

1.3.1 Palygorskite and sepiolite

Palygorskite, also named attapulgite (because it was found in the deposit of Attapulgus, Georgia – USA), and sepiolite are hydrated magnesium (and aluminum in the case of palygorskite) phyllosilicate clay minerals. Both have a fibrous morphology resulting from the modulated molecular organization, which consists of a layer structure of ribbons of tetrahedral silica and central magnesium octahedra oriented along the fibers (2:1 phyllosilicate structure). Figure 1.6 shows representations of the structures of palygorskite and sepiolite. The octahedral sheet is sandwiched between two tetrahedral sheets that have periodic inversion of apical oxygen in every two (palygorskite) or three (sepiolite) silicate chairs, causing a periodic discontinuity of the octahedral sheet. As a result, alternated blocks and well-defined one-dimensional cavities or tunnels (Doménech et al., 2011; Sánchez Del Río et al., 2009) with dimensions 3.7 x 6.4 Å for palygorskite and 3.7 x 10.6 Å for sepiolite (Brigatti et al., 2006) are formed. On the external surface of the clay fibers, the partially open channels form grooves (Martínez-Martínez et al., 2011; Ruiz-Hitzky, 2001). As the octahedral sheet is discontinuous, coordinated water molecules (bonded to Mg ions), protons and a small number of exchangeable cations complete the coordination and charge balance. Furthermore, water molecules adsorbed on the external surface and a variable amount within the tunnels, commonly called zeolitic water which is associated to the structure by hydrogen bonding, completes the various types of water in the structure of these clay minerals (Brigatti et al., 2006; Giustetto et al., 2006; Madejová et al., 2017).

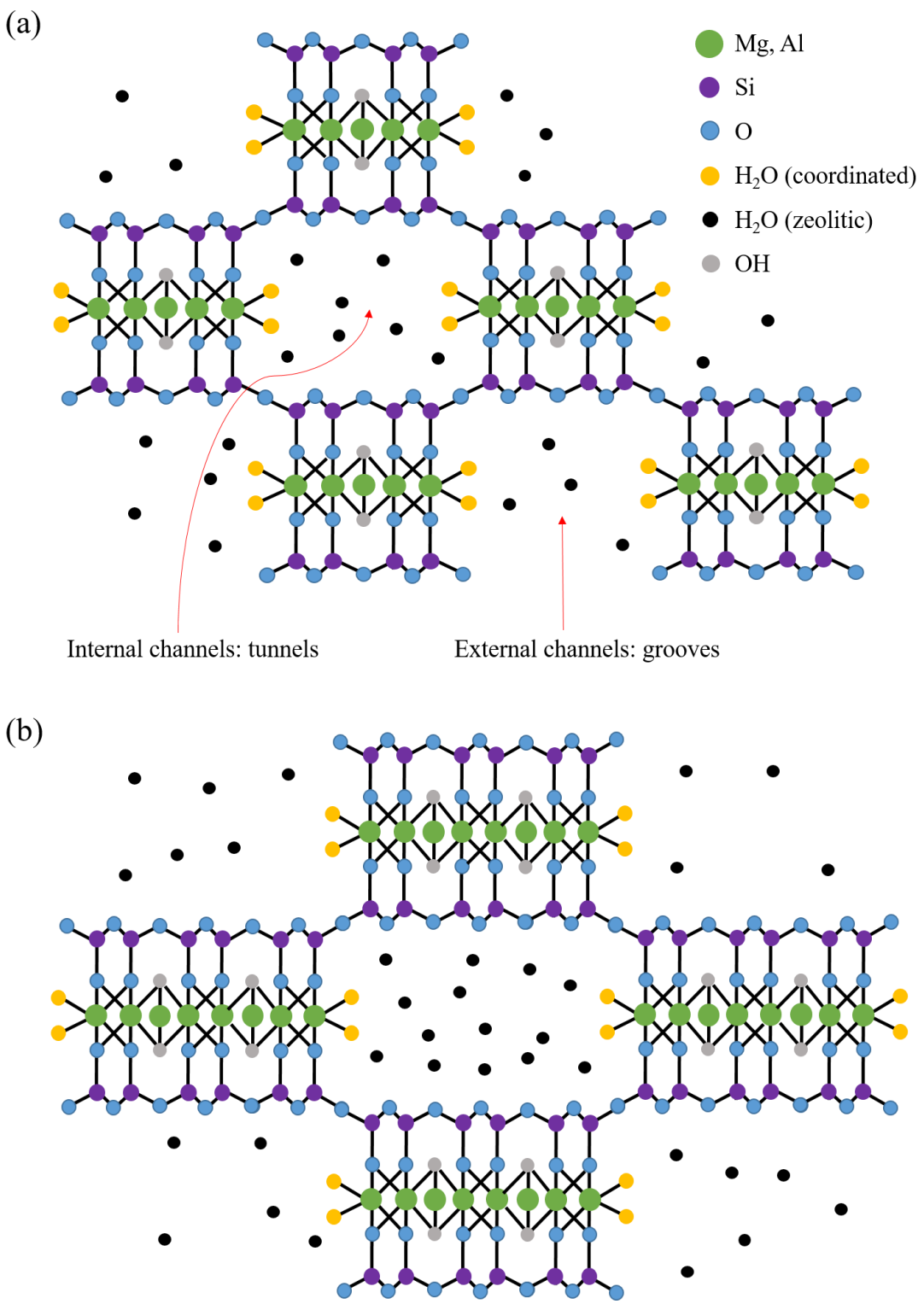

Figure 1.6 – Two-dimensional representation of the structures of (a) palygorskite and (b) sepiolite.

The structure of these clays can undergo isomorphic substitution of cations by other cations with lower valence, for example replacement of Si^{4+} by Al^{3+} in the tetrahedral sheets, and additionally for palygorskite Al^{3+} by Mg^{2+} in the octrahedral layers, resulting in negatively charged sites (Martínez-Martínez et al., 2011; Tunç et al., 2011). In general, the partial charge generated in the clay structure is low, which results in a low cation exchange capacity (CEC).

Three types of active sorption sites are present in the structure of these clays: water molecules coordinated to Mg ions at the edges of structural ribbons; oxygen ions on the tetrahedral sheets of the ribbons; and SiOH groups (along the fibre axis) formed by the broken Si-O-Si bonds at external surfaces and of acceptance of a proton and/or a hydroxyl group for charge balance (Galan, 1996).

The porous structure of these clays, which provide good surface properties for sorption, colloidal-rheological properties and catalyst supports has increased the interest in and the applicability of these clays, ranging from the use as adsorbents of dyes (Eren et al., 2010; Moreira et al., 2017; Tabak et al., 2009) and heavy metals (Bahabadi et al., 2017; Potgieter et al., 2006; Wang et al., 2018) to the production of hybrid materials in general, such as bionanocomposites (Ruiz-Hitzky et al., 2013), organoclays (Paiva et al., 2008) and hybrid pigments (Li et al., 2018; Wang et al., 2016b). In relation to the latter, both clays are well known to play an important role in the constitution of the Maya Blue pigment (see next sections).

1.4 Hybrid materials

The definition recommended by the International Union of Pure and Applied Chemistry (IUPAC) for a hybrid material is a material composed of an intimate mixture

of inorganic components, organic components, or both types of components, in which the components usually interpenetrate on scales of less than 1 µm (Alemán et al., 2007). Therefore, the definition of hybrid materials is completely linked to their constitution, which is composed of two or more components (more commonly of different nature) and structurally organized at the nanometer or molecular level.

The great advantage of hybrid materials is that they often exhibit multifunctional properties, better than those of their isolated components; consequently, they can have better potential for applications. Hybrid materials with organic dyes adsorbed on inorganic substracts, such as clays for example, have aroused the interest of several researchers for the development of materials with variable structures, functionalities, properties and excellent stability approaching that of Maya Blue.

1.4.1 Maya Blue

The Maya Blue pigment was widely used in murals, codices, ceramics and sculptures by the Mayan civilization in the Pre-Columbian era. It is probably, the oldest and most famous type of dye/clay hybrid material. First identified in 1931, Maya Blue pigment stands out for its amazing stability, able to resist concentrated nitric acid, bases, organic solvents, oxidants, reducing agents, moderate heat and light, without losing its color (Arnold et al., 2008; Chiari et al., 2008; José-Yacamán et al., 1996; Sánchez Del Río and Martinetto, 2006). Thus, Maya blue paintings have lasted for a millenium, despite being exposed to harsh climatic conditions, high temperature and humidity. As shown in Figure 1.7, the famous wall paintings at Cacaxtla (an archaeological site located in Mexico) are an example of this amazing stabilty, where Maya Blue has displayed

remarkable durability over hundreds of years of exposure under humid conditions (Chiari et al., 2008).

Figure 1.7 - Maya blue pigment in the famous wall paintings at Cacaxtla, Mexico. Image reproduced from: Chiari et al., 2008.

After the first identification of Maya Blue, it took a few decades to actually conclude that Maya blue pigment is a nanostructured material formed by the mixture of palygorskite clay (there are also cases with sepiolite) and the natural dye indigo extracted from plants (such as *Indigofera suffruticosa* specie). Based on the study of Van Olphen (Van Olphen, 1966), who produced a pigment with properties similar to those of Maya blue from the blend of palygorskite and synthetic indigo (less than 0.5 %), indigo and palygorskite were recognized as the main components used to prepare Maya Blue pigment. He also pointed out that an analogous stable pigment could be prepared from sepiolite and indigo (Van Olphen, 1966).

Nowadays, it is well known that, although palygorskite and sepiolite do not contribute to the pigmentation of Maya Blue, they play an importante and active role in the chemical, photo- and thermal stabilization of the indigo dye. In the Maya Blue structure, indigo is located (apparently irreversibly) in the tunnels of palygorskite or

sepiolite clay, protected from external treatments (Chiari et al., 2008; Giustetto et al., 2011, 2006, 2005; Tilocca and Fois, 2009).

Because of its excellent color stability, the Maya Blue pigment has inspired the development of new materials based on the association of dyes with inorganic compounds, such as clays, zeolites and mesoporous materials, among others. Consequently, the use of paygorskite and sepiolite for hybrid strategies has increased, associating similar properties and enhanced stability with other colors and potential applications. These include hybrids with interesting self-cleaning properties (Wu et al., 2019; Zhang et al., 2016a, 2016b) and highly stable hybrid pigments with a range of colors, formed from organic dyes (Fan et al., 2014; Giustetto et al., 2014; Giustetto and Wahyudi, 2011; Wang et al., 2016b; Wu et al., 2018, 2017; Yuan Zhang et al., 2015; Yujie Zhang et al., 2015b, 2015a) or inorganic pigments (Li et al., 2018; Tian et al., 2017; Wang et al., 2016a).

1.5 Objectives

In view of the aforementioned considerations, our attention in this thesis was drawn to the formation of hybrid pigments from palygorskite and sepiolite fibrous clays as part of our interest in manipulating and controlling the chemistry of flavylium and pyranoflavylium cations in order to promote an improvement in their fluorescence properties and chemical, thermal and photochemical stabilities.

In Chapter 2, we investigated the preparation of flavylium cation/palygorskite (FL/PAL) complexes as prototypes for fluorescent hybrid anthocyanin/palygorskite pigments, as well the evaluation of the color stability and photophysical properties of the hybrid pigments formed. Following a similar strategy, in Chapter 3, we report results for

hybrids prepared by the adsorption of a series of flavylium and pyranoflavylium cations on sepiolite clay. Dictated by the fact that the tunnels and grooves of sepiolite are wider than those of palygorskite, we have also used pyranoflavylium cations as potential prototypes for fluorescent hybrid red wine pyranoanthocyanin/sepiolite pigments.

References

Alemán, J. V., Chadwick, A. V., He, J., Hess, M., Horie, K., Jones, R.G., Kratochvíl, P., Meisel, I., Mita, I., Moad, G., Penczek, S., Stepto, R.F.T., 2007. Definitions of terms relating to the structure and processing of sols, gels, networks, and inorganic-organic hybrid materials (IUPAC Recommendations 2007). Pure Appl. Chem. 79, 1801–1829. https://doi.org/10.1351/pac200779101801

Arnold, D.E., Branden, J.R., Williams, P.R., Feinman, G.M., Brown, J.P., 2008. The first direct evidence for the production of Maya Blue: Rediscovery of a technology. Antiquity 82, 151–164. https://doi.org/10.1017/S0003598X00096514

Azevedo, J., Oliveira, J., Cruz, L., Teixeira, N., Brás, N.F., De Freitas, V., Mateus, N., 2014. Antioxidant features of red wine pyranoanthocyanins: Experimental and theoretical approaches. J. Agric. Food Chem. 62, 7002–7009. https://doi.org/10.1021/jf404735j

Bahabadi, F.N., Farpoor, M.H., Mehrizi, M.H., 2017. Removal of Cd, Cu and Zn ions from aqueous solutions using natural and Fe modified sepiolite, zeolite and palygorskite clay minerals. Water Sci. Technol. 75, 340–349. https://doi.org/10.2166/wst.2016.522

Bergaya, F., Lagaly, G., 2006. General introduction: Clays, clay minerals, and clay science, in: Chapter 1, Handbook of Clay Science, Developments in Clay Science.

pp. 1–18. https://doi.org/10.1016/B978-0-08-098258-8.00001-8

Brigatti, M.F., Galan, E., Theng, B.K.G., 2006. Structures and Mineralogy of Clay Minerals, in: Chapter 2, Handbook of Clay Science, Developments in Clay Science. pp. 19–86. https://doi.org/10.1016/S1572-4352(05)01002-0

Brouillard, R., Chassaing, S., Fougerousse, A., 2003. Why are grape/fresh wine anthocyanins so simple and why is it that red wine color lasts so long? Phytochemistry 64, 1179–1186. https://doi.org/10.1016/S0031-9422(03)00518-1

Casassa, L.F., Harbertson, J.F., 2014. Extraction, Evolution, and Sensory Impact of Phenolic Compounds During Red Wine Maceration. Annu. Rev. Food Sci. Technol. 5, 83–109. https://doi.org/10.1146/annurev-food-030713-092438

Castañeda-Ovando, A., Pacheco-Hernández, M. de L., Páez-Hernández, M.E., Rodríguez, J.A., Galán-Vidal, C.A., 2009. Chemical studies of anthocyanins: A review. Food Chem. https://doi.org/10.1016/j.foodchem.2008.09.001

Cavalcanti, R.N., Santos, D.T., Meireles, M.A.A., 2011. Non-thermal stabilization mechanisms of anthocyanins in model and food systems-An overview. Food Res. Int. 44, 499–509. https://doi.org/10.1016/j.foodres.2010.12.007

Chiari, G., Giustetto, R., Druzik, J., Doehne, E., Ricchiardi, G., 2008. Pre-columbian nanotechnology: Reconciling the mysteries of the maya blue pigment. Appl. Phys. A Mater. Sci. Process. 90, 3–7. https://doi.org/10.1007/s00339-007-4287-z

de Freitas, V., Mateus, N., 2011. Formation of pyranoanthocyanins in red wines: A new and diverse class of anthocyanin derivatives. Anal. Bioanal. Chem. 401, 1463–1473. https://doi.org/10.1007/s00216-010-4479-9

Doménech, A., Doménech-Carbó, M.T., Edwards, H.G.M., 2011. On the interpretation of the Raman spectra of Maya Blue: A review on the literature data. J. Raman Spectrosc. 42, 86–96. https://doi.org/10.1002/jrs.2642

Eren, E., Cubuk, O., Ciftci, H., Eren, B., Caglar, B., 2010. Adsorption of basic dye from aqueous solutions by modified sepiolite: Equilibrium, kinetics and thermodynamics study. Desalination 252, 88–96. https://doi.org/10.1016/j.desal.2009.10.020

Fan, L., Zhang, Y., Zhang, J., Wang, A., 2014. Facile preparation of stable palygorskite/cationic red X-GRL@SiO_2 "Maya Red" pigments. RSC Adv. 4, 63485–63493. https://doi.org/10.1039/C4RA13739F

Fernandes, I., Faria, A., de Freitas, V., Calhau, C., Mateus, N., 2015. Multiple-approach studies to assess anthocyanin bioavailability. Phytochem. Rev. 14, 899–919. https://doi.org/10.1007/s11101-015-9415-3

Ferreira Da Silva, P., Lima, J.C., Freitas, A.A., Shimizu, K., Maçanita, A.L., Quina, F.H., 2005. Charge-transfer complexation as a general phenomenon in the copigmentation of anthocyanins. J. Phys. Chem. A 109, 7329–7338. https://doi.org/10.1021/jp052106s

Figueiredo-González, M., Cancho-Grande, B., Simal-Gándara, J., Teixeira, N., Mateus, N., De Freitas, V., 2014. The phenolic chemistry and spectrochemistry of red sweet wine-making and oak-aging. Food Chem. 152, 522–530. https://doi.org/10.1016/J.FOODCHEM.2013.12.018

Freitas, A.A., Silva, C.P., Silva, G.T.M., Maçanita, A.L., Quina, F.H., 2018. Ground- and Excited-State Acidity of Analogs of Red Wine Pyranoanthocyanins,. Photochem. Photobiol. 94, 1086–1091. https://doi.org/10.1111/php.12944

Fulcrand, H., Dueñas, M., Salas, E., Cheynier, V., 2006. Phenolic reactions during winemaking and aging. Am. J. Enol. Vitic. 57, 289–297.

Galan, E., 1996. Properties and applications of palygorskite-sepiolite clays. Clay Miner. 31, 443–453.

García-Estévez, I., Cruz, L., Oliveira, J., Mateus, N., de Freitas, V., Soares, S., 2017. First

evidences of interaction between pyranoanthocyanins and salivary proline-rich proteins. Food Chem. 228, 574–581. https://doi.org/10.1016/j.foodchem.2017.02.030

Giustetto, R., Levy, D., Chiari, G., 2006. Crystal structure refinement of Maya Blue pigment prepared with deuterated indigo, using neutron powder diffraction. Eur. J. Mineral. 18, 629–640. https://doi.org/10.1127/0935-1221/2006/0018-0629

Giustetto, R., Levy, D., Wahyudi, O., Ricchiardi, G., Vitillo, J.G., 2011. Crystal structure refinement of a sepiolite/indigo Maya Blue pigment using molecular modelling and synchrotron diffraction. Eur. J. Mineral. 23, 449–466. https://doi.org/10.1127/0935-1221/2011/0023-2105

Giustetto, R., Llabrés I Xamena, F.X., Ricchiardi, G., Bordiga, S., Damin, A., Gobetto, R., Chierotti, M.R., 2005. Maya blue: A computational and spectroscopic study. J. Phys. Chem. B 109, 19360–19368. https://doi.org/10.1021/jp048587h

Giustetto, R., Vitillo, J.G., Corazzari, I., Turci, F., 2014. Evolution and reversibility of host/guest interactions with temperature changes in a methyl red@palygorskite polyfunctional hybrid nanocomposite. J. Phys. Chem. C 118, 19322–19337. https://doi.org/10.1021/jp4091238

Giustetto, R., Wahyudi, O., 2011. Sorption of red dyes on palygorskite: Synthesis and stability of red/purple Mayan nanocomposites. Microporous Mesoporous Mater. 142, 221–235. https://doi.org/10.1016/j.micromeso.2010.12.004

Held, B., Tang, H., Natarajan, P., Da Silva, C.P., De Oliveira Silva, V., Bohne, C., Quina, F.H., 2016. Cucurbit[7]uril inclusion complexation as a supramolecular strategy for color stabilization of anthocyanin model compounds. Photochem. Photobiol. Sci. 15, 752–757. https://doi.org/10.1039/c6pp00060f

Heras-Roger, J., Díaz-Romero, C., Darias-Martín, J., 2016. What Gives a Wine Its Strong

Red Color? Main Correlations Affecting Copigmentation. J. Agric. Food Chem. 64, 6567–6574. https://doi.org/10.1021/acs.jafc.6b02221

José-Yacamán, M., Rendon, L., Arenas, J., Puche, M.C.S., 1996. Maya Blue Paint : An Ancient Nanostructured Material. Science (80-.). 273, 223–225.

Khoo, H.E., Azlan, A., Tang, S.T., Lim, S.M., 2017. Anthocyanidins and anthocyanins: colored pigments as food, pharmaceutical ingredients, and the potential health benefits. Food Nutr. Res. 61, 1361779. https://doi.org/10.1080/16546628.2017.1361779

Kohno, Y., Hoshino, R., Ikoma, S., Shibata, M., Matsushima, R., Tomita, Y., Maeda, Y., Kobayashi, K., 2010. Stabilization of Flavylium Dye by Incorporation into Bentonite Clay. J. Jpn. Soc. Colour Mater. 83, 103–107. https://doi.org/https://doi.org/10.4011/shikizai.83.103

Kohno, Y., Hoshino, R., Matsushima, R., Tomita, Y., Kobayashi, K., 2007. Stabilization of Flavylium Dyes by Incorporation in the Clay Interlayer. J. Jpn. Soc. Colour Mater. 80, 6–12. https://doi.org/https://doi.org/10.4011/shikizai1937.80.6

Kohno, Y., Kinoshita, R., Ikoma, S., Yoda, K., Shibata, M., Matsushima, R., Tomita, Y., Maeda, Y., Kobayashi, K., 2009. Stabilization of natural anthocyanin by intercalation into montmorillonite. Appl. Clay Sci. 42, 519–523. https://doi.org/10.1016/j.clay.2008.06.012

Kohno, Y., Senga, M., Shibata, M., Yoda, K., Matsushima, R., Tomita, Y., Maeda, Y., Kobayashi, K., 2011. Stabilization of flavylium dye by incorporation into Fe-containing mesoporous silicate. Microporous Mesoporous Mater. 141, 77–80. https://doi.org/10.1016/j.micromeso.2010.11.004

Kohno, Y., Shibata, Y., Oyaizu, N., Yoda, K., Shibata, M., Matsushima, R., 2008. Stabilization of flavylium dye by incorporation into the pore of protonated zeolites.

Microporous Mesoporous Mater. 114, 373–379. https://doi.org/10.1016/j.micromeso.2008.01.023

Li, H., Zhang, A., Wang, A., Mu, B., An, X., 2018. Cobalt blue hybrid pigment doped with magnesium derived from sepiolite. Appl. Clay Sci. 157, 111–120. https://doi.org/10.1016/j.clay.2018.02.032

Lima, J.C., Vautier-Giongo, C., Lopes, A., Melo, E., Quina, F.H., Maçanita, A.L., 2002. Color stabilization of anthocyanins: Effect of SDS micelles on the acid-base and hydration kinetics of malvidin 3-glucoside (Oenin). J. Phys. Chem. A 106, 5851–5859. https://doi.org/10.1021/jp014081c

Madejová, J., Gates, W.P., Petit, S., 2017. IR Spectra of Clay Minerals, in: Chapter 5, Handbook of Clay Science, Developments in Clay Science. pp. 107–149. https://doi.org/10.1016/B978-0-08-100355-8.00005-9

Marquez, A., Serratosa, M.P., Merida, J., 2013. Pyranoanthocyanin Derived Pigments in Wine: Structure and Formation during Winemaking. J. Chem. 2013, 1–15. https://doi.org/10.1155/2013/713028

Martínez-Martínez, V., Corcóstegui, C., Bañuelos Prieto, J., Gartzia, L., Salleres, S., López Arbeloa, I., 2011. Distribution and orientation study of dyes intercalated into single sepiolite fibers. A confocal fluorescence microscopy approach. J. Mater. Chem. 21, 269–276. https://doi.org/10.1039/c0jm02211j

Moreira, M.A., Ciuffi, K.J., Rives, V., Vicente, M.A., Trujillano, R., Gil, A., Korili, S.A., de Faria, E.H., 2017. Effect of chemical modification of palygorskite and sepiolite by 3-aminopropyltriethoxisilane on adsorption of cationic and anionic dyes. Appl. Clay Sci. 135, 394–404. https://doi.org/10.1016/j.clay.2016.10.022

Oliveira, H., Wu, N., Zhang, Q., Wang, J., Oliveira, J., De Freitas, V., Mateus, N., He, J., Fernandes, I., 2016. Bioavailability studies and anticancer properties of malvidin

based anthocyanins, pyranoanthocyanins and non-oxonium derivatives. Food Funct. 7, 2462–2468. https://doi.org/10.1039/c6fo00445h

Oliveira, J., Mateus, N., de Freitas, V., 2014. Previous and recent advances in pyranoanthocyanins equilibria in aqueous solution. Dye. Pigment. 100, 190–200. https://doi.org/10.1016/J.DYEPIG.2013.09.009

Oliveira, R.N., Acchar, W., Soares, G.D.A., Barreto, L.S., 2013. The increase of surface area of a Brazilian palygorskite clay activated with sulfuric acid solutions using a factorial design. Mater. Res. 16, 924–928. https://doi.org/10.1590/s1516-14392013005000075

Paiva, L.B., Morales, A.R., Valenzuela Díaz, F.R., 2008. Organoclays: Properties, preparation and applications. Appl. Clay Sci. 42, 8–24. https://doi.org/10.1016/j.clay.2008.02.006

Pina, F., Melo, M.J., Laia, C.A.T., Parola, A.J., Lima, J.C., 2012. Chemistry and applications of flavylium compounds: A handful of colours. Chem. Soc. Rev. 41, 869–908. https://doi.org/10.1039/c1cs15126f

Potgieter, J.H., Potgieter-Vermaak, S.S., Kalibantonga, P.D., 2006. Heavy metals removal from solution by palygorskite clay. Miner. Eng. 19, 463–470. https://doi.org/10.1016/j.mineng.2005.07.004

Quina, F.H., Bastos, E.L., 2018. Chemistry inspired by the colors of fruits, flowers and wine. An. Acad. Bras. Cienc. 90, 681–695. https://doi.org/10.1590/0001-3765201820170492

Quina, F.H., Moreira, P.F., Vautier-Giongo, C., Rettori, D., Rodrigues, R.F., Freitas, A.A., Silva, P.F., Macanita, A.L., 2009. Photochemistry of anthocyanins and their biological role in plant tissues. Pure Appl. Chem. 81, 1687–1694. https://doi.org/10.1351/Pac-Con-08-09-28

Ruiz-Hitzky, E., 2001. Molecular access to intracrystalline tunnels of sepiolite. J. Mater. Chem. 11, 86–91. https://doi.org/10.1039/b003197f

Ruiz-Hitzky, E., Darder, M., Fernandes, F.M., Wicklein, B., Alcântara, A.C.S., Aranda, P., 2013. Fibrous clays based bionanocomposites. Prog. Polym. Sci. 38, 1392–1414. https://doi.org/10.1016/j.progpolymsci.2013.05.004

Sánchez Del Río, M., Boccaleri, E., Milanesio, M., Croce, G., Van Beek, W., Tsiantos, C., Chyssikos, G.D., Gionis, V., Kacandes, G.H., Suárez, M., García-Romero, E., 2009. A combined synchrotron powder diffraction and vibrational study of the thermal treatment of palygorskite-indigo to produce Maya blue. J. Mater. Sci. 44, 5524–5536. https://doi.org/10.1007/s10853-009-3772-5

Sánchez Del Río, M., Martinetto, P., 2006. Synthesis and Acid Resistance of Maya Blue Pigment. Archaeometry 48, 115–130. https://doi.org/10.1111/j.1475-4754.2006.00246.x

Schwarz, M., Wabnitz, T.C., Winterhalter, P., 2003. Pathway Leading to the Formation of Anthocyanin−Vinylphenol Adducts and Related Pigments in Red Wines. J. Agric. Food Chem. 51, 3682–3687. https://doi.org/10.1021/JF0340963

Siddique, F., Silva, C.P., Silva, G.T.M., Lischka, H., Quina, F.H., Aquino, A.J.A., 2019. The electronic transitions of analogs of red wine pyranoanthocyanin pigments. Photochem. Photobiol. Sci. 18, 45–53. https://doi.org/10.1039/C8PP00391B

Silva, G.T.M., Thomas, S.S., Silva, C.P., Schlothauer, J.C., Baptista, M.S., Freitas, A.A., Bohne, C., Quina, F.H., 2019. Triplet Excited States and Singlet Oxygen Production by Analogs of Red Wine Pyranoanthocyanins. Photochem. Photobiol. 95, 176–182. https://doi.org/10.1111/php.12973

Silva, V.O., Freitas, A.A., Maçanita, A.L., Quina, F.H., 2016. Chemistry and photochemistry of natural plant pigments: the anthocyanins. J. Phys. Org. Chem. 29,

594–599. https://doi.org/10.1002/poc.3534

Tabak, A., Eren, E., Afsin, B., Caglar, B., 2009. Determination of adsorptive properties of a Turkish Sepiolite for removal of Reactive Blue 15 anionic dye from aqueous solutions. J. Hazard. Mater. 161, 1087–1094. https://doi.org/10.1016/j.jhazmat.2008.04.062

Tang, K., Liu, T., Han, Y., Xu, Y., Li, J.M., 2017. The Importance of Monomeric Anthocyanins in the Definition of Wine Colour Properties. South African J. Enol. Vitic. 38, 1–10. https://doi.org/10.21548/38-1-661

Tian, G., Wang, W., Wang, D., Wang, Q., Wang, A., 2017. Novel environment friendly inorganic red pigments based on attapulgite. Powder Technol. 315, 60–67. https://doi.org/10.1016/j.powtec.2017.03.044

Tilocca, A., Fois, E., 2009. The color and stability of maya blue: TDDFT calculations. J. Phys. Chem. C 113, 8683–8687. https://doi.org/10.1021/jp810945a

Tománková, E., Balík, J., Soural, I., Bednář, P., Papoušková, B., 2016. Colour and antioxidant properties of malvidin-3-glucoside and Vitisin A. Acta Aliment. 45, 85–92. https://doi.org/10.1556/066.2016.45.1.11

Tunç, S., Duman, O., Çetinkaya, A., 2011. Electrokinetic and rheological properties of sepiolite suspensions in the presence of hexadecyltrimethylammonium bromide. Colloids Surfaces A Physicochem. Eng. Asp. 377, 123–129. https://doi.org/10.1016/j.colsurfa.2010.12.036

Van Olphen, H., 1966. Maya Blue : A Clay-Organic Pigment? Science (80-.). 154, 645–646.

Wang, Q., Mu, B., Wang, W., Wang, A., Tian, G., 2016a. Cost-efficient, vivid and stable red hybrid pigments derived from naturally available sepiolite and halloysite. Ceram. Int. 43, 1862–1869. https://doi.org/10.1016/j.ceramint.2016.10.145

Wang, Q., Mu, B., Zhang, Y., Zhang, J., Wang, A., 2016b. Palygorskite-based hybrid fluorescent pigment: Preparation, spectroscopic characterization and environmental stability. Microporous Mesoporous Mater. 224, 107–115. https://doi.org/10.1016/j.micromeso.2015.11.034

Wang, Z., Liao, L., Hursthouse, A., Song, N., Ren, B., 2018. Sepiolite-Based Adsorbents for the Removal of Potentially Toxic Elements from Water: A Strategic Review for the Case of Environmental Contamination in Hunan, China. Int. J. Environ. Res. Public Health 15, 1653. https://doi.org/10.3390/ijerph15081653

Wu, S., Cui, H., Wang, C., Hao, F., Liu, P., Xiong, W., 2018. In situ self-assembled preparation of the hybrid nanopigment from raw sepiolite with excellent stability and optical performance. Appl. Clay Sci. 163, 1–9. https://doi.org/10.1016/j.clay.2018.07.009

Wu, S., Duan, Z., Hao, F., Xiong, S., Xiong, W., Lv, Y., Liu, P., Luo, H., 2017. Preparation of acid-activated sepiolite/Rhodamine B@SiO2 hybrid fluorescent pigments with high stability. Dye. Pigment. 137, 395–402. https://doi.org/10.1016/J.DYEPIG.2016.10.030

Wu, S., Huang, J., Cui, H., Ye, T., Hao, F., Xiong, W., Liu, P., Luo, H., 2019. Preparation of organic–inorganic hybrid methylene blue polymerized organosilane/sepiolite pigments with superhydrophobic and self-cleaning properties. Text. Res. J. https://doi.org/10.1177/0040517519829924

Zhang, Y., Dong, J., Sun, H., Yu, B., Zhu, Z., Zhang, J., Wang, A., 2016a. Solvatochromic Coatings with Self-Cleaning Property from Palygorskite@Polysiloxane/Crystal Violet Lactone. ACS Appl. Mater. Interfaces 8, 27346–27352. https://doi.org/10.1021/acsami.6b09252

Zhang, Y., Fan, L., Chen, H., Zhang, J., Zhang, Y., Wang, A., 2015a. Learning from

ancient Maya: Preparation of stable palygorskite/methylene blue@SiO2 Maya Blue-like pigment. Microporous Mesoporous Mater. 211, 124–133. https://doi.org/10.1016/j.micromeso.2015.03.002

Zhang, Y., Wang, W., Mu, B., Wang, Q., Wang, A., 2015. Effect of grinding time on fabricating a stable methylene blue/palygorskite hybrid nanocomposite. Powder Technol. 280, 173–179. https://doi.org/10.1016/j.powtec.2015.04.046

Zhang, Y., Zhang, J., Wang, A., 2016b. From Maya blue to biomimetic pigments: Durable biomimetic pigments with self-cleaning property. J. Mater. Chem. A 4, 901–907. https://doi.org/10.1039/c5ta09300g

Zhang, Y., Zhang, J., Wang, A., 2015b. Facile preparation of stable palygorskite/methyl violet@SiO2 “Maya Violet” pigment. J. Colloid Interface Sci. 457, 254–263. https://doi.org/10.1016/j.jcis.2015.07.030

CHAPTER 2

Organic/inorganic hybrid pigments from flavylium cations and palygorskite

This chapter, which was published in *Applied Clay Science* (https://doi.org/10.1016/j.clay.2018.07.002) as a research paper, reports the preparation, photophysical properties and stabilities of a series of hybrid pigments based on flavylium cations adsorbed on palygorskite clay.

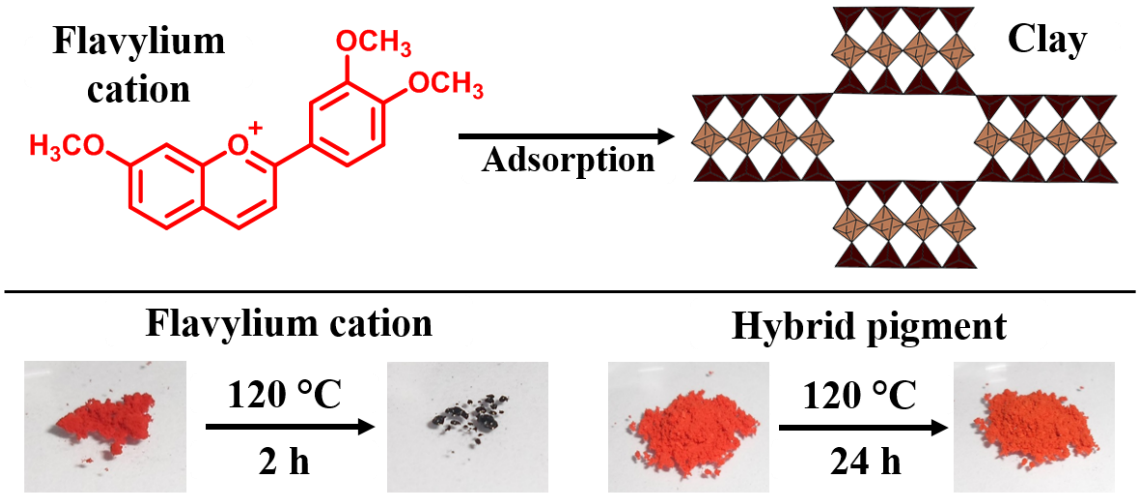

Abstract

Features such as color, brightness and fluorescence are extremely important in applications of pigments. Hybrid materials inspired by the ancient Maya Blue pigment are a promising alternative to improve the properties and applicability of natural and synthetic dyes. In this Chapter, we report the preparation, photophysical properties, and stability of several fluorescent hybrid pigments based on flavylium cations (FL) adsorbed on palygorskite (PAL). Five flavylium cations were investigated, viz., the 3',4',7-trimethoxyflavylium (FL1), 7-hydroxy-4'-methoxy-flavylium (FL2), 7-hydroxy-4-methylflavylium (FL3), 5,7-dihydroxy-4-methylflavylium (FL4) and 7-methoxy-4-methylflavylium (FL5) cations. Only FL1 and FL2, without a methyl substituent at the 4-position that could hinder inclusion in palygorskite channels, adsorbed strongly on PAL, producing fluorescent hybrid pigments with attractive colors. The spectroscopic and fluorescence properties of the FL1/PAL and FL2/PAL hybrid pigments were characterized. The color of the adsorbed dyes was somewhat more resistant to changes in external pH, photochemical stability was maintained and the thermal lability was markedly improved in the FL/PAL hybrid pigments, pointing to flavylium cations as promising chromophores for the development of fluorescent hybrid pigments with attractive colors.

2.1 Introduction

Hybrid materials prepared by the combination of dyes with inorganic substrates have been extensively studied in search of materials with unique properties and color attributes (preferably bright and/or fluorescent) that are chemically, thermally and light stable (Laguna et al., 2007; Teixeira-Neto et al., 2009, 2012; Dejoie et al., 2010; Giustetto et al., 2014; Lin et al., 2014). One of the oldest and perhaps the most famous example of an organic-inorganic hybrid material is the Maya Blue pigment, which was widely used in murals, codices, ceramics and sculptures by the Maya civilization in the Pre-Columbian era. Maya Blue is extremely stable, able to resist the attack of concentrated nitric acid, bases and organic solvents without losing its color (Sánchez Del Río and Martinetto, 2006; Arnold and Branden, 2008; Chiari et al., 2008; Giustetto et al., 2011). The amazing chemical and photochemical stability of Maya Blue is presumably due to its unique structure, which consists of the dye indigo protectively (and apparently irreversibly) inserted into the channels of palygorskite or sepiolite clay (Giustetto et al., 2005, 2006, 2011; Chiari et al., 2008; Tilocca and Fois, 2009).

Palygorskite (PAL) is a hydrated magnesium and aluminum phyllosilicate clay mineral. Unlike most clays, PAL has fibrous morphology, consisting of a layer structure of ribbons of tetrahedral silica and central magnesium octahedra oriented along the fibers. The octahedral sheet is sandwiched between two tetrahedral sheets that have periodic inversion of the apical oxygen, resulting in well-defined one-dimensional cavities or tunnels (Sánchez Del Río et al., 2009; Doménech et al., 2011) with dimensions 3.7 x 6.4 Å (Brigatti et al., 2006) and, on the external surface of the clay fibers, partially open grooves or channels (as denominated for sepiolite by, e.g., Ruiz-Hitzky (2001) and Martínez-Martínez et al. (2011)). Several studies have shown that palygorskite has two main types of acidic sites, sites of stronger acidity with an effective pK_a in the range of

5-5.5 and more weakly acidic sites with a pK_a around 9-9.5 (Frini-Srasra and Srasra, 2008; Acebal and Vico, 2017). The porous structure of this clay allows the insertion and/or adsorption of organic molecules and ions, making it a good adsorbent (Giustetto et al., 2014; Mu and Wang, 2016). Recent studies involving dyes and PAL clay have obtained several novel Maya Blue-like pigments (Lima et al., 2012; Fan et al., 2014; Zhang et al., 2015a, 2015b; Zhang et al., 2015c, 2015d), some of which are materials with interesting self-cleaning properties (Zhang et al., 2016a, 2016b). Adsorption of dyes onto PAL and PAL composites (Mu and Wang, 2016) and biomedical applications clay-drug hybrid materials (Kim et al., 2016) have been recently reviewed and the use of PAL as an adsorbent for environmental remediation continues to be of interest (Ugochukwu et al., 2013; Boudriche et al., 2015; Yang et al, 2018).

The chromophoric group of anthocyanins, which are responsible for most of the purple, blue and red colors of flowers and fruits, is a 7-hydroxyflavylium cation. The chemical and photochemical reactivity of synthetic flavylium cations mimics that of natural anthocyanins, with the advantage of the facility and versatility of modifying the substituents on the flavylium chromophore and consequently their reactivity. Although anthocyanins and synthetic flavylium cations have great potential for practical applications as dyes or antioxidants, these applications are limited by their chemical reactivity, which is affected by several factors including pH, temperature, light, oxygen, among others (Ferreira da Silva et al., 2005; Castañeda-Ovando et al., 2009; Quina et al., 2009; Cavalcanti et al., 2011; Silva et al., 2016).

The inclusion and/or adsorption of anthocyanins and flavylium cations in/on inorganic substrates such as mesoporous materials (Kohno et al., 2008a, 2011, 2015; Gago et al., 2017) and clays (Lima et al., 2007; Kohno et al., 2007, 2009, 2010; Ogawa et al., 2017; Ribeiro et al., 2018), may represent promising alternatives for preventing the

undesirable chemistry of these dye molecules. In the present work, we have investigated the preparation of flavylium cation/palygorskite (FL/PAL) complexes as prototypes for fluorescent hybrid anthocyanin/palygorskite pigments. The complexes that retained the more intense colors and fluorescence after exhaustive washing with acidic methanol were chosen for evaluation of the thermal, photochemical and pH stability of their color and fluorescence.

2.2 Experimental Section

2.2.1 Materials

The flavylium cation salts 3',4',7-trimethoxyflavylium chloride (FL1), 7-hydroxy-4'-methoxy-flavylium chloride (FL2), 7-hydroxy-4-methylflavylium chloride (FL3), 5,7-dihydroxy-4-methylflavylium chloride (FL4) and 7-methoxy-4-methylflavylium chloride (FL5) used in this work (Scheme 2.1) were available from previous studies of the group and the syntheses have been previously reported (Freitas et al., 2013; Held et al., 2016; Silva et al., 2018). The palygorskite used in this work was the Source Clay PFl-1 from the Clay Minerals Society. The chemical composition, characterization and properties of this clay have been described (Shariatmadari et al., 1999; Borden and Giese, 2001; Chipera and Bish, 2001; Guggenheim and Koster van Groos, 2001; Madejová and Komadel, 2001; Mermut and Cano, 2001; Li et al., 2003; Dogan et al., 2006; Frost et al., 2010). Hydrochloric acid (HCl, Vetec) was used as received, methanol (Merck) was treated with sodium and ultrapure water was used for the preparation of all aqueous solutions.

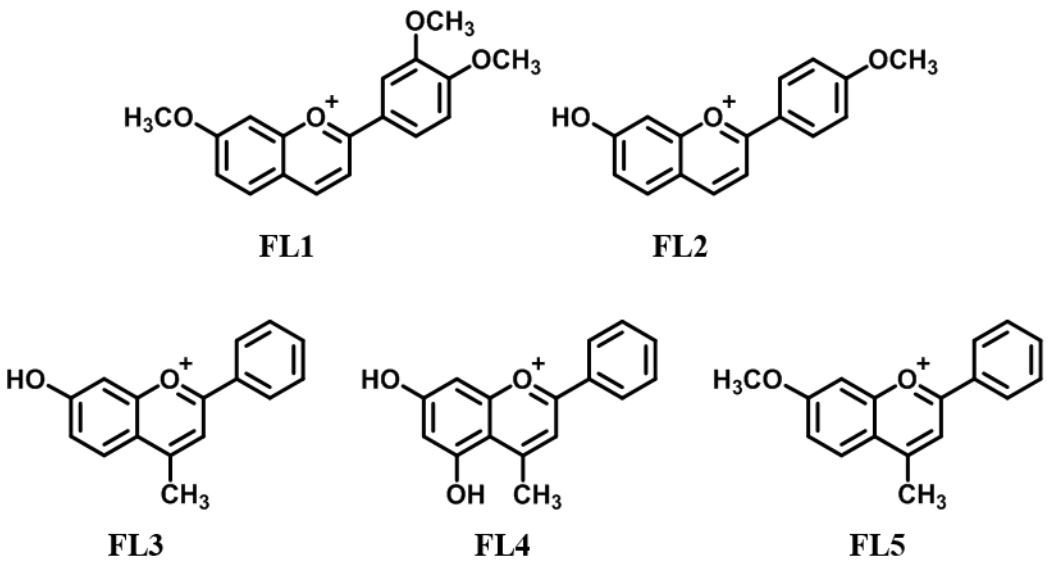

Scheme 2.1. - Structures of the flavylium cations (FL) used in this work.

2.2.2 Preparation and physical characterization of the FL/PAL hybrid pigments

Aliquots of solutions of the FL in methanol (in which FL cations are highly soluble) containing 1% 1.0 mol dm^{-3} HCl (in order to suppress proton transfer and hydration of the flavylium cations) were added to the appropriate amount of PAL clay powder. The initial FL/PAL ratios utilized were 0.050, 0.075, 0.100 and 0.125 mmol g^{-1}. The resulting dispersions were stirred for 24 h in the dark at room temperature, centrifuged and the solid washed exhaustively with HCl-acidified methanol and dried at 45 °C under vacuum for 2 h. The amount of flavylium cation adsorbed was estimated from the decrease in the absorbance of the supernatant employing the known molar attenuation coefficient of each FL.

Powder X-ray diffractograms of PAL and FL1/PAL were determined with a Bruker D2 Phase diffractometer using Cu-K_α radiation (1.5418 Å, 30 kV, 15 mA) employing a scan step of 0.05°. Nitrogen adsorption/desorption isotherms were determined at -196 °C using a Quantachrome volumetric adsorption analyzer (Model

100E). The samples were outgassed for 24 h under reduced pressure at 80 °C. The specific surface areas (S_{BET}) and total pore volumes (V_{tot}) of the samples were determined by the BET (Brunauer et al., 1938) and BJH (Barrett et al., 1951) methods, respectively. Surface areas of the micropores (S_{micro}), the external surface areas (S_{ext}), the micropore volumes (V_{micro}) and the sum of meso- and macropore volumes ($V_{meso+macro}$) were estimated by the *t*-plot method (Lippens and de Boer, 1965).

2.2.3 Spectroscopic measurements

For the infrared measurements, about 1.50 mg of solid sample was added to approximately 150 mg of dry KBr in a small agate mortar and mixed by grinding. The resulting powder was pressed into a pellet using a hydraulic press (Caver, model 3912, Wabash). Infrared spectra of the pellets were collected using a Bruker Vector 22 FTIR spectrophotometer in the frequency range of 4000-500 cm^{-1}, 32 scans at 0.5 cm^{-1} digital resolution.

The UV-Vis-diffuse reflectance (DR) spectra were measured with a Varian Cary 50 UV-vis Bio spectrophotometer equipped with a *Barrelino*™ diffuse reflectance probe (Harrick Scientific Products, Inc.). Samples with greater amounts of adsorbed flavylium (FL1 and FL2) were diluted in barium sulfate. The diffuse reflectance spectra were converted to the corresponding remission function, F(R), employing the Kubelka-Munk equation (Tomasini et al., 2009):

$$F(R) = \frac{(1-R)^2}{2R}$$

where R is the measured reflectance at each wavelength. CIELAB Color coordinates (CIE L*a*b*) (Gilchrist and Nobbs, 1999) were obtained from the UV-vis-DR measurements by using the software Agilent Cary WinUV Color. In this case, the samples were not diluted in barium sulfate in order to obtain the true color coordinates of the samples. Absorbance spectra were measured using the same spectrophotometer or a Hewlett Packard 8452A diode array spectrometer.

All steady state fluorescence measurements were performed with a Hitachi F-4500 fluorescence spectrophotometer. For analysis of the solid samples, the instrument was equipped with a solid sample holder. The excitation and emission wavelengths are indicated in the figure legends. The slits were set to bandwidths of 5.0 nm for both excitation and emission monochromators of the hybrid pigments, and for FL1 and FL2 were 10/20 and 2.5/5.0 nm (excitation and emission), respectively. The experiments with the hybrid pigments were conducted in the solid state. For the steady-state fluorescence anisotropy measurements, the fluorescence spectrophotometer (Hitachi F-4500) was fitted with manual polarizers placed in the excitation and emission light pathways. The steady-state anisotropy (r) was calculated for the emission intensities determined for the four orientations of the polarizers: vertical-vertical (VV), vertical-horizontal (VH), horizontal-horizontal (HH) and horizontal-vertical (HV) employing the following equation (Lakowicz, 2006):

$$r = \frac{I_{\mathrm{VV}} - GI_{\mathrm{VH}}}{I_{\mathrm{VV}} + 2GI_{\mathrm{VH}}}$$

where $G = I_{HV}/I_{HH}$ is a correction factor for the relative sensitivity of the detection system to horizontally and vertically polarized light.

Time-resolved fluorescence decay experiments were carried out using an OB920 single photon counting system (Edinburgh Instruments), exciting the sample with a 405 nm Picosecond Pulsed Diode Laser (EPL405). The solid sample was placed in a shallow quartz cell that was covered with a quartz glass and was placed in a front-face sample holder which is tilted so as to minimize specular reflections (Zhang et al., 2014). The bandwidth for the emission monochromator was 16 nm. A neutral density filter was employed for control of the photon flux from the excitation source that reached the sample. The emission wavelengths set for the collection of the decays for the FL1/PAL and FL2/PAL samples were 575 and 525 nm, respectively. The fluorescence decays were collected with a 50 ns time window and the number of counts in the channel with maximum intensity was 10,000. Barium sulfate powder was used as a scatterer to collect the instrument response function (IRF). The fluorescence decays were fit to a sum of exponentials employing Edinburgh Instruments F900 software for reconvolution to extract the lifetimes. The quality of the fits was determined by the randomness of the residuals and the χ^2 values, which are ideally between 0.9 and 1.3.

For the anisotropy experiments, the diode laser was rotated to achieve vertical and horizontal polarizations of the excitation beam. For the emission collection, the polarizer between the sample and the emission monochromator was set to the required angles. The anisotropy decay measurements were performed with a 20 ns time window and the time required to collect 10000 counts was estimated. This time and the neutral density setting for the excitation beam were kept constant for the collection of the 4 decays with the different polarizations. The four decays were collected for each anisotropy calculation (I_{VV}, I_{VH}, I_{HV}, I_{HH}) and combined to obtain the anisotropy decay (Lakowicz, 2006):

$$r(t) = \frac{I_{VV}(t) - GI_{VH}(t)}{I_{VV}(t) + 2GI_{VH}(t)}$$

The anisotropy decay, calculated using the F900 software, was then fit to a sum of exponentials to estimate rotational correlation lifetimes.

2.2.4 Wide field and confocal fluorescence microscopy

Confocal fluorescence images were obtained using a plate scanning instrument based on a microscope (Olympus IX71) with a digital piezoelectric controller and stage (PI, E-710.3CD and P-517.3CD) for nanometric sample scanning. The excitation of the samples at 473 nm was provided by a Cobolt Blue diode laser. The circularly polarized laser beam was focused on the samples with an UPLFLN 40X Olympus objective. The emission signal was separated from the laser excitation beam using Chroma Z470rd and ZET 473NF dichroic and notch filter, respectively. Photons were counted using an avalanche photodiode point detector (Perkin Elmer, SPCM-AQR-14) aligned with a 50 μm pinhole in the confocal line. Transistor-transistor logic (TTL) detector signals were registered in a counter/timer PCI card (NI 6601) and transferred to a personal computer for 2D plotting using a scanning control program written in C# (Ferreira et al., 2011). Fluorescence images were recorded using false-color mapping, reaching the best contrast enhancement according to the difference in intensity of the fluorescence signal. Wide-field images were obtained with the same fluorescence microscope by adapting an optical lens in the epifluorescence entrance with focus on the back aperture of the objective. The samples were excited at 405 nm with a Coherent Cube CW laser and the emission was selected by a dichroic cube (Chroma, z405lp) and images were registered in a color camera (ThorLabs DCU223C) coupled to the right primary port of the Olympus IX71 (Lauer et al., 2014).

2.2.5 Photochemical and thermal stability and sensitivity to pH

The UV radiation resistance tests of the samples were performed using an Oriel® (California, USA) Sol UV-2 Solar simulator (85.7 % UV-A, 11 % UV-B and 3.3 % of visible light). The samples were exposed to a radiation intensity of 75.0 W m^{-2} UV-A (365 nm) and 43.0 W m^{-2} UV-B (312 nm). The irradiations were carried out at room temperature (25 °C) with an exposure time of 6 h. UV-vis-DR measurements were used to verify any spectral and color changes.

In order to verify the reactivity of the FL cations adsorbed into/onto PAL, FL1/PAL and FL2/PAL samples were added to 5 mL of 10 mmol dm^{-3} phosphate buffer solution at pH = 9. After 24 h, the samples were centrifuged and dried. UV-vis-DR measurements were used to verify any spectral and color changes. In order to compare the stability of the hybrid pigments with the respective free FL, the spectra of FL in 10 mmol dm^{-3} phosphate buffer solution, pH = 8.5, were also obtained. The reversibility was examined by adding FL to 10 mmol dm^{-3} acetate buffer solutions at pH = 4, 5 or 6, followed by addition of 0.1 g of PAL after discoloration of the solutions due to hydration of the flavylium cation. This test was carried out under stirring at room temperature (ca. 20 ºC) and accomplished by taking digital images as a function of the time.

Thermal stability was investigated by submitting FL1/PAL and FL2/PAL samples to heating at 120 °C under vacuum for 24 h and comparing with FL cations in solid form that were submitted to the same temperature for 2 h. Measurements of the color coordinates and digital images were used to verify any color changes.

2.3 Results and discussion

2.3.1 Hybrid pigment formation

Initial studies clearly showed that the relative amount of flavylium cation adsorbed and the colors of the samples were influenced by the substituents on the FL cations. Five FL cations with similar substituents at different positions but with different pH-dependent equilibria and different molecular sizes and solvophobicity/solvophilicity, were chosen for evaluation. Both FL1 and FL2 adsorbed strongly on PAL (Table 2.1) and imparted attractive colors to the samples (Figure 2.S1 of the Supplementary Material), even after exhaustive washing with acidic methanol with the objective of removing loosely physiosorbed dye. In contrast, the other three flavylium cations all have a methyl group at the 4-position, i.e., FL3, FL4 and FL5, and all adsorbed poorly on PAL, failing to impart attractive coloration to the clay. In the case of FL4, the amount adsorbed was miniscule, as shown in Table 2.1 and in Figure 2.S2 of the Supplementary Material. Since affinity and stability should parallel each other, our subsequent studies of the hybrid pigments focused on those derived from FL1 and FL2, i.e., FL1/PAL and FL2/PAL, respectively.

Table 2.1. Relative amounts of flavylium cation adsorbed, in μmol per g of PAL.

Initial FL/PAL ratio	**FL1**	**FL2**	**FL3**	**FL4**	**FL5**
50	40	24	12	< 0.1	< 1
75	59	29	7	< 0.1	9
100	67	31	19	< 0.1	3
125	72	33	12	< 0.1	14

2.3.2 X-Ray diffraction and N_2 adsorption isotherms

The powder X-ray diffractograms of FL1/PAL with the highest dye loading were indistinguishable from that of the raw PAL clay itself (Figure 2.S3 of the Supplementary Material), which was in turn the same as that published for the raw PFl-1 Source Clay (Chipera and Bish, 2001). This is an expected result since the dye loading was nonetheless still relatively low and the interlayer spacings of one-dimensional clays such as palygorskite are known to be fairly insensitive to the inclusion of organic molecules (Giustetto et al., 2014; Chang et al., 2016; Yang et al., 2018).

Table 2.2 shows the specific surface areas (S_{BET}) and total pore volumes (V_{tot}) of the FL1/PAL and FL2/PAL samples with the highest amounts of adsorbed dyed (72 and 33 μmol g^{-1}, respectively) and of a PAL reference sample exhaustively washed with methanol containing 1% 1.0 mol dm^{-3} HCl determined from N_2 adsorption isotherms by the BET (Brunauer et al., 1938) and BJH (Barrett et al., 1951) methods, respectively. Table 2.2 also indicates the surface areas of the micropores (S_{micro}), the external surface areas (S_{ext}), the micropore volumes (V_{micro}) and the sum of meso- and macropore volumes ($V_{meso+macro}$) estimated by the *t*-plot method (Lippens and de Boer, 1965). For FL1/PAL, the reduction in surface area was primarily due to the decrease in the external area S_{ext}, while FL2/PAL exhibited decreases in both the external and micropore surface areas and in the accessible pore volumes.

Table 2.2. Surface areas and pore volumes of acid-washed PAL, FL1/PAL = 72 and FL2/PAL = 33.

Sample	S_{BET} / m^2g^{-1}	S_{micro} / m^2g^{-1}	S_{ext} / m^2g^{-1}	V_{micro} / cm^3g^{-1}	$V_{meso+macro}$ / cm^3g^{-1}	V_{tot} / cm^3g^{-1}
PAL[a]	137	21	116	0.011	0.475	0.486
FL1/PAL	126	22	104	0.011	0.462	0.473
FL2/PAL	126	15	111	0.008	0.420	0.428

[a] after washing with HCl-acidified methanol.

2.3.3 Spectroscopic and photophysical studies

FTIR spectra of PAL clay and of the FL1 and FL2 derived hybrid pigments were recorded in the region from 4000 cm^{-1} to 500 cm^{-1} (Figure 2.S4 of the Supplementary Material). The raw clay exhibits absorption bands in the range 3000-3600 cm^{-1}, along with a band at 1654 cm^{-1}, corresponding respectively to the stretching and bending vibrations of water molecules (coordinated and zeolitic) (Frost et al., 2010; Giustetto and Wahyudi, 2011; Fan et al., 2014; Zhang et al., 2015b; Zhang et al., 2015c, 2015d). The region 3000-3600 cm^{-1} also includes contributions from the OH-stretching vibrations of Mg/Al-OH groups (Frost et al., 2010; Zhang et al., 2015a; Zhang et al., 2015d). The band at 3615 cm^{-1} corresponds to Al-OH stretching (Frost et al., 2010; Zhang et al., 2015b; Zhang et al., 2015d) and/or Si-OH stretching (Giustetto and Wahyudi, 2011). Bands in the range from 975 to 1196 cm^{-1} are attributed to Si-O vibrations (Frost et al., 2010; Zhang et al., 2015b; Zhang et al., 2015c) and the weak band at 797 cm^{-1} is characteristic of quartz impurities (Frost et al., 2010; Zhang et al., 2015b). In the infrared spectra of the FL/PAL samples, additional bands characteristic of FL cations were detected in the range of 1200-1600 cm^{-1} (Figure 2.1). In particular, the absorption bands at 1356 cm^{-1} and 1352 cm^{-1} for

FL1/PAL and FL2/PAL samples, respectively, correspond to C-O-C stretching. The intensities of the FL bands are quite weak because of the relatively small amount of flavylium cation in relation to clay and exhibit hypsochromic shifts compared to the FL cation salts, reflecting the interactions between FL and PAL.

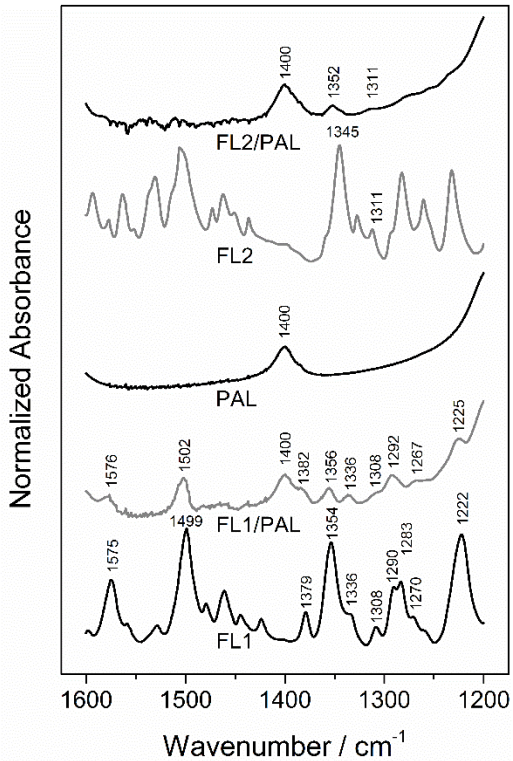

Figure 2.1. Infrared spectra of PAL, FL1, FL2, FL1/PAL (72 µmol) and FL2/PAL (33 µmol) in the range 1200-1600 cm^{-1}. Note: The broad peak at 1400 cm^{-1} is an impurity in the KBr used.

UV-vis absorption spectra of FL1 and FL2 in 1% 1.0 mol dm^{-3} HCl/methanol solution present absorption maxima at 478 and 465 nm, respectively (Figures 2.2a and b). The UV-vis-DR spectra of the hybrid pigments in the same Figures exhibit a small red shift from 478 nm to around 492 nm for FL1, and 465 nm to 470 nm for FL2. Spectral shifts of this type have been attributed to the effect of electrostatic interactions between organic molecules and the inorganic substrate (Kohno et al., 2008a, 2009) or to the acidity

of the inorganic substrate (Kohno et al., 2008b). Although aggregates are relatively common for the adsorption of dyes on clays (Valandro et al., 2015, 2017), the spectra did not present any evidence of the presence of FL aggregates, indicating that the washing step as part of the adsorption procedure efficiently removed excess FL cations that might participate in aggregate formation.

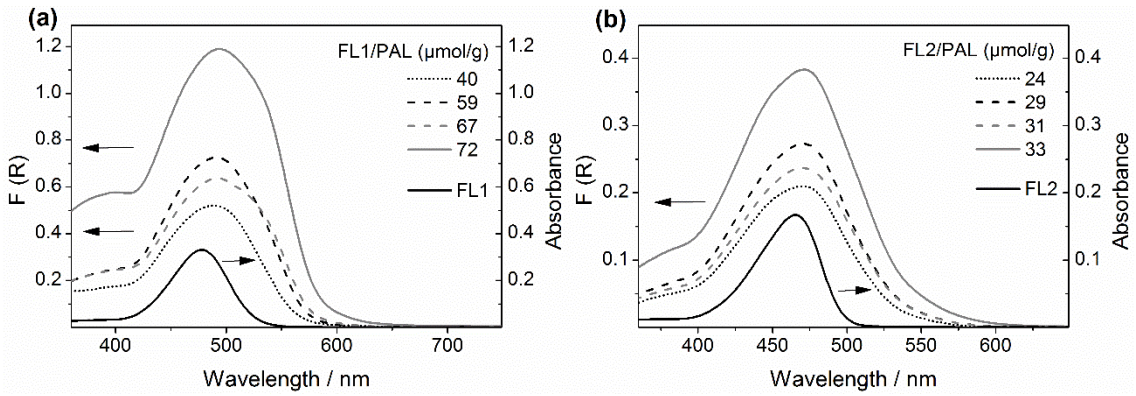

Figure 2.2. UV-vis and UV-vis-DR spectra (Kubelka-Munk mode) of (a) FL1 and FL1/PAL, and (b) FL2 and FL2/PAL samples.

Figure 2.3 shows the fluorescence excitation and emission spectra of the hybrid pigments FL1/PAL and FL2/PAL, together with those of FL1 and FL2 in 1% 1.0 mol dm^{-3} HCl/methanol solution. In 1% 1.0 mol dm^{-3} HCl/methanol solution, FL1 presented a broad fluorescence emission band with a maximum around 577 nm and FL2 a maximum at 509 nm. The corresponding fluorescence excitation spectra resemble the absorption spectra, with maxima at 487 and 468 nm for FL1 and FL2, respectively. The two hybrid pigments showed emission in the same region as the corresponding FL in solution. For FL2/PAL, the maximum fluorescence emission was at ca. 525 nm and did not shift significantly with increasing amount of adsorbed FL. For FL1/PAL, however, the fluorescence emission maximum underwent a red-shift from 577 to 600 nm with increasing amount of adsorbed FL1. In the case of Auramine O adsorbed on SYn-1 and

SAz-1 clays, a decrease in intensity and shift to longer wavelengths of the fluorescence emission with increasing dye adsorption was attributed to H-aggregate formation (Valandro et al., 2015). However, FL/PAL hybrid pigments exhibited no additional absorption bands of the type expected for J- or H-aggregates, suggesting that the apparent shift with increasing adsorbed FL1 is more likely a distortion of the emission spectrum due to reabsorption, i.e., to an inner filter effect. For both solid hybrid pigments, the front-face geometry emission intensity decreased as the amount of adsorbed flavylium cation increased (Figure 2.3), suggesting self-quenching.

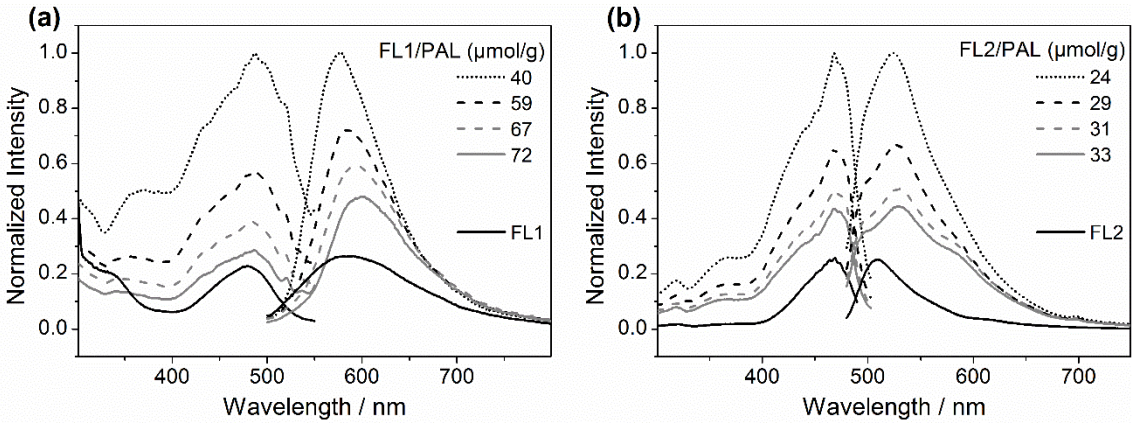

Figure 2.3. Excitation and emission spectra of (a) FL1 (Ex. 480 and Em. 576 nm) in 1% 1.0 mol dm^{-3} HCl/methanol solution and solid FL1/PAL (Ex. 470 and Em. 576 nm; adsorbed amounts of FL1 are indicated in μmol/g); (b) FL2 (Ex. 467 and Em. 508 nm) in 1% 1.0 mol dm^{-3} HCl/methanol solution and solid FL2/PAL (Ex. 467 and Em. 525 nm; adsorbed amounts of FL1 are indicated in μmol/g) samples.

Time-resolved emission measurements (405 nm excitation; 575 nm emission for FL1/PAL and 525 nm emission for FL2/PAL) indicated fast biexponential decay with lifetimes (± 15%) of FL1/PAL (0.35 and 1.0 ns with normalized preexponentials of ca.

0.8 and 0.2, respectively) about half those of FL2/PAL (0.6 and 2.0 ns with normalized preexponentials of ca. 0.6 and 0.4, respectively). Steady-state fluorescence anisotropies (*r*) ranged from 0.03-0.05 for FL1/PAL and 0.06-0.07 for FL2/PAL, apparently insensitive to the amount of adsorbed FL. Time-resolved anisotropy measurements showed an extremely fast initial depolarization, within ca. ≤ 100 ps, with a residual anisotropy at long times consistent with that found in the steady-state measurements. This suggests that fast intermolecular energy transfer or migration between FL molecules is the main mechanism responsible for the rapid loss of anisotropy and could also contribute to the decrease in fluorescence intensity with increasing amount of adsorbed flavylium cation.

Wide field true color fluorescence images (Figure 2.4) indicate a homogeneous distribution of adsorbed FL without differentiating between adsorption inside or on the edges of the channels, with the difference in intensities due largely to differences in the focal planes. In agreement with the red shift of the emission seen in the fluorescence spectra, the fluorescence color of the FL1/PAL particles changes with the amount of FL1 adsorbed, as can be seen in Figure 2.4. Images recorded by confocal fluorescence microscopy using false-color mapping are shown in Figure 2.S5 of the Supplementary Material. Although these images indicate that the particles are not homogeneous in size or shape, all are strongly fluorescent, with the highest intensities in the regions of the focal plane around the particle core. Unfortunately, the dye loadings were much too high to make single-molecule measurements on isolated particles or fibers (Martínez-Martínez et al., 2011).

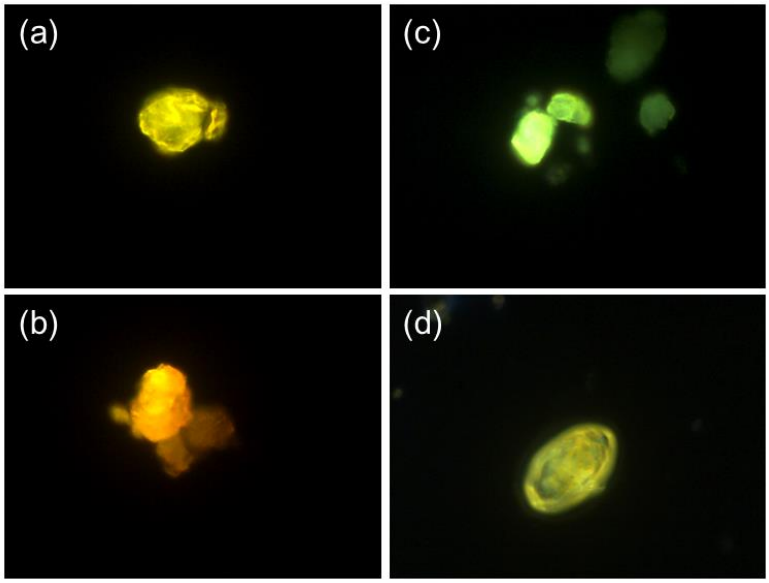

Figure 2.4. True color wide-field fluorescence images of the hybrid pigments with a nominal horizontal field of view of 150 μm. FL1/PAL = 40 μmol/g (a) and 72 μmol/g (b); FL2/PAL = 24 μmol/g (c) and 33 μmol/g (d).

2.3.4 Stability tests of the hybrid pigments

Resistance of the adsorbed dye to extraction with organic solvent and acid is, in essence, intrinsic to the method of preparation of the hybrid pigments. Thus, the flavylium dissolved in acidic methanol were allowed to adsorb by contact with the clay and the resultant materials then washed exhaustively with acidic methanol to remove any readily extractable dye. Although the dyes are also highly soluble in water, water did not extract the dye from either FL1/PAL or FL2/PAL.

The photochemical stability of flavylium cations is usually much better than their thermal stability. Indeed, both the solid pigments and the hybrid pigments showed good photostability, with the color being essentially unaltered by irradiation for 6 h in a solar UV simulator. Thus, adsorption of the dyes onto the clay does not markedly reduce their photostability. On the other hand, there was substantial improvement in the thermal

stability of both FL1 and FL2 adsorbed on palygorskite, as has been reported for flavylium cations adsorbed on other types of clay (Kohno et al., 2007, 2010) or protonated zeolites (Kohno et al., 2008a). A temperature of 120 ^{o}C. was chosen for the thermal stability tests since temperatures up to 120-150 ^{o}C have been used for the thermal analysis sepiolite/indigo and PAL/indigo hybrid materials (Hubbard et al., 2003) and, in the case of PAL (Guggenheim and Koster van Gross, 2001), this temperature is just above the range where most of the weakly adsorbed water has been lost and where the more strongly adsorbed water only begins to be lost. Thus, while both FL1 and FL2 degraded substantially in < 2 h at this temperature in a vacuum oven, both hybrid pigments largely retained their characteristic colors after 24 h under these conditions (Figure 2.5 and Figures 2.S6-S7 and Tables 2.S1 and 2.S2 of the Supplementary Material).

Figure 2.5. Photographs of FL1 (upper) and FL2 (lower) after heating at 120 ^{o}C for 2 h and photographs of the corresponding hybrid pigments (FL1/PAL = 72 and FL2/PAL = 33) after heating at 120 °C for 24h

In aqueous solution, both FL1 and FL2 undergo hydration above about pH 3 to form the hemiacetal (B), followed by ring-opening tautomerization to form the *cis*-chalcone (ZC) and then slow isomerization to the *trans*-chalcone (EC) (Held et al., 2016). The 7-hydroxy group of FL2 can also deprotonate at slightly higher pH, resulting in the conjugate base (A); the corresponding equilibria are shown for FL2 in Scheme 2.S1 of

the Supplementary Material. Spectra of FL1 or FL2 registered after 1 h in pH = 8.5 phosphate buffer solution and of the hybrid pigments after immersion for 24 h in pH = 9 phosphate buffer solution are shown in Figure 2.6. For FL1 a new band appeared around 380 nm corresponding to a mixture of B, ZC and EC, while FL2 presented two new bands, one at around 490 nm assigned to a conjugate base formed by deprotonation of the hydroxyl group of one or more of the species resulting from the hydration-induced equilibria. The spectra of FL1/PAL and FL2/PAL also showed two bands at longer wavelength, one in the region of the adsorbed cation and the other in the same regions as FL1 and FL2 in solution at similar alkaline pH.

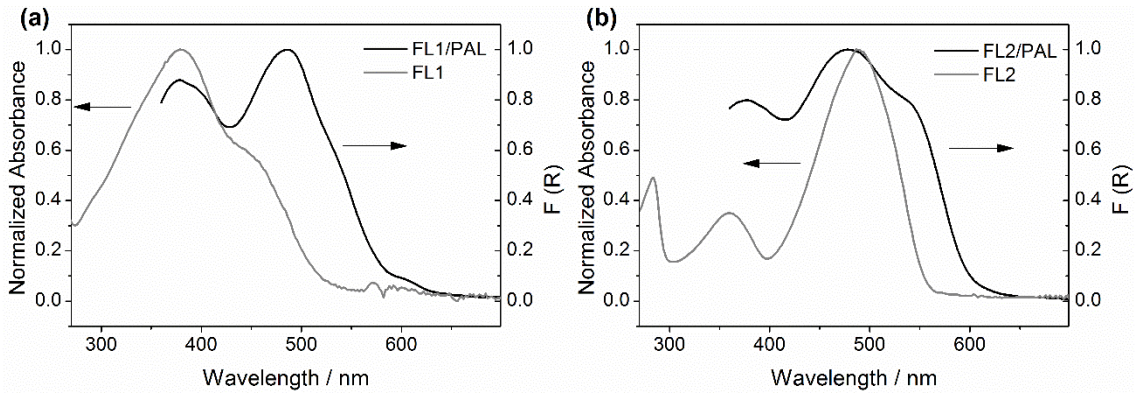

Figure 2.6. Absorbance and diffuse reflectance spectra (Kubelka-Munk mode) for (a) FL1 and FL1/PAL and (b) FL2 and FL2/PAL. The absorbance spectra were collected for FL1 and FL2 incubated for 1 h in pH 8.5 solution, and the UV-vis-DR spectra were collected after FL1/PAL and FL2/PAL were immersed for 24 h in pH 9 solution, centrifuged and dried.

Figure 2.S8 of the Supplementary Material illustrates the impact of the basic aqueous medium on the color of the hybrid pigments before and after immersion at pH 9 and Table 2.S3 of the Supplementary Material shows the CIELAB color coordinate data. Although the color of FL1/PAL became less intense upon immersion in pH 9 aqueous

solution, it still showed an attractive color compared to FL1 at the same pH, indicating that the adsorption process made it less prone to hydration. However, FL2/PAL changed color completely, indicating that the adsorption process did not prevent deprotonation of a significant fraction of the adsorbed FL2 molecules. In both cases, the dye did not leach from the clay and the color changes were reversible upon acidification of the medium, indicating chemical stability under these conditions.

2.3.5 The dye-clay interaction

Since flavylium cations are highly soluble in methanol, the exhaustive washing with acidic methanol should remove any excess or weakly physiosorbed dye, leaving only strongly bound dye. This points to ion exchange as potentially the most important mode of interaction of these cationic dyes with palygorskite. In this regard, the final amounts of the flavylium cations adsorbed (Table 2.1) were all well below the cation exchange capacity (CEC) values reported for the PFl-1 Source Clay palygorskite utilized in this work: 175 (Borden and Giese, 2001) and 165 (Li et al., 2003) and, after a partial purification, 140 μmol g^{-1} (Shariatmadari et a., 1999). Nonetheless, because all five of the initially tested dyes are cationic, ion exchange alone cannot explain the marked differences in affinity for the clay. Thus, the presence of a methyl group at the 4 position of the flavylium chromophore of FL3 and FL5 substantially reduced the net adsorption and, in the case of FL4, the presence of an additional hydroxyl group at position 5 of the chromophore completely eliminated its adsorption after washing (Table 2.1). Indeed, as shown in Figure 2.7, the additional methyl group makes these compounds too wide to insert into the tunnels or external grooves of PAL. However, the two compounds without the 4-methyl group could insert partially, though not totally into the tunnels and/or

interact with the open grooves on the external surface. Because FL2 is slightly smaller than FL1, it should fit into the tunnels somewhat better than FL1. This is consistent with the surface area and pore volume measurements (Table 2.2), which suggest a preference of FL1 for the external grooves and of FL2 for both external grooves and partial insertion into tunnels.

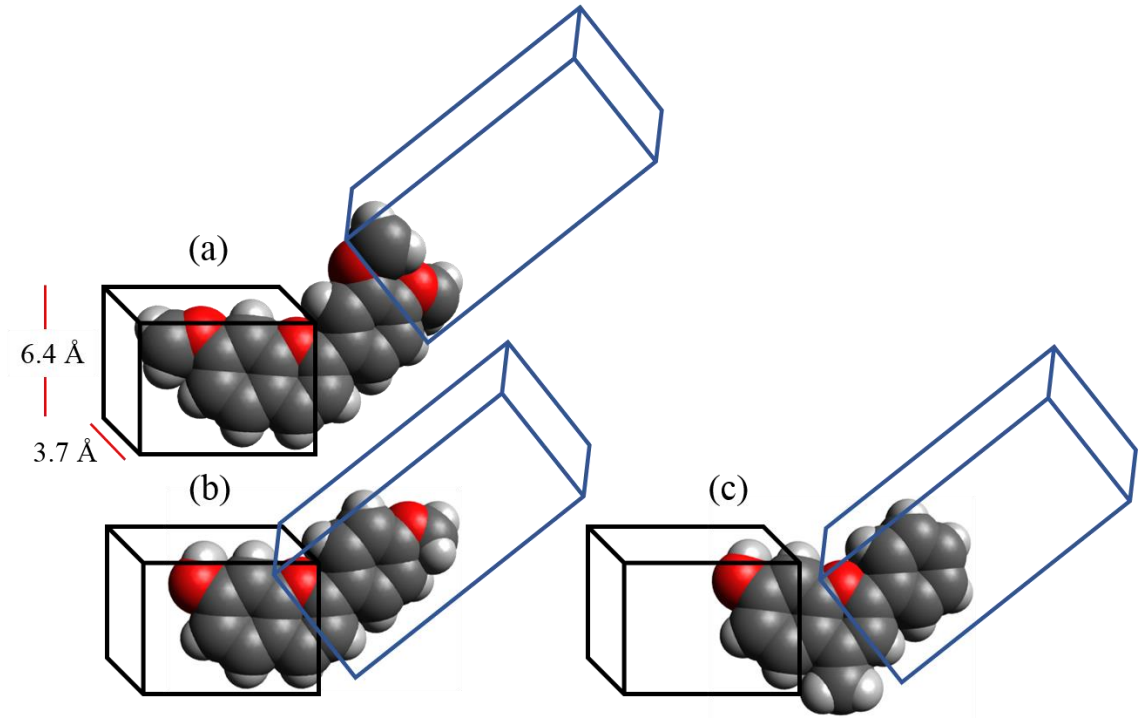

Figure 2.7. Comparison of the molecular sizes of (a) FL1, (b) FL2 and (c) FL3 with the dimensions of the tunnels of palygorskite (Brigatti et al., 2006).

Several studies have shown that the cationic form of anthocyanins and flavylium ions can be selectively stabilized aqueous solution by incorporating them into anionic micelles (Lima et al., 2002; Quina et al., 2009) or by inclusion in supramolecular complexes (Held et al., 2016). Because the apparent hydration constant of FL1 (pK_h, or the pH at which half of the cation form is hydrated) is 3.0 ± 0.3 (Held et al., 2016), solutions of FL1 in acetate buffer at pH 4, 5 or 6 are nearly colorless (Figures 2.S9-2.S11

of the Supplementary Material), reflecting the almost complete conversion of the flavylium cation form of FL1 to the hydrated species. Upon addition of PAL to these solutions, the suspended clay gradually acquired the red color of the adsorbed FL1 cation as a function of time, indicating the conversion of the hydrated forms in solution to the adsorbed cationic form on the clay. If only the cationic form adsorbed from solution onto the clay, there should be a clear difference in the apparent rates of adsorption at these three distinct pH values due to the large pH-dependent differences in the equilibrium concentration of this form. However, the rates of appearance of the coloration were qualitatively very similar at pH 4 and pH 5, but clearly much faster than at pH 6. Likewise, the maximum intensity of the color at long times (2 weeks) was similar for the two lower pH values, and much more intense than at pH 6 (Figures 2.S9-2.S11 of the Supplementary Material). Indeed, this strongly suggests that it is the hydrated forms that adsorb on PAL under these conditions and that they are subsequently converted to the cationic form by interaction with the more highly acidic sites of the clay with effective pK_a around pH 5-5.5 (*vide supra*).

4. Conclusions

Simple electrostatic interactions are incompatible with the observed differences in adsorption of FL cations on PAL. The adsorption was particularly inefficient for FL cations bearing a 4-methyl group, consistent with steric inhibition of interaction with the palygorskite tunnels or external grooves as the major contributor to differences in adsorption. Adsorption on PAL stabilized the cationic form of the flavylium cations FL1 and FL2 against hydration to at least pH 5, apparently reflecting the participation of the more highly acidic sites on the PAL surface. The photochemical stability was retained

and the chemical and thermal stabilities of the cation form of FL1 and FL2 were substantially improved by adsorption on PAL, pointing to flavylium cations of this type as promising chromophores for the development of novel fluorescent hybrid pigments with attractive colors.

Supplementary Material

Figures

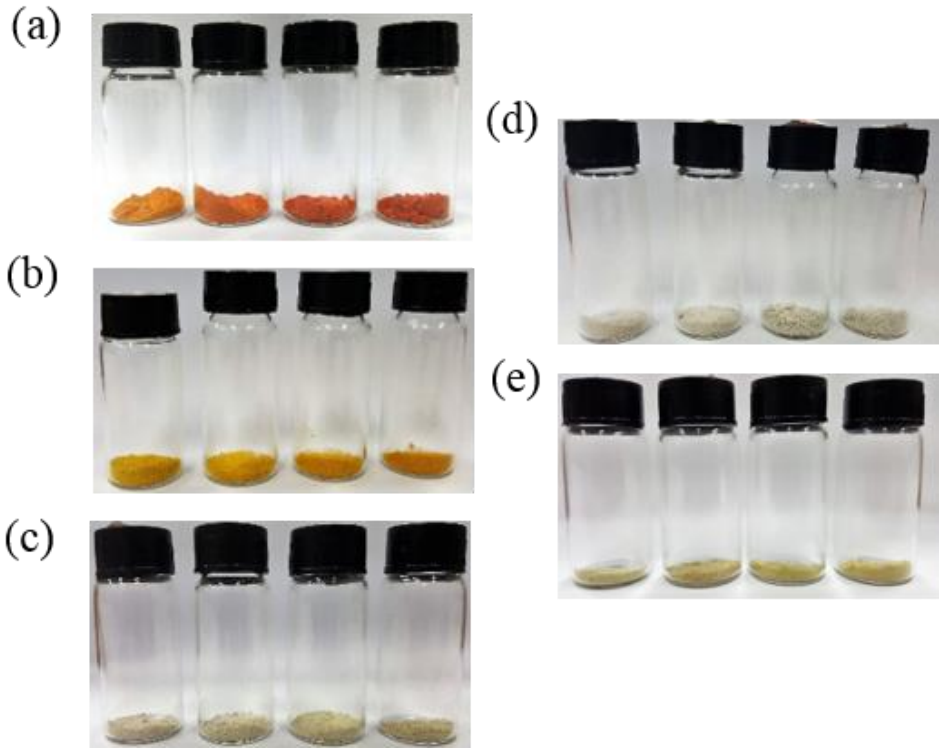

Figure 2.S1 Digital images of the hybrid pigments obtained. (a) From FL1; (b) From FL2; (c) From FL3; (d) From FL4 and (e) from FL5. The FL/PAL ratios increase from left to right (from 0.050 to 0.125 mmol of initially added FL per 1 g of PAL).

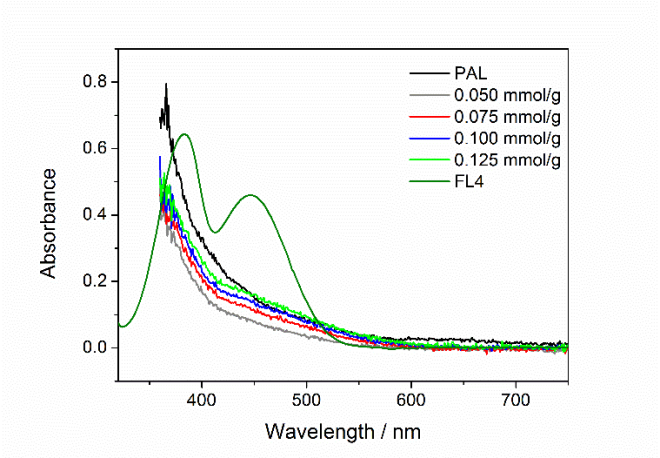

Figure 2.S2. Absorption spectrum of FL4 and UV-vis-DR spectra of PAL and the hybrid pigments at the initial FL4/PAL ratios indicated.

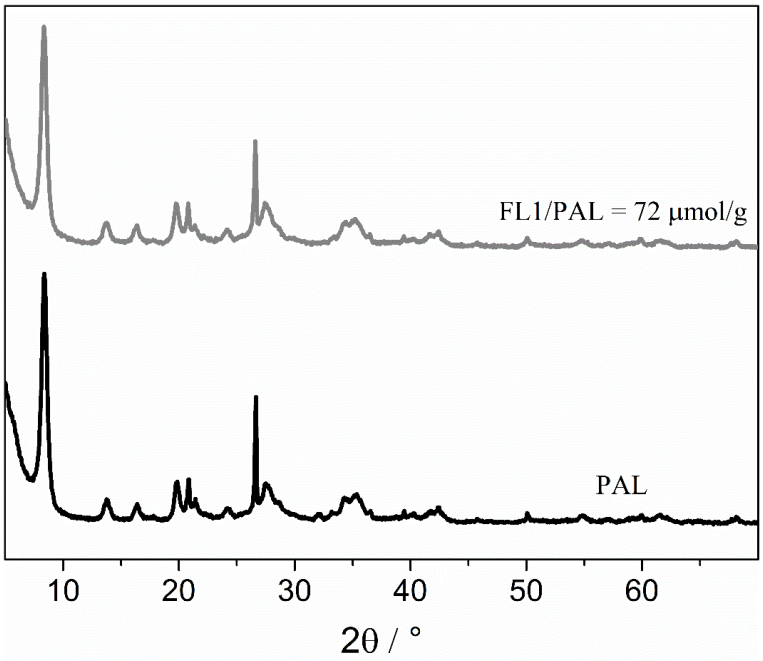

Figure 2.S3. Powder X-ray diffractograms of PAL and FL1/PAL.

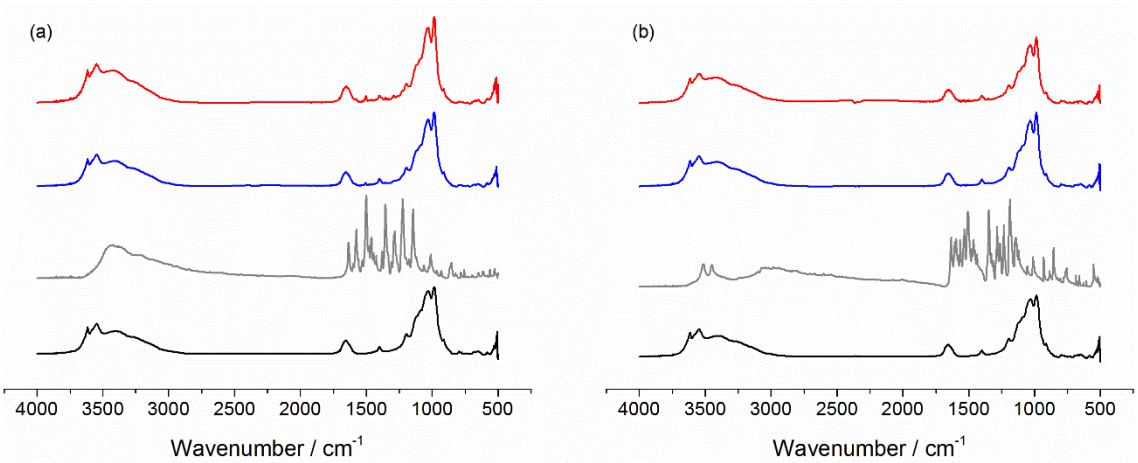

Figure 2.S4. Infrared spectra of PAL and the hybrid pigments in the range 4000-500 cm^{-1}. (a) PAL (black); FL1 (gray); FL1/PAL 40 and 72 µmol/g (blue and red). (b) PAL (black); FL2 (gray); FL2/PAL 24 and 33 µmol/g (blue and red).

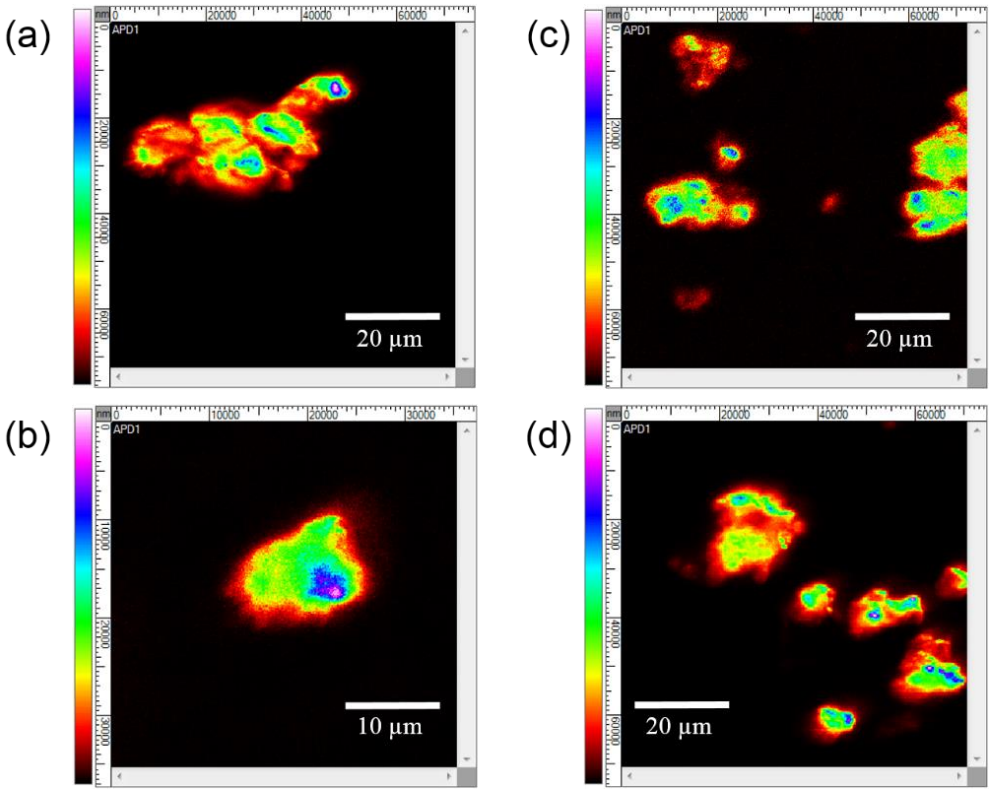

Figure 2.S5. False color confocal fluorescence images of the hybrid pigments. FL1/PAL = 40 µmol/g (a) and 72 µmol/g (b); FL2/PAL = 24 µmol/g (c) and 33 µmol/g (d).

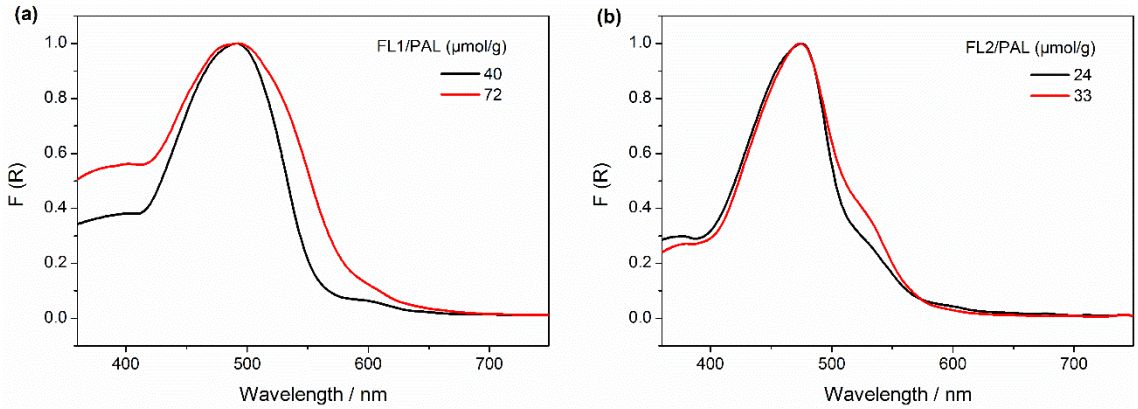

Figure 2.S6. Diffuse reflectance spectra of the hybrid pigments after heating at 120 °C for 24h: (a) FL1/PAL and (b) FL2/PAL.

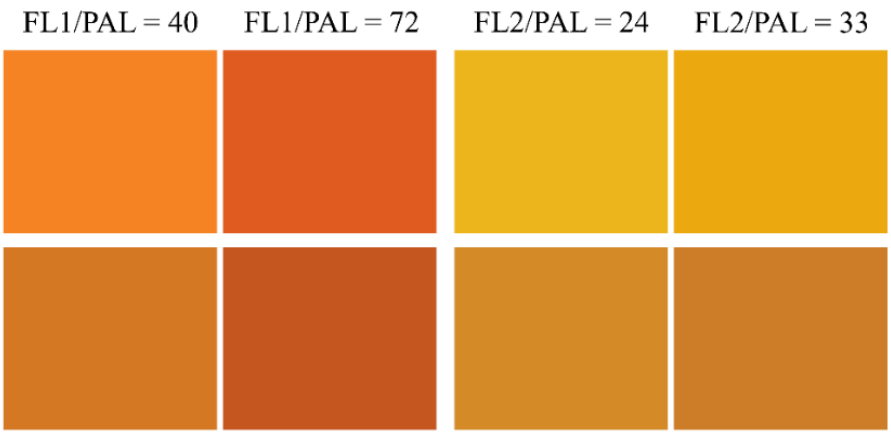

Figure 2.S7. Images of the colors from CIELAB (1931) color coordinate data for the hybrid pigments FL/PAL (μmol/g) before (top) and after (bottom) heating at 120 °C for 24h.

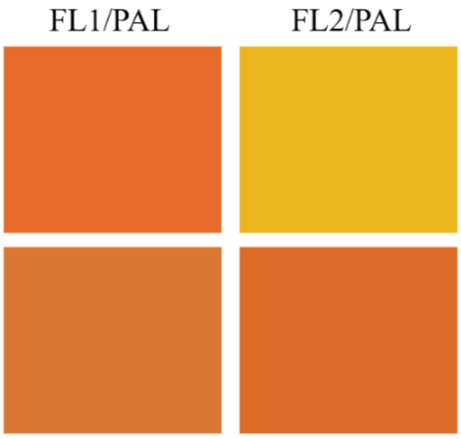

Figure 2.S8. Images of the colors from CIELAB (1931) color coordinate data for the hybrid pigments before (top) and after immersion in pH 9 solution (bottom).

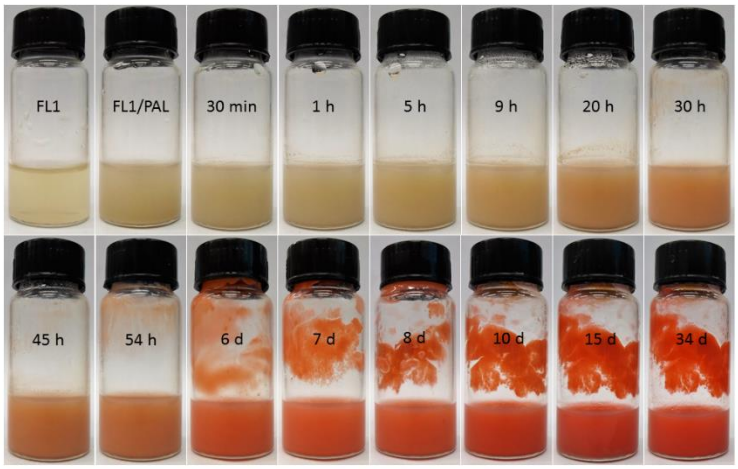

Figure 2.S9. Images of FL1 and the mixture of FL1 and PAL as a function of time at pH 4.

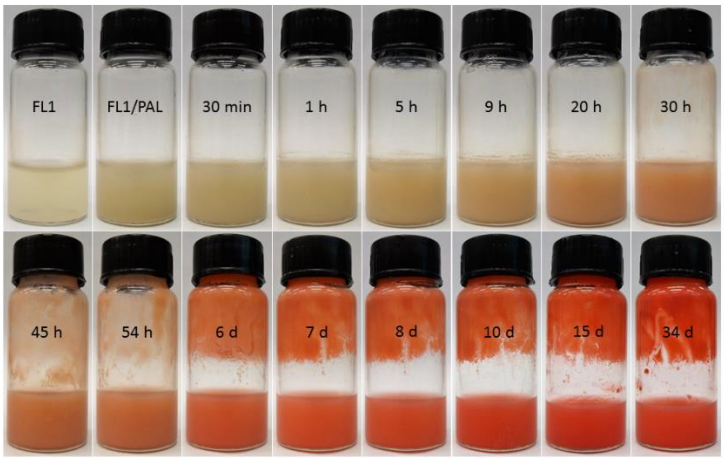

Figure 2.S10. Images of FL1 and the mixture of FL1 and PAL as a function of time at pH 5.

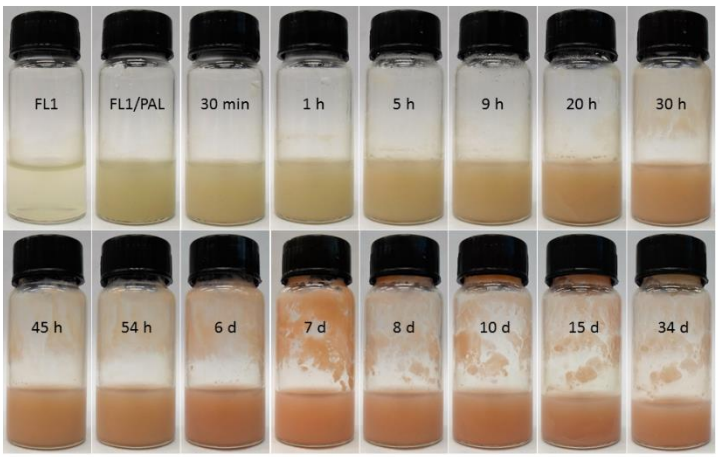

Figure 2.S11. Images of FL1 and the mixture of FL1 and PAL as a function of time at pH 6.

Schemes

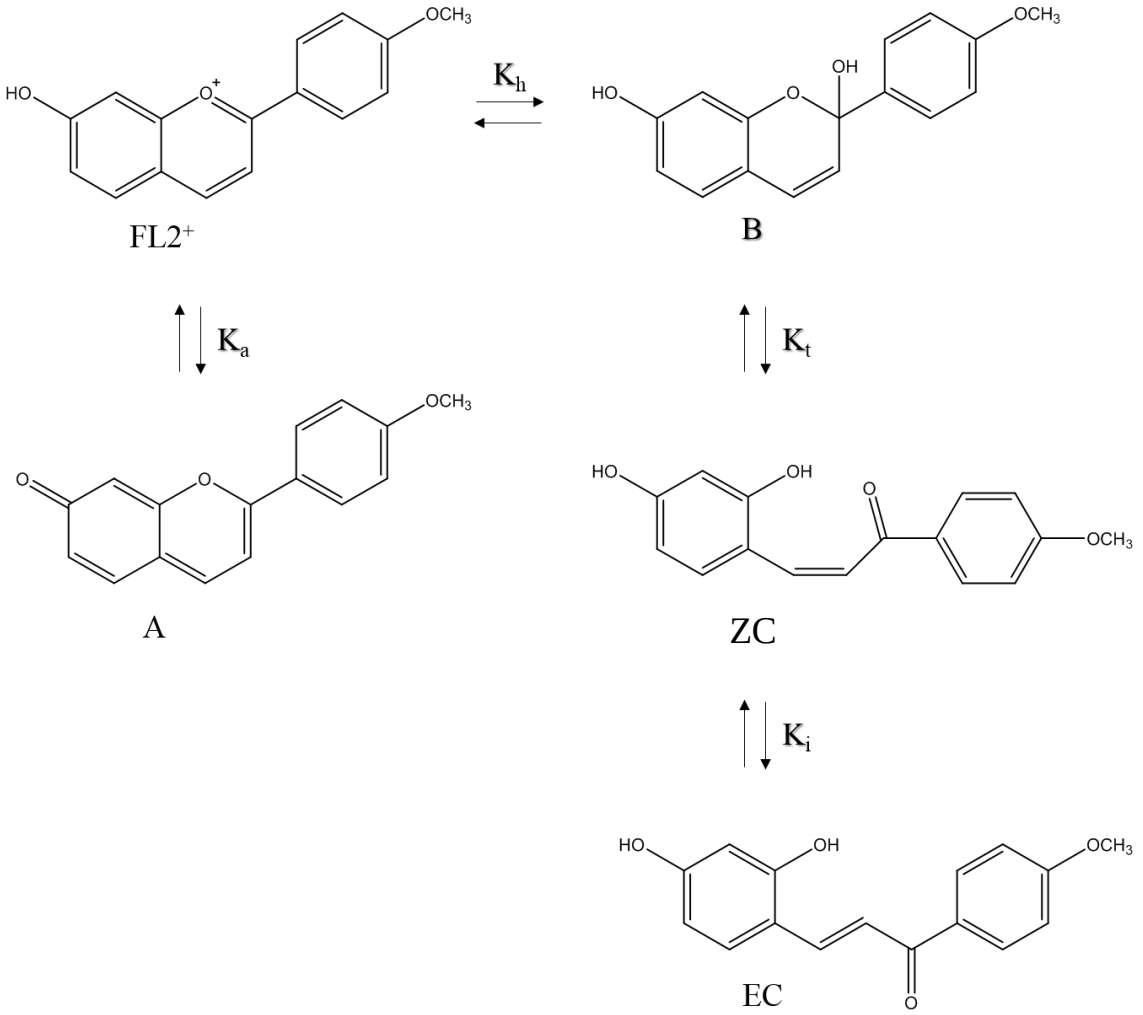

Scheme 2.S1. pH-dependent multiequilibria of FL2 in aqueous solution, including deprotonation (K_a) to form the conjugate base (**A**), hydration (K_h) to form the hemiketal (**B**) and subsequent ring-opening tautomerization (K_t) to form the *cis*-chalcone (**ZC**) and isomerization (K_i) to the *trans*-chalcone (**EC**).

Tables

Table 2.S1. CIELAB color coordinates for the hybrid pigments before heating.

Samples	L*	a*	b*
FL1/PAL = 40	66.5246	40.1775	66.7167
FL1/PAL = 72	55.8438	50.5605	58.3429
FL2/PAL = 24	77.4972	12.1733	75.3793
FL2/PAL = 33	73.6264	17.4510	79.0872

Table 2.S2. CIELAB color coordinates for the hybrid pigments after heating at 120 °C for 24h.

Heated Samples	L*	a*	b*
FL1/PAL = 40	59.5868	32.5089	59.1578
FL1/PAL = 72	51.1756	43.4934	52.4811
FL2/PAL = 24	64.0634	22.6563	60.5227
FL2/PAL = 33	60.3541	28.2977	56.6914

Table 2.S3. CIELAB color coordinates for the hybrid pigments before and after immersed in pH 9 aqueous solution.

Samples	L*	a*	b*
FL1/PAL	59.9179	45.5669	57.9132
FL1/PAL (pH = 9)	60.6742	36.8762	53.3205
FL2/PAL	77.4972	12.1733	75.3793
FL2/PAL (pH = 9)	58.5622	41.7290	55.5043

References

Acebal, S.G., Vico, L.I., 2017. Acid-Base Properties of Aqueous Suspensions of Homoionic Sepiolite and Palygorskite. Nat. Resour. 8, 432–444. https://doi.org/10.4236/nr.2017.86028

Arnold, E., Branden, J., 2008. The first direct evidence for the production of Maya Blue: rediscovery of a technology. Antiquity 82, 151–164. https://doi.org/10.1017/S0003598X00096514

Barrett, E. P., Joyner, L. G., Halenda, P. P. 1951. The Determination of Pore Volume and Area Distributions in Porous Substances. I. Computations from Nitrogen Isotherms. J. Am. Chem. Soc. 73, 373-380. https://doi.org/10.1021/ja01145a126

Borden, D., Giese, R. F. 2001. Baseline studies of the Clay Minerals Society source clays: Cation exchange capacity measurements by the ammonia-electrode method. Clays Clay Miner. 49, 444-445. https://doi.org/10.1346/CCMN.2001.0490510

Boudriche, L., Calvet, R., Chamayou, A., Hamdi, B., Balard, H., 2015. Removal of lead(II) from aqueous solution using modified palygorskite, contribution of inverse gas chromatography. J. Chromatogr. A 1408, 207-216. https://doi.org/10.1016/j.chroma.2015.07.011

Brigatti, M.F., Galan, E., Theng, B.K.G., 2006. Structures and Mineralogy of Clay Minerals, in: Chapter 2, Handbook of Clay Science, Developments in Clay Science. pp. 19–86. https://doi.org/10.1016/S1572-4352(05)01002-0

Brunauer, S., Emmett, P. H., Teller, E., 1938. Adsorption of Gases in Multimolecular Layers**.** J. Am. Chem. Soc. 60, 309-319. https://doi.org/10.1021/ja01269a023

Castañeda-Ovando, A., Pacheco-Hernández, M. de L., Páez-Hernández, M.E., Rodríguez, J.A., Galán-Vidal, C.A., 2009. Chemical studies of anthocyanins: A review. Food Chem. 113, 859–871. https://doi.org/10.1016/j.foodchem.2008.09.001

Cavalcanti, R.N., Santos, D.T., Meireles, M.A.A., 2011. Non-thermal stabilization mechanisms of anthocyanins in model and food systems-An overview. Food Res. Int. 44, 499–509. https://doi.org/10.1016/j.foodres.2010.12.007

Chang, P.-H., Jiang, W.-T., Li, Z., Kuo, C.-Y., Wu, Q., Jean, J. S., Lv, G. 2016. Interaction of ciprofloxacin and probe compounds with palygorskite PFL-1. J. Hazard. Mater. 303, 55-63. https://doi.org/10.1016/j.hazmat.2015.10.012

Chiari, G., Giustetto, R., Druzik, J., Doehne, E., Ricchiardi, G., 2008. Pre-columbian nanotechnology: Reconciling the mysteries of the maya blue pigment. Appl. Phys. A Mater. Sci. Process. 90, 3–7. https://doi.org/10.1007/s00339-007-4287-z

Chipera, S. J., Bish, D. L. 2001. Baseline studies of the Clay Minerals Society Source Clays: Powder X-ray diffraction analysis. Clays Clay Miner. 49, 398-409.

Dejoie, C., Martinetto, P., Dooryhée, E., Strobel, P., Blanc, S., Bordat, P., Brown, R., Porcher, F., Sanchez Del Rio, M., Anne, M., 2010. Indigo@silicalite: A new

organic-inorganic hybrid pigment. ACS Appl. Mater. Interfaces 2, 2308–2316. https://doi.org/10.1021/am100349b

Dogan, A. U., Dogan, M., Onal, M., Sarikaya, Aburub, A., Wurster, D. E. 2006. Baseline studies of the Clay Minerals Society Source Clays: Specific surface area by the Brunauer Emmett Teller (BET) method. Clays Clay Miner. 54, 62-66.

Doménech, A., Doménech-Carbó, M.T., Edwards, H.G.M., 2011. On the interpretation of the Raman spectra of Maya Blue: A review on the literature data. J. Raman Spectrosc. 42, 86–96. https://doi.org/10.1002/jrs.2642

Fan, L., Zhang, Y., Zhang, J., Wang, A., 2014. Facile preparation of stable palygorskite/cationic red X-GRL@SiO_2 "Maya Red" pigments. RSC Adv. 4, 63485–63493. https://doi.org/10.1039/C4RA13739F

Ferreira da Silva, P., Lima, J. C., Freitas, A. A., Shimizu, K., Maçanita, A. L., Quina, F. H., 2005. Charge-transfer complexation as a general phenomenon in the copigmentation of anthocyanins. J. Phys. Chem. A 109, 7329–7338. https://doi.org/10.1021/jp052106s

Ferreira, A. P. G., Frederice, R., Janssen, K. P. F., Gehlen, M. H., 2011. Dually fluorescent silica nanoparticles. J. Lumin. 131, 888–893. https://doi.org/10.1016/j.jlumin.2010.12.019

Freitas, A. A, Maçanita, A. A. L., Quina, F.H., 2013. Improved analysis of excited state proton transfer kinetics by the combination of standard and convolution methods. Photochem. Photobiol. Sci. 12, 902–10. https://doi.org/10.1039/c3pp25445c

Frini-Srasra, N., Srasra, E., 2008. Determination of Acid-Base Properties of HCl Acid Activated Palygorskite by Potentiometric Titration. Surf. Eng. Appl. Electrochem. 44, 401–409. https://doi.org/10.3103/S1068375508050116

Frost, R.L., Xi, Y., He, H., 2010. Synthesis, characterization of palygorskite supported

zero-valent iron and its application for methylene blue adsorption. J. Colloid Interface Sci. 341, 153–161. https://doi.org/10.1016/j.jcis.2009.09.027

Gago, S., Pessêgo, M., Laia, C.A.T., Parola, A.J., 2017. pH-Tunable Fluorescence and Photochromism of a Flavylium-Based MCM-41 Pigment. ACS Omega 2, 122–126. https://doi.org/10.1021/acsomega.6b00381

Gilchrist, A., Nobbs, J. 1999. Colorimetry, Theory. In Encyclopedia of Spectroscopy and Spectrometry, Second Ed. (2010), J. Lindon, G. Tranter, D. Koppenaal, Eds. - Academic Press, NY; pp. 380-385.

Giustetto, R., Wahyudi, O., 2011. Sorption of red dyes on palygorskite: Synthesis and stability of red/purple Mayan nanocomposites. Microporous Mesoporous Mater. 142, 221–235. https://doi.org/10.1016/j.micromeso.2010.12.004

Giustetto, R., Llabrés I Xamena, F.X., Ricchiardi, G., Bordiga, S., Damin, A., Gobetto, R., Chierotti, M.R., 2005. Maya blue: A computational and spectroscopic study. J. Phys. Chem. B 109, 19360–19368. https://doi.org/10.1021/jp048587h

Giustetto, R., Levy, D., Wahyudi, O., Chiari, G., 2006. Crystal structure refinement of Maya Blue pigment prepared with deuterated indigo, using neutron powder diffraction. Eur. J. Mineral. 18, 629–640. https://doi.org/10.1127/0935-1221/2006/0018-0629

Giustetto, R., Levy, D., Wahyudi, O., Ricchiardi, G., Vitillo, J.G., 2011. Crystal structure refinement of a sepiolite/indigo Maya Blue pigment using molecular modelling and synchrotron diffraction. Eur. J. Mineral. 23, 449–466. https://doi.org/10.1127/0935-1221/2011/0023-2105

Giustetto, R., Vitillo, J.G., Corazzari, I., Turci, F., 2014. Evolution and reversibility of host/guest interactions with temperature changes in a methyl red@palygorskite polyfunctional hybrid nanocomposite. J. Phys. Chem. C 118, 19322–19337.

https://doi.org/10.1021/jp4091238

Guggenheim, S., Koster van Groos, A. F. 2001. Baseline studies of the Clay Minerals Society Source Clays: Thermal Analysis. Clays Clay Miner. 49, 433-443. https://doi.org/10.1346/CCMN.2001.0490507

Held, B., Tang, H., Natarajan, P., da Silva, C.P., Silva, V. O., Bohne, C., Quina, F.H., 2016. Cucurbit[7]uril inclusion complexation as a supramolecular strategy for color stabilization of anthocyanin model compounds. Photochem. Photobiol. Sci. 15, 752–757. https://doi.org/10.1039/C6PP00060F

Hubbard, B., Kuang, W., Moser, A., Facey, G. A., Detellier, C. 2003. Structural study of Maya blue: textural, thermal and solid state multinuclear magnetic resonance characterization of the palygorskite-indigo and sepiolite-indigo adducts. Clays Clay Miner. 51, 318-326.

Kim, M. H., Choi, G., Elzatahry, A., Vinu, A. Choy, Y. B., Choy, J.-H., 2016. Review of clay-drug hybrid materials for biomedical applications: administration routes. Clays Clay Miner. 64, 115-130. https://doi.org/10.1346/CCMN.2016.0640204

Kohno, Y., Hoshino, R., Matsushima, R., Tomita, Y., Kobayashi, K., 2007. Stabilization of Flavylium Dyes by Incorporation in the Clay Interlayer. J. Jpn. Soc. Colour Mater. 80, 6–12. https://doi.org/https://doi.org/10.4011/shikizai1937.80.6

Kohno, Y., Shibata, Y., Oyaizu, N., Yoda, K., Shibata, M., Matsushima, R., 2008a. Stabilization of flavylium dye by incorporation into the pore of protonated zeolites. Microporous Mesoporous Mater. 114, 373–379. https://doi.org/10.1016/j.micromeso.2008.01.023

Kohno, Y., Tsubota, S., Shibata, Y., Nozawa, K., Yoda, K., Shibata, M., Matsushima, R., 2008b. Enhancement of the photostability of flavylium dye adsorbed on mesoporous silicate. Microporous Mesoporous Mater. 116, 70–76.

https://doi.org/10.1016/j.micromeso.2008.03.014

Kohno, Y., Kinoshita, R., Ikoma, S., Yoda, K., Shibata, M., Matsushima, R., Tomita, Y., Maeda, Y., Kobayashi, K., 2009. Stabilization of natural anthocyanin by intercalation into montmorillonite. Appl. Clay Sci. 42, 519–523. https://doi.org/10.1016/j.clay.2008.06.012

Kohno, Y., Hoshino, R., Ikoma, S., Shibata, M., Matsushima, R., Tomita, Y., Maeda, Y., Kobayashi, K., 2010. Stabilization of Flavylium Dye by Incorporation into Bentonite Clay. J. Jpn. Soc. Colour Mater. 83, 103–107. https://doi.org/https://doi.org/10.4011/shikizai.83.103

Kohno, Y., Senga, M., Shibata, M., Yoda, K., Matsushima, R., Tomita, Y., Maeda, Y., Kobayashi, K., 2011. Stabilization of flavylium dye by incorporation into Fe-containing mesoporous silicate. Microporous Mesoporous Mater. 141, 77–80. https://doi.org/10.1016/j.micromeso.2010.11.004

Kohno, Y., Kato, Y., Shibata, M., Fukuhara, C., Maeda, Y., Tomita, Y., Kobayashi, K., 2015. Enhanced stability of natural anthocyanin incorporated in Fe-containing mesoporous silica. Microporous Mesoporous Mater. 203, 232–237. https://doi.org/10.1016/j.micromeso.2014.10.042

Laguna, H., Loera, S., Ibarra, I.A., Lima, E., Vera, M.A., Lara, V., 2007. Azoic dyes hosted on hydrotalcite-like compounds: Non-toxic hybrid pigments. Microporous Mesoporous Mater. 98, 234–241. https://doi.org/10.1016/j.micromeso.2006.09.009

Lakowicz, J. R. 2006. Principles of Fluorescence Spectroscopy, 3rd edition, Springer, New York; pp. 353-412.

Lauer, M.H., Gehlen, M.H., De Jesus, K., Berlinck, R.G.S., 2014. Fluorescence spectroscopy and confocal microscopy of the mycotoxin citrinin in condensed phase and hydrogel films. J. Fluoresc. 24, 745–750. https://doi.org/10.1007/s10895-013-

1347-y

Li, Z., Willms, C. A., Kniola, K. 2003. Removal of anionic contaminants using surfactant-modified palygorskite and sepiolite. Clays Clay Miner., 51, 445-451.

Lima E, Martinez-Ortiz MJ, Fregoso E, Mendez-Vivar J. 2007. Capturing natural chromophores on natural and synthetic aluminosilicates. Stud. Surf. Sci. Catal. 170, 2110-2115. https://doi.org/10.1016/S0167-2991(07)81107-4

Lima, E., Guzmán, A., Vera, M., Rivera, J.L., Fraissard, J., 2012. Aged natural and synthetic Maya Blue-like pigments: What difference does it make? J. Phys. Chem. C 116, 4556–4563. https://doi.org/10.1021/jp207602m

Lima, J. C., Vautier-Giongo, C., Lopes, A., Melo, E., Quina, F. H., Maçanita, A. L. 2002. Color Stabilization of Anthocyanins: Effect of SDS Micelles on the Acid−Base and Hydration Kinetics of Malvidin 3-Glucoside (Oenin). J Phys. Chem. A, 106, 5851-5859. https://doi.org/10.1021/jp014081c

Lin, Y.H., Hori, Y., Hoshino, S., Miyazawa, C., Kohno, Y., Shibata, M., 2014. Fluorescent colored material made of clay mineral and phycoerythrin pigment derived from seaweed. Dye. Pigment. 100, 97–103. https://doi.org/10.1016/j.dyepig.2013.08.022

Lippens, B. C., de Boer, J. H. 1965. Studies on pore systems in catalysts: V. The *t* method. J. Catal. 4, 319-323. https://doi.org/10.1016/0021-9517(65)90307-6

Madejová, J., Komadel, P. 2001. Baseline studies of the Clay Minerals Society Source Clays: Infrared methods. Clays Clay Miner. 49, 410-432.

Martínez-Martínez, V., Corcóstegui, C., Prieto, J. B., Gartzia, L., Sallares, S., Arbeloa, I. L. 2011. Distribution and orientation study of dyes intercalated into single sepiolite fibers. A confocal fluorescence microscopy approach. J. Mater. Chem. 21, 269-276. https://doi.org/10.1039/c0jm02211j

Mermut, A.R., Cano, A. F. 2001. Baseline studies of the Clay Minerals Society Source Clays: Chemical analyses of major elements. Clays Clay Miner. 49, 381-386.

Mu, B., Wang, A., 2016. Adsorption of dyes onto palygorskite and its composites: A review. J. Environ. Chem. Eng. 4, 1274–1294. https://doi.org/10.1016/j.jece.2016.01.036

Ogawa, M., Takee, R., Okabe, Y., Seki, Y. 2017. Bio-geo hybrid pigment; clay-anthocyanin complex which changes color depending on the atmosphere. Dyes Pigments, 139, 561-565. https://doi.org/10.1016/j.dyepig.2016.12.054

Quina, F.H., Moreira, P.F., Vautier-Giongo, C., Rettori, D., Rodrigues, R.F., Freitas, A.A., Silva, P.F., Macanita, A.L., 2009. Photochemistry of anthocyanins and their biological role in plant tissues. Pure Appl. Chem. 81, 1687–1694. https://doi.org/10.1351/Pac-Con-08-09-28

Ribeiro, H. L., Oliveira, A. V. D., Brito, E. S. D., Ribeiro, P. R. V., Souza Filho, M. D. S. M., Azeredo, H. M. C. 2018, Stabilizing effect of montmorillonite on acerola juice anthocyanins. Food Chem, 245, 966-973. https://doi.org/10.1016/j.foodchem.2017.11.076

Ruiz-Hitzky, E. 2001. Molecular access to the intracrytalline tunnels of sepiolite. J. Mater. Chem. 11, 86-91. https://doi.org/10.1039/b003197f

Sánchez Del Río, M., Martinetto, P., 2006. Synthesis and Acid Resistance of Maya Blue Pigment. Archaeometry 48, 115–130. https://doi.org/10.1111/j.1475-4754.2006.00246.x

Sánchez Del Río, M., Boccaleri, E., Milanesio, M., Croce, G., Van Beek, W., Tsiantos, C., Chyssikos, G.D., Gionis, V., Kacandes, G.H., Suárez, M., García-Romero, E., 2009. A combined synchrotron powder diffraction and vibrational study of the thermal treatment of palygorskite-indigo to produce Maya blue. J. Mater. Sci. 44,

5524–5536. https://doi.org/10.1007/s10853-009-3772-5

Shariatmadari, H., Mermut, A. R., Benke, M. B. 1999. Sorption of selected cationic and neutral organic molecules on palygorskite and sepiolite. Clays Clay Miner. 47, 44-53.

Silva, V.O., Freitas, A.A., Maçanita, A.L., Quina, F.H., 2016. Chemistry and photochemistry of natural plant pigments: the anthocyanins. J. Phys. Org. Chem. 29, 594–599. https://doi.org/10.1002/poc.3534

Silva, C. P., Pioli, R. M., Liu, L., Zheng, S., Zhang, M., Silva, G. T. de M., Carneiro, V. M. T., Quina, F. H., 2018. Improved Synthesis of Analogues of Red Wine Pyranoanthocyanin Pigments. ACS Omega 3, 954–960. https://doi.org/10.1021/acsomega.7b01955

Teixeira-Neto, Â.A., Shiguihara, A.L., Izumi, C.M.S., Bizeto, M.A., Leroux, F., Temperini, M.L.A., Constantino, V.R.L., 2009. A hybrid material assembled by anthocyanins from açaí fruit intercalated between niobium lamellar oxide. Dalt. Trans. 4136–4145. https://doi.org/10.1039/b820610d

Teixeira-Neto, Â.A., Izumi, C.M.S., Temperini, M.L.A., Ferreira, A.M.D.C., Constantino, V.R.L., 2012. Hybrid Materials Based on Smectite Clays and Nutraceutical Anthocyanins from the Açaí Fruit. Eur. J. Inorg. Chem. 2012, 5411–5420. https://doi.org/10.1002/ejic.201200702

Tilocca, A., Fois, E., 2009. The color and stability of maya blue: TDDFT calculations. J. Phys. Chem. C 113, 8683–8687. https://doi.org/10.1021/jp810945a

Tomasini, E.P., Román, E.S., Braslavsky, S.E., 2009. Validation of fluorescence quantum yields for light-scattering powdered samples by laser-induced optoacoustic spectroscopy. Langmuir 25, 5861–5868. https://doi.org/10.1021/la803492k

Ugochukwu, U. C., Jones, M. D., Head, I. M., Manning, D. A. C., Fialips, C. I. 2014.

Biodegradation of crude oil saturated fraction supported on clays. Biodegradation 25, 153-165. https://doi.org/10.1007/s10532-013-9647-0

Valandro, S.R., Poli, A.L., Neumann, M.G., Schmitt, C.C., 2015. Photophysics of auramine O adsorbed on solid clays. J. Lumin. 161, 209–213. https://doi.org/10.1016/j.jlumin.2015.01.023

Valandro, S.R., Poli, A.L., Correia, T.F.A., Lombardo, P.C., Schmitt, C.C., 2017. Photophysical Behavior of Isocyanine/Clay Hybrids in the Solid State. Langmuir 33, 891–899. https://doi.org/10.1021/acs.langmuir.6b03898

Yang, R., Li, D., Li, A., Yang, H. 2018. Adsorption properties and mechanisms of palygorskite for remocal of various ionic dyes from water. Appl. Clay Sci. 151, 20-28. https://doi.org/10.1016/j.clay.2017.10.016

Zhang, H.T., Li, R., Yang, Z., Yin, C.-X., Gray, M.R., Bohne, C., 2014. Evaluating steady-state and time-resolved fluorescence as a tool to study the behavior of asphaltene in toluene. Photochem. Photobiol. Sci. 13, 917–928. https://doi.org/10.1039/c4pp00069b

Zhang, Y., Wang, W., Mu, B., Wang, Q., Wang, A., 2015a. Effect of grinding time on fabricating a stable methylene blue/palygorskite hybrid nanocomposite. Powder Technol. 280, 173–179. https://doi.org/10.1016/j.powtec.2015.04.046

Zhang, Y., Wang, W., Zhang, J., Liu, P., Wang, A., 2015b. A comparative study about adsorption of natural palygorskite for methylene blue. Chem. Eng. J. 262, 390–398. https://doi.org/10.1016/j.cej.2014.10.009

Zhang, Y., Fan, L., Chen, H., Zhang, J., Zhang, Y., Wang, A., 2015c. Learning from ancient Maya: Preparation of stable palygorskite/methylene blue@SiO2 Maya Blue-like pigment. Microporous Mesoporous Mater. 211, 124–133. https://doi.org/10.1016/j.micromeso.2015.03.002

Zhang, Y., Zhang, J., Wang, A., 2015d. Facile preparation of stable palygorskite/methyl violet@SiO2 “Maya Violet” pigment. J. Colloid Interface Sci. 457, 254–263. https://doi.org/10.1016/j.jcis.2015.07.030

Zhang, Y., Dong, J., Sun, H., Yu, B., Zhu, Z., Zhang, J., Wang, A., 2016a. Solvatochromic Coatings with Self-Cleaning Property from Palygorskite@Polysiloxane/Crystal Violet Lactone. ACS Appl. Mater. Interfaces 8, 27346–27352. https://doi.org/10.1021/acsami.6b09252

Zhang, Y., Zhang, J., Wang, A., 2016b. From Maya blue to biomimetic pigments: durable biomimetic pigments with self-cleaning property. J. Mater. Chem. A 4, 901–907. https://doi.org/10.1039/C5TA09300G

CHAPTER 3

Highly fluorescent hybrid pigments from anthocyanin- and red wine pyranoanthocyanin-analogs adsorbed on sepiolite clay

This chapter was published in *Photochemical and Photobiological Sciences* (https://doi.org/10.1039/C9PP00141G) as an Advanced Article. Herein we report results for hybrid materials prepared by the adsorption of a series of flavylium and pyranoflavylium cations on sepiolite clay, with focus in fluorescence properties and stability.

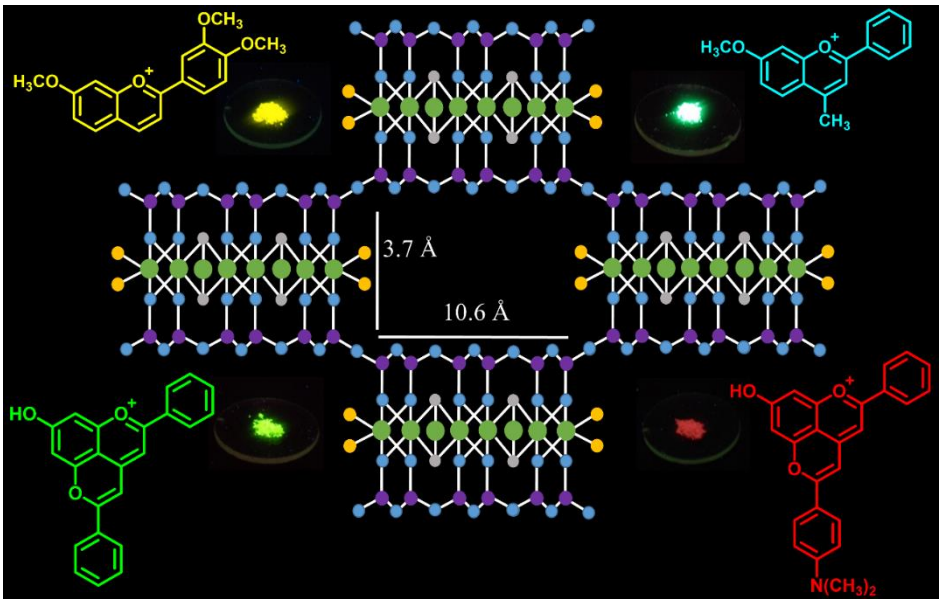

Abstract

Flavylium cations serve as models for the chemical and photochemical reactivity of anthocyanins, the natural plant pigment responsible for many of the red, blue and purple colors of fruits and flowers. Likewise, pyranoflavylium cations serve as models of the fundamental chromophoric moiety of pyranoanthocyanins, molecules that can form from reactions of grape anthocyanins in red wines during their maturation. In the present work, hybrid pigments are prepared by the adsorption of a series of five synthetic flavylium cations (FL) and five synthetic pyranoflavylium cations (PFL) on sepiolite clay (SEP). The FL are smaller in size than the PFL, but both can in principle fit into the tunnels and/or external grooves (with dimensions of 3.7 x 10.6 Å) of SEP. Measurements of the fluorescence quantum yields of the adsorbed dyes indicate that they are at least as fluorescent as in acidic acetonitrile solution, and in a few cases substantially more fluorescent. The observation of biexponential fluorescence decays is consistent with emission from dye molecules adsorbed at two distinct sites, presumably tunnels and grooves. These hybrid materials also have improved properties in terms of stability of the color in contact with pH 10 aqueous solution and resistance to thermal degradation of the dye. SEP thus appears to be a promising substrate for the development of highly fluorescent flavylium or pyranoflavylium cation-derived hybrid pigments with improved color and thermal stability.

3.1 Introduction

Sepiolite is a hydrated magnesium phyllosilicate clay mineral with fibrous morphology whose structure consists ribbons of octahedral sheets of magnesium oxides sandwiched between two tetrahedral sheets of silicon oxides with periodic inversion of the apical oxygen in every three silicate chairs. This causes a periodic discontinuity of the octahedral sheet that results in the formation of a structure with alternating blocks and one-dimensional tunnels with dimensions of 3.7 x 10.6 Å (Brigatti et al., 2006; Galan, 1996) and, on the external surface of the clay fibers, partially open channels or grooves (Martínez-Martínez et al., 2011; Ruiz-Hitzky, 2001). Two types of water molecules complete the tunnel structure of the sepiolite, weakly bound water in the tunnels (commonly called zeolitic water) and more tightly bound water coordinated to Mg ions at the ribbon borders (structural water molecules) (Ruiz-Hitzky, 2001). Its wide tunnels allows the penetration and/or adsorption of organic molecules, making SEP a good host, but its well-defined porous structure, similar to that of zeolites, does not permit lamellar expansion of SEP (Karataş et al., 2017; Martínez-Martínez et al., 2011; Ovarlez et al., 2009; Ruiz-Hitzky, 2001).

Sepiolite was one of the clays used in the preparation of Maya Blue pigment, an ancient organic-inorganic hybrid material used in murals, codices, ceramic and sculptures by the Maya civilization in the Pre-Columbian era. Maya blue has attracted attention due to its exceptional chemical and photochemical stability, being able to withstand the attacks of acids, bases and organic solvents and exposure to light without losing its color (Arnold and Branden, 2008; Chiari et al., 2008; Sánchez Del Río and Martinetto, 2006). The structure of Maya Blue, which is responsible for promoting this amazing stability, consists of the dye indigo protectively (and apparently irreversibly) inserted into the

tunnels of palygorskite or sepiolite clay (Chiari et al., 2008; Giustetto et al., 2006, 2005; Roberto Giustetto et al., 2011a; Tilocca and Fois, 2009). Many studies have focused on the characterization and stabilities of these complexes with the objective of understanding the indigo-palygorskite or indigo-sepiolite interactions in Maya Blue (Chiari et al., 2003; Doménech-Carbó et al., 2013; Doménech et al., 2011; Giustetto et al., 2006, 2005; R. Giustetto et al., 2011; Roberto Giustetto et al., 2011b, 2011a; Lima et al., 2012; Tilocca and Fois, 2009; Tsiantos et al., 2012). Maya Blue has also inspired the development of new materials based on the association of other dyes with palygorskite and sepiolite, associating similar properties and enhanced stability with other colors and potential applications. These include hybrid materials with interesting self-cleaning properties (Wu et al., 2019; Zhang et al., 2016a, 2016b) and highly stable hybrid pigments with a range of colors formed with both organic dyes (Fan et al., 2014; Giustetto et al., 2014; Giustetto and Wahyudi, 2011; Wang et al., 2016b; Wu et al., 2018, 2017; Yuan Zhang et al., 2015; Yujie Zhang et al., 2015b, 2015a) and inorganic pigments (Li et al., 2018; Tian et al., 2017; Wang et al., 2016a).

Our attention was drawn to these hybrid materials as part of our interest in manipulating and controlling the chemistry of flavylium and pyranoflavylium cations. Flavylium cations are synthetic analogues containing the same fundamental chromophore as anthocyanins, the natural plant pigments responsible by the most of the blue, red and purple colors of flowers, fruits and leaves. Pyranoflavylium cations are analogs of the chromophore of pyranoanthocyanins, compounds that are formed during the maturation of red wine (Casassa and Harbertson, 2014; Heras-Roger et al., 2016; Tang et al., 2017) via chemical reactions of grape anthocyanins with yeast metabolic products, colorless copigment molecules or other additives present in the wine (Brouillard et al., 2003; Figueiredo-González et al., 2014; Fulcrand et al., 2006; Marquez et al., 2013; Oliveira et

al., 2014; Schwarz et al., 2003). Unlike these much more complex natural products, synthetic flavylium and pyranoflavylium cations have the advantage of relatively facile and versatile modification of the substituents and consequently the reactivity and photophysical properties of the chromophore. Having recently shown that the adsorption of flavylium cations on palygorskite resulted in hybrid pigments with greatly improved chemical and thermal stability (G. T. M. Silva et al., 2018), we now report results for hybrid materials prepared by the adsorption of a series of flavylium and pyranoflavylium cations on sepiolite clay. The choice of sepiolite was dictated by the fact that its tunnels and grooves are wider than those of palygorskite and hence more attractive as a substrate for the adsorption of the larger pyranoflavylium cations.

3.2 Experimental section

3.2.1 Materials

The flavylium (FL) and pyranoflavylium (PFL) cations used in this work (Scheme 3.1) were available from previous studies of the group and the syntheses have been reported previously (Freitas et al., 2013; Held et al., 2016; C. P. Silva et al., 2018). The sepiolite (SEP) used in this work was SepSp-1 reference clay from the Clay Minerals Society Source Clay Minerals Repository; this material was manually ground to a powder that passed freely through a 40 mesh wire sieve but otherwise used with no additional purification. The chemical composition, characterization and properties of this clay have been described (Gionis et al., 2007; He et al., 1996; Hubbard et al., 2003; Li et al., 2003; Madejová et al., 2017; Vogt et al., 2002; Wang et al., 2009; Weir et al., 2002). Trifluoroacetic acid, (TFA, Sigma-Aldrich) and ethanol (Merck) were used as received.

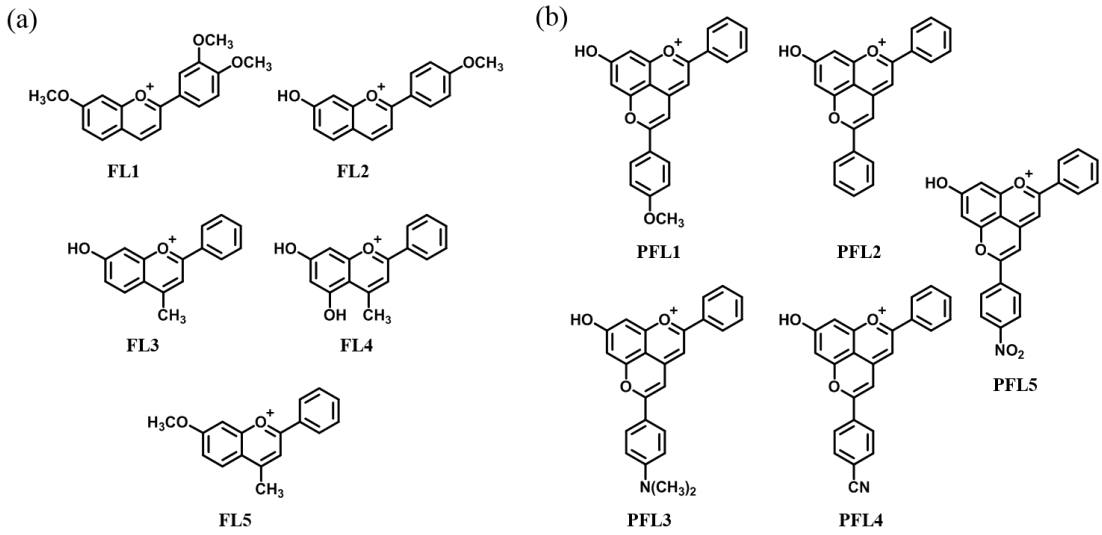

Scheme 3.1. Structures of the (a) flavylium cations, FL, and (b) pyranoflavylium cations, PFL, used in this work.

3.2.2 Preparation of the FL/SEP and PFL/SEP hybrid materials

Aliquots of solutions of the FL and PFL in ethanol (EtOH) acidified with 0.01 M TFA (in order to maintain the 7-OH group protonated) were added to a weighed amount of SEP clay powder. The initial FL/SEP and PFL/SEP ratios utilized were ca. 0.03 mmol/g. The resulting suspensions were stirred for 24 h in the dark at room temperature, centrifuged and the solid washed exhaustively with TFA-acidified EtOH and then dried under vacuum for 2 h at room temperature. The amounts of FL and PFL adsorbed on SEP were estimated from the decrease in the absorbance of the supernatant employing the known molar attenuation coefficients of the FL and PFL cations (Freitas et al., 2013; Held et al., 2016; C. P. Silva et al., 2018).

3.2.3 UV-Vis-diffuse reflectance and fluorescence measurements

A Varian Cary 50 UV-Vis Bio spectrophotometer equipped with a *Barrelino*™ diffuse reflectance probe (Harrick Scientific Products, Inc.) was used for obtain UV-Vis-diffuse reflectance (DR) spectra. The corresponding CIELAB Color coordinates (CIE L*a*b*) (Gilchrist and Nobbs, 1999) were determined with the software Agilent Cary WinUV Color employing natural daylight illuminant CIE D65 as the standard illuminant and an observer angle of 2 degrees. The remission spectra were obtained from the UV-Vis-DR employing the Kubelka-Munk equation (Tomasini et al., 2009):

$$F(R) = \frac{(1-R)^2}{2R}$$

where R is the absolute reflectance at each wavelength.

Steady state fluorescence measurements were performed with a Hitachi F-4500 fluorescence spectrophotometer equipped with a solid sample holder. The excitation and emission wavelengths are indicated in the figure legends. The bandwidths were 2.5 nm for both excitation and emission monochromators for all measurements, except for the FL4/SEP samples (5.0 nm).

Time-resolved fluorescence decay experiments were performed as described previously in the chapter 2 (G. T. M. Silva et al., 2018). The powder samples were excited at 405 nm (Edinburgh Instruments EPL 405 picosecond pulsed diode laser) in a solid sample holder and the decays collected at: 475 nm (for PFL2/SEP), 490 nm (for FL2/SEP), 500 nm (for FL3/SEP, FL4/SEP, FL5/SEP and PFL1/SEP), 515 nm (for PFL4/SEP), 525 nm (for PFL3/SEP and PFL5/SEP) or 555 nm (for FL1/SEP).

3.2.4 Confocal fluorescence microscopy

Confocal fluorescence images were obtained with the instrument and conditions described in the chapter 2 (G. T. M. Silva et al., 2018), with the exception of the excitation wavelength and the objective. The samples were excited at 405 nm with a Coherent Cube CW laser and the polarized laser beam was focused on the samples with a 100x objective.

3.2.5 Solid state fluorescence quantum yields

The solid-state fluorescence quantum yields (Φ_f) of the powder samples were measured with a Hamamatsu Quantaurus QY absolute photoluminescence quantum yield spectrometer model C11347 (integrating sphere), using raw SEP as the reference at the excitation wavelength used to obtain the spectra.

3.2.6 Sensitivity to pH and thermal stability

The reactivity of the FL and PFL cations adsorbed on SEP was investigated by addition of 15 mg of the FL1/SEP and PFL3/SEP samples to 5 mL of 10 mmol dm^{-3} sodium borate buffer solution, pH = 10. The samples were stirred for 24 h, then centrifuged and dried. UV-Vis-DR spectra as well as color coordinates were obtained in order to verify any spectral or color variations. To investigate the reversibility of the adsorption, FL1 was added to 10 mmol dm^{-3} sodium acetate buffer solutions at pH = 4, 5, and 6, followed by the addition of 0.05 g of SEP after discoloration of the solutions

due to the hydration of FL1. This experiment was carried out under stirring at room temperature (ca. 20 °C) and accomplished by taking digital images as a function of time.

Thermal stability was investigated by submitting FL1/SEP and PFL3/SEP samples to heating at 105 °C and 120 °C under vacuum for 24 h. Measurements of the color coordinates and UV-Vis-DR were used to verify any color or spectral changes.

3.3 Results and discussion

3.3.1 Fluorescent hybrid pigment formation

The cation exchange capacity (CEC) reported for the SepSp-1 Source Clay Sepiolite utilized in this work is 15 µmol g^{-1} (Li et al., 2003), well below the values in the range of 90-150 µmol g^{-1} for SEP from Zafer Mining Co. (Balıkesir, Turkey) (Tunç et al., 2008), Eskishehir Turkey (Shariatmadari et al., 1999) or Pangel-S9, Tolsa S.A. (Arbeloa et al., 2002). Taking into account this value of the SEP cation exchange capacity, 30 µmol of FL and PFL per g of SEP (twice the CEC) were added initially in the adsorption process. Since both FL and PFL cations are highly soluble in ethanol, exhaustive washing with acidic ethanol should remove any excess or weakly physiosorbed dye, leaving only the more strongly bound dye, indicating ion exchange as potentially the most important mode of interaction of these cationic dyes with the SEP clay. Substituents on the FL or PFL cations had little or no effect on the adsorption since the final amounts of adsorbed dye were similar for all dyes after the washing step. In addition, all of the amounts of adsorbed dye were inferior to the reported cation exchange capacity (CEC) of 15 µmol g^{-1} (Li et al., 2003) for the clay, suggestive of the importance of ion exchange in the adsorption process under these conditions. Although FL cations are slightly smaller in

size than PFL cations, the dimensions of both classes of dyes relative to those of the tunnels (Figure 3.1) should permit some insertion of the dyes into the tunnels, in addition to inclusion in the external grooves.

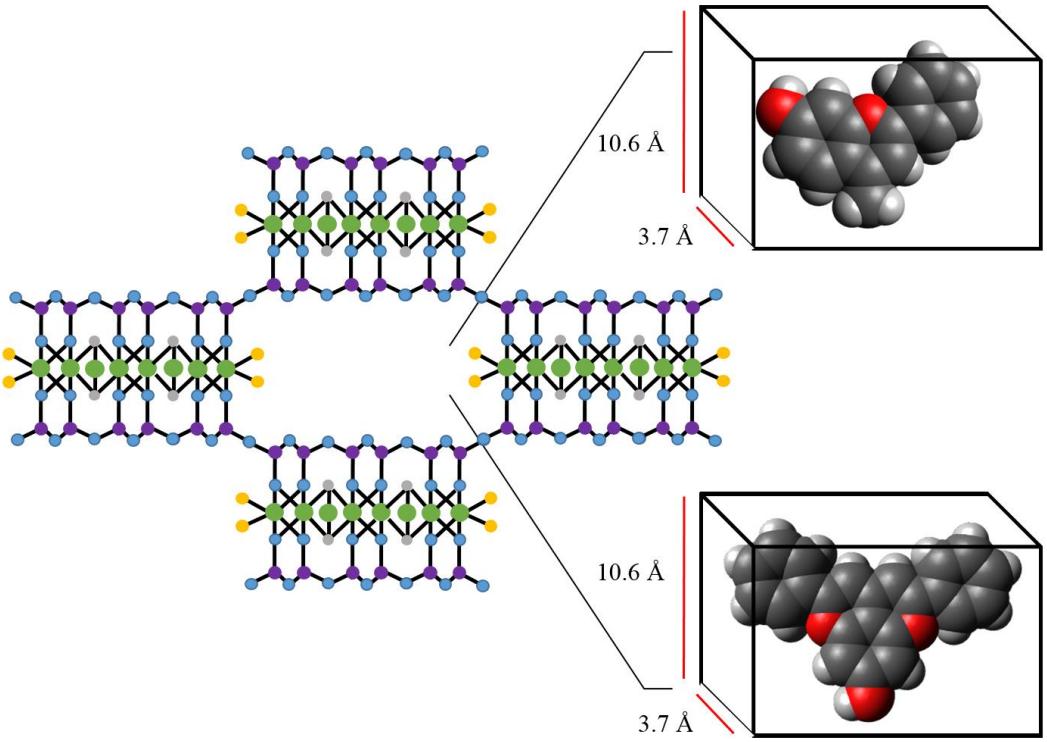

Figure 3.1. Comparison of the molecular sizes of FL3 (top) and PFL2 (bottom) with the dimensions of the tunnels of SEP.

The visible colors of some samples are more pronounced than those of others (Figure 3.2), a consequence of the relatively small quantities of FL and PFL cations adsorbed and differences in their molar absorptivities. More importantly, adsorption on the clays did have a significant effect on the chemical and thermal stability of the dyes, as well as the fluorescence efficiencies of several of them, as outlined in the following sections.

Figure 3.2. Images of the samples (a) FL/SEP and (b) PFL/SEP.

3.3.2 Chemical and thermal stability

For the thermal and chemical stability studies, the samples with most pronounced colors. i.e., FL1/SEP and PFL3/SEP (Figure 3.2) were chosen. The two classes of dyes studied here are largely unstable at high temperatures. Thus, while both FL1 and PFL3 degrade substantially in < 2 h at either 105 °C or 120 °C, FL1/SEP largely retained its characteristic colors for 24 h at both of these temperatures. At 105 ºC, PFL3/SEP still retained its characteristic color for 24 h, but at 120 °C major degradation occurred (Figure 3.3), with an accompanying obvious change in color (Figure 3.4).

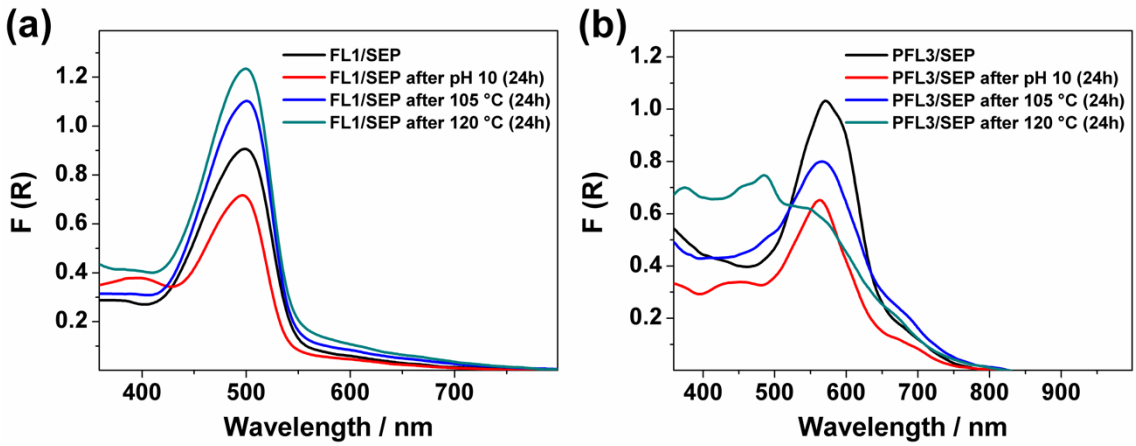

Figure 3.3. UV-Vis-DR spectra (Kubelka-Munk mode) of (a) FL1/SEP and (b) PFL3/SEP before and after immersion in pH 10 aqueous buffer.

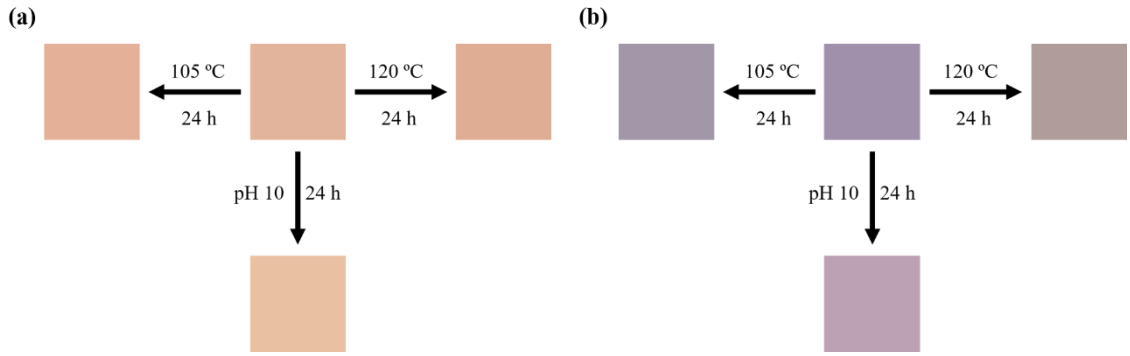

Figure 3.4. Images of the colors from CIELAB coordinate data for (a) FL1/SEP and (b) PFL3/SEP after the thermal stability tests.

In aqueous solution, FL1 begins to lose its color above about pH 3 (pK_h, or the pH at which half of the cation form is hydrated, is 3.0 ± 0.3) (Held et al., 2016) due to the formation of the corresponding hemiacetal, followed by ring-opening tautomerization to form a cis-chalcone and then slow isomerization to the trans-chalcone (Held et al., 2016). PFL3 (like all of the PFLs used in this work) undergoes deprotonation of the 7-hydroxy group at basic pH (Freitas et al., 2018) (see Figure 3.S1 of the Supplementary Material). Figures 3 and 4 also show the impact on the spectra and colors of FL1/SEP and PFL3/SEP before and after immersion in a pH 10 aqueous buffer medium. The corresponding CIELAB color coordinates are listed in Table 3.S1 of the Supplementary Material. Although the color of FL1/SEP became less intense, substantial color still remained, indicating that adsorbed FL1 is less prone to hydration. For PFL3/SEP, a new band appeared around 450 nm, similar to the band that appears for PFL3 in solution at high pH (Figure 3.S2 of the Supplementary Material). However, the color of the sample only faded slightly and did not change abruptly as it does for PFL3 in solution (Figure 3.S1 of the Supplementary Material). In neither case did the dye leach from the clay into the pH 10 aqueous medium.

The selective stabilization of the cationic form of FL1 by adsorption on SEP was further demonstrated by experiments in which FL1 was incubated with SEP in acetate buffers at pH 4, 5 or 6. Prior to the addition of SEP (Figure 3.5a), the solution is nearly colorless due to the hydration reaction. Upon addition of SEP to these solutions, the suspended clay gradually acquired the orange color of the adsorbed FL1 cation as a function of time (Figure 3.5b). The rates of appearance of the coloration were qualitatively very similar at pH 4, 5 and 6 and the maximum intensity of the color was similar at all three pH values (Figure 3.5c). Because there are large pH-dependent differences in the equilibrium concentration of the cationic form in solution, this result strongly suggests that the hydrated forms of FL1 initially adsorb on SEP, where they subsequently convert to the cationic form by interaction with acidic sites of the SEP clay. Indeed, SEP clay has been reported to have two kinds of acid surface sites, one that is strongly acidic with an effective pK_a around 3.2 - 3.3 (Çelik, 2004; Tunç et al., 2008) and another that is moderately acidic with a pK_a in the range of 6.3 – 6.6 (Alkan et al., 2005; Çelik, 2004).

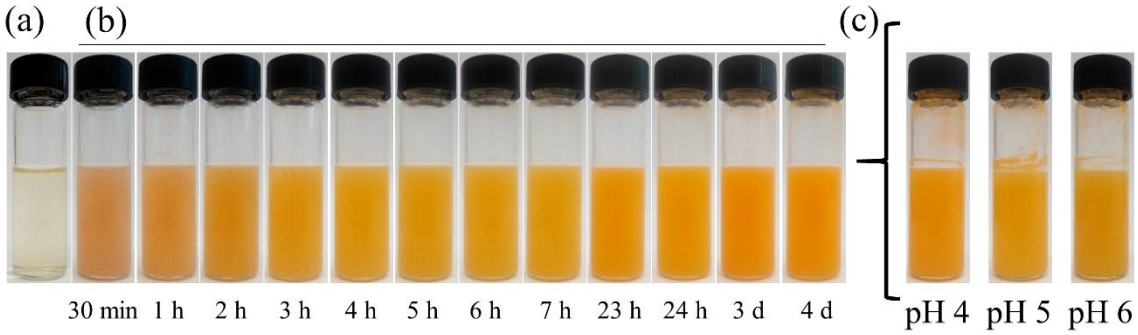

Figure 3.5. Images of (a) FL1 at pH 4; (b) mixture of FL1 and SEP as a function of time at pH 4; and (c) mixture of FL1 and SEP at pH 4, 5 and 6, after 27 days.

3.3.3 Spectroscopic studies

Figure 3.6 presents the UV-Vis-DR spectra for all of the hybrid pigments prepared in this work, plotted in the Kubelka-Munk mode as reemission spectra (Eq. 1). All spectra had an underlying background absorption due to the SEP clay itself (the spectrum of SEP clay is shown in Figure 3.S3 of the Supplementary Material). With the exception of FL4/SEP, PFL1/SEP and PFL2/SEP, the spectra are red shifted from those in acidic solution (1 % 1.0 mol dm^{-3} HCl/methanol for the FL cations (G. T. M. Silva et al., 2018) and acetonitrile containing 0.10 mol dm^{-3} TFA for the PFL cations (Siddique et al., 2019)), with the largest red shifts for FL1/SEP (ca. 22 nm), FL2/SEP (ca. 10 nm) and PFL3/SEP (ca. 20 nm). Red shifts of this type have been attributed to electrostatic interactions (Kohno et al., 2009, 2008a) or to the acidity of the inorganic substrate (Kohno et al., 2008b). The exhaustive washing following the initial adsorption procedure was effective, eliminating any excess of FL and PFL cations since the spectra did not exhibit any evidence of the presence of aggregates of FL or PFL.

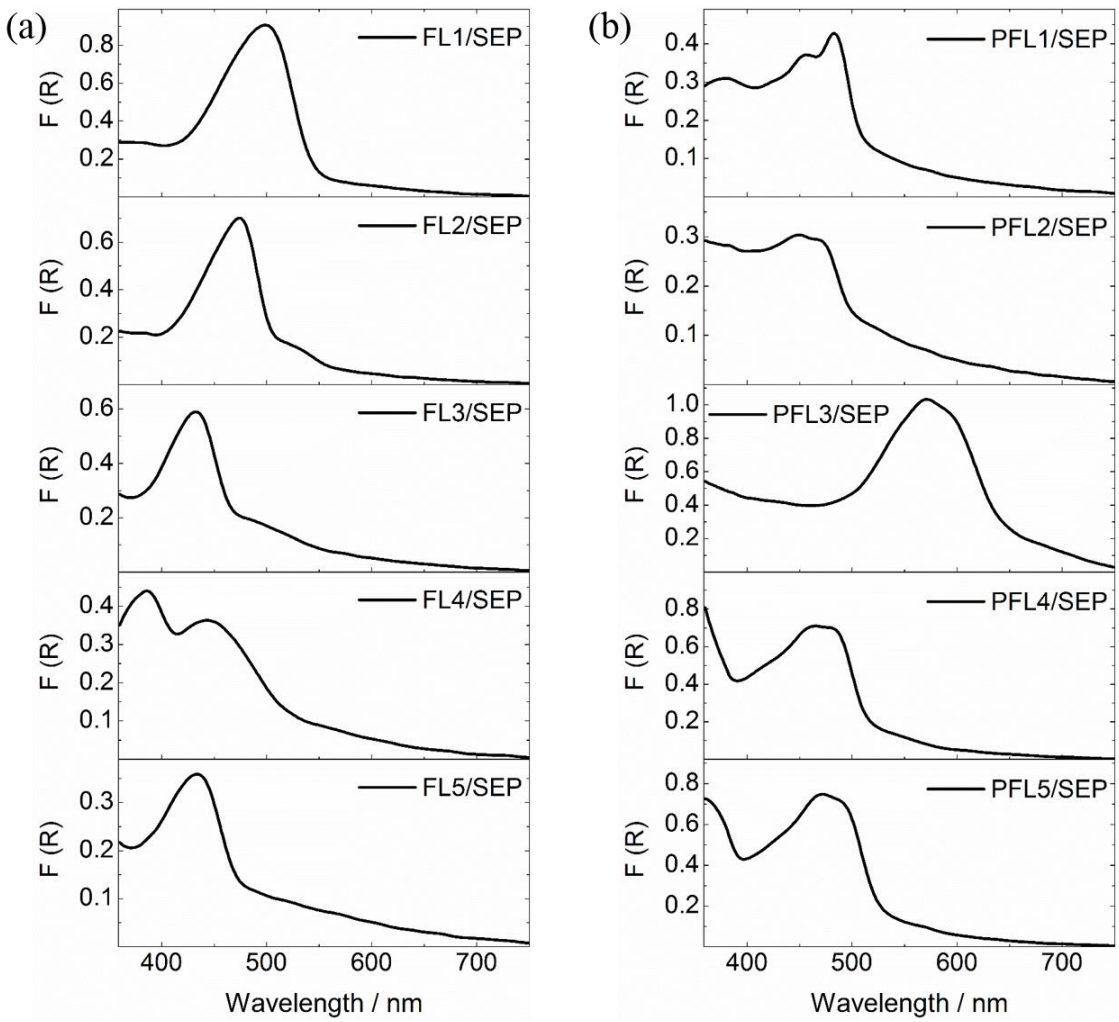

Figure 3.6. UV-Vis-DR spectra (Kubelka-Munk mode) of the (a) FL/SEP and (b) PFL/SEP samples.

Steady-state fluorescence excitation and emission spectra of the hybrid pigments are shown in Figure 3.7. The fluorescence excitation spectra for both classes of hybrid pigments are generally similar to the reemission spectra (Figure 3.6), with the exception of FL4/SEP whose emission was too weak to obtain a reliable spectrum. The fact that fluorescence could be observed at all from FL4/SEP and PFL3/SEP was an indication itself that the interaction with SEP improved the fluorescence of the dyes since both FL4 and PFL3 are essentially non-fluorescent in solution.

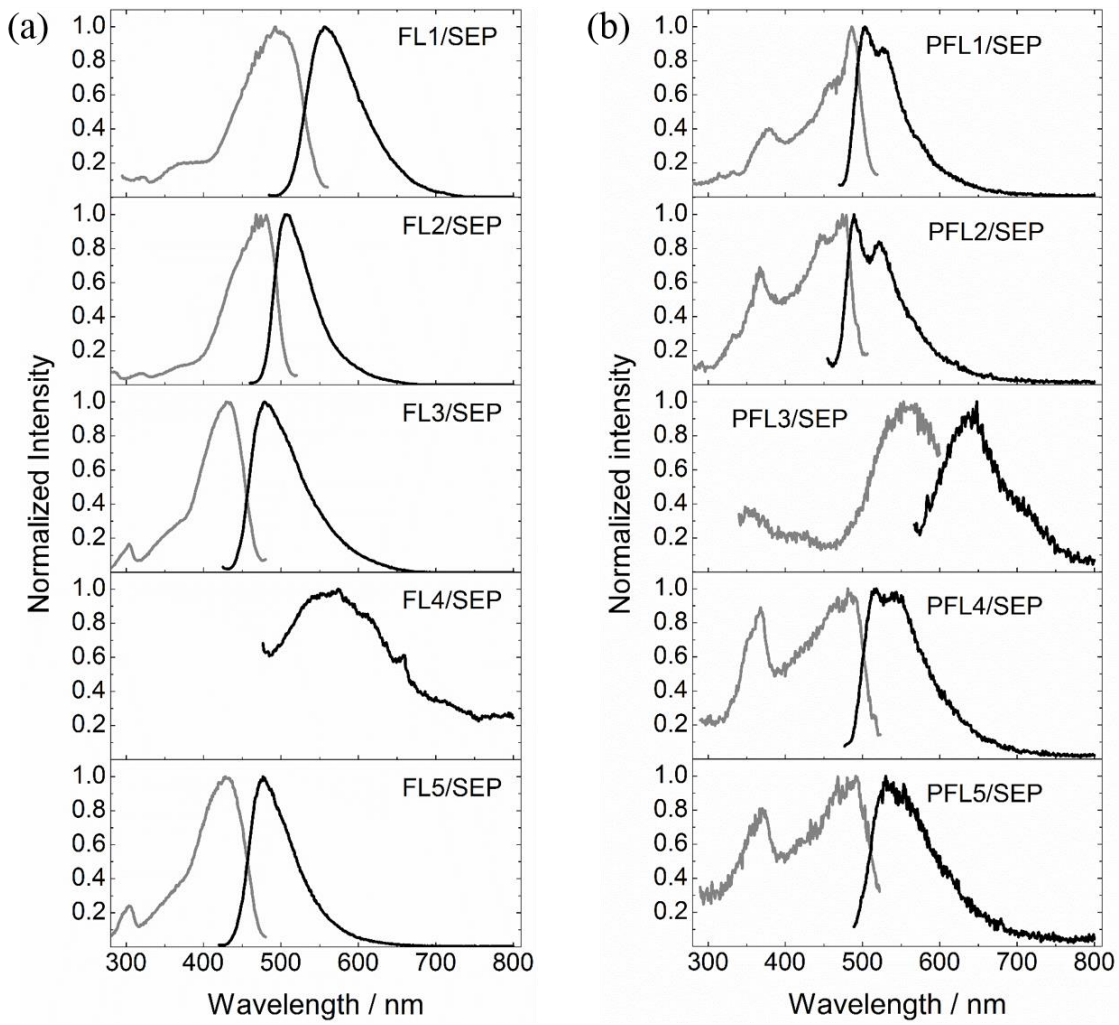

Figure 3.7. Excitation and emission spectra of the hybrid pigments (a) FL1/SEP (Ex. 480 and Em. 576 nm), FL2/SEP (Ex. 450 and Em. 530 nm), FL3/SEP (Ex. 415 and Em. 490 nm), FL4/SEP (Ex. 450), FL5/SEP (Ex. 410 and Em. 490 nm), and (b) PFL1/SEP (Ex. 455 and Em. 530 nm), PFL2/SEP (Ex. 445 and Em. 523 nm), PFL3/SEP (Ex. 555 and Em. 640 nm), PFL4/SEP (Ex. 450 and Em. 545 nm), PFL5/SEP (Ex. 455 and Em. 555 nm).

Figure 3.8 presents confocal fluorescence microscopic images (false-color mapping) of some of the more strongly fluorescent hybrid clay particles, pointing to relatively uniform emission across the whole particle. The impressive fluorescence of these solid samples instigated us to perform measurements of fluorescence quantum yields. The results, presented in Table 3.1, show that the fluorescence quantum yields of

the FLs and PFLs tend to be equal to or slightly higher than those of the FLs and PFLs in acetonitrile containing 0.1 mol dm^{-3} TFA. Particularly noteworthy are the large increase in the fluorescence quantum yield of FL1 in SEP and the observation of fluorescence from PFL3 in SEP. PFL3 is non-emissive in solution due to relaxation to a twisted intramolecular charge transfer (TICT) state (Siddique et al., 2019) and encapsulation of FL1 in a CB[7] cucurbituril cavity was also found to strongly enhance its fluorescence (Held et al., 2016). Unlike FL5, which is quite fluorescent in solution, FL1 has an electron-rich dimethoxyphenil B-ring that favors intramolecular charge-transfer interactions with the cationic portion of the molecule. Thus, adsorption of FL1 and PFL3 on sepiolite presumably inhibits the conformational changes in the excited singlet states that transform the fluorescent locally excited state into a much less fluorescent or non-fluorescent TICT state. The time-resolved emission decay measurements (Table 3.1) indicate two lifetime components that make roughly equal contributions to the emission. In the case of FL1 and FL2, the longer lifetime exceeds that of the dyes adsorbed on PAL (Table 3.1). Since no aggregates of FL or PFL cations were detected, the two lifetime components suggest the existence of at least two different adsorption sites, potentially reflecting binding of the dye in the external grooves and in the internal tunnels of SEP.

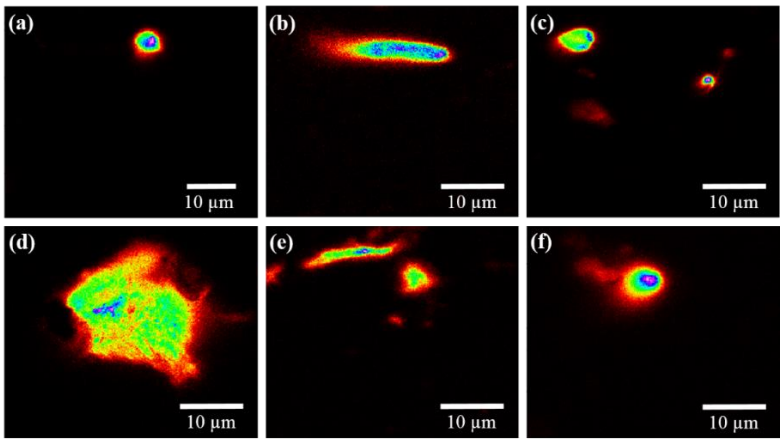

Figure 3.8. Confocal fluorescence images (false color) of the samples (a-b) FL2/SEP; (c) FL5/SEP; (d-e) PFL5/SEP and (f) PFL2/SEP.

Table 3.1. Quantum yield (Φ_f) and lifetime (τ_f) for fluorescence of the FL and PFL cations adsorbed into/onto SEP.

Hybrid pigments	Φ_f*	Φ_f[a]	$\tau_{f,1}$* / ns	$\tau_{f,2}$* / ns	τ_f[b] / ns
FL1/SEP	0.37	0.001	1.33 (41%)	3.10 (59%)	0.35 (80%)
					1.0 (20%)
FL2/SEP	0.41	0.42	1.11 (47%)	2.95 (53%)	0.6 (60%)
					2.0 (40%)
FL3/SEP	0.310	0.26	1.51 (52%)	4.08 (48%)	
FL4/SEP	0.006	0.001	-	-	
FL5/SEP	0.61	0.53	1.86 (33%)	5.72 (67%)	
PFL1/SEP	0.36	0.43[c] 0.41[d]	0.83 (56%)	3.61 (44%)	
PFL2/SEP	0.22	0.16[c]	2.13 (47%)	6.48 (53%)	
PFL3/SEP	0.027	-	-	-	
PFL4/SEP	0.067	0.048[c]	1.36 (61%)	3.96 (39%)	
PFL5/SEP	0.044	0.030[c]	0.79 (74%)	2.62 (26%)	

*±10 %; [a]FLs and PFLs at 20°C in air-equilibrated acetonitrile containing 0.10 mol dm^{-3} TFA. [b]FLs adsorbed on PAL, Chapter 2 Ref. (G. T. M. Silva et al., 2018). [c]Ref. (Silva et al., 2019). [d]Ref. (Freitas et al., 2017).

3.4 Conclusions

The adsorption of flavylium (FL) and pyranoflavylium (PFL) cations on sepiolite (SEP) clay results in hybrid materials with a series of improved properties in terms of stability of the color in contact with mildly basic aqueous solution, resistance to thermal degradation of the dye, while maintaining excellent fluorescence properties. In all cases,

the SEP-adsorbed dyes are at least as fluorescent as in solution, with particular attention to FL1, which is substantially more fluorescent. The thermal stability of FL1/SEP is better than that of PFL3/SEP, suggesting that the smaller FL1 dye molecules are perhaps more readily incorporated in the tunnels of SEP than the larger PFL3 dye molecules. FL1 is also more resistant to color loss due to hydration when adsorbed on SEP, with its wider tunnels and grooves, than on PAL clay (G. T. M. Silva et al., 2018) with narrower tunnels and grooves. The fluorescence decays of FL and PFL adsorbed on SEP are biexponential, with a somewhat greater contribution from the longer decay time for FL than for PFL, suggesting that the longer and shorter fluorescence lifetimes arise from dye adsorbed in the SEP tunnels and grooves, respectively. SEP thus appears to be a promising substrate for the development of highly fluorescent hybrid pigments with improved color and thermal stability.

Supplementary Materials

Figures

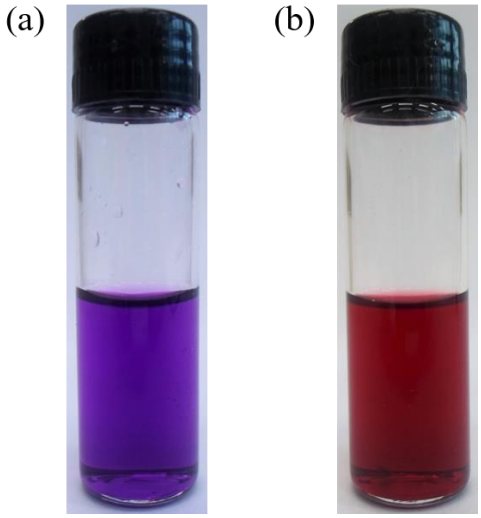

Figure 3.S1. Images of PFL3 in (a) acidified and (b) basified methanol.

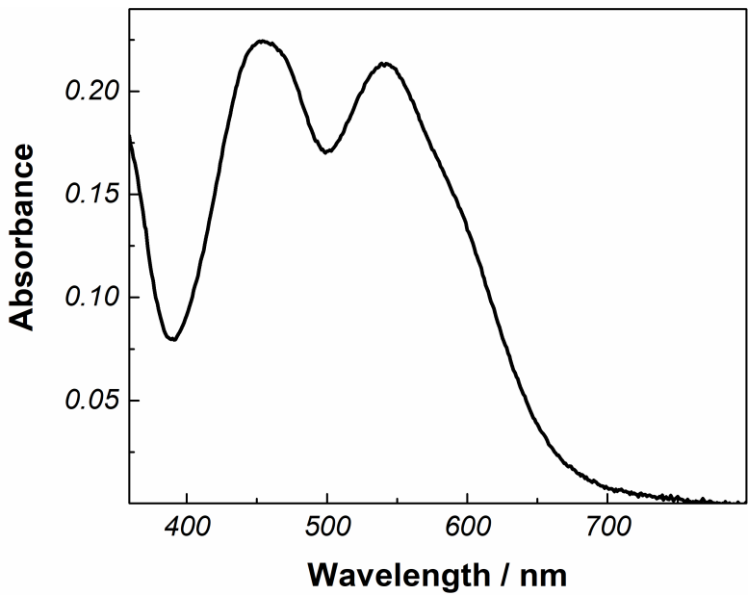

Figure 3.S2. UV-Vis absorbance spectral of PFL3 in phosphate buffer solution pH 9.2.

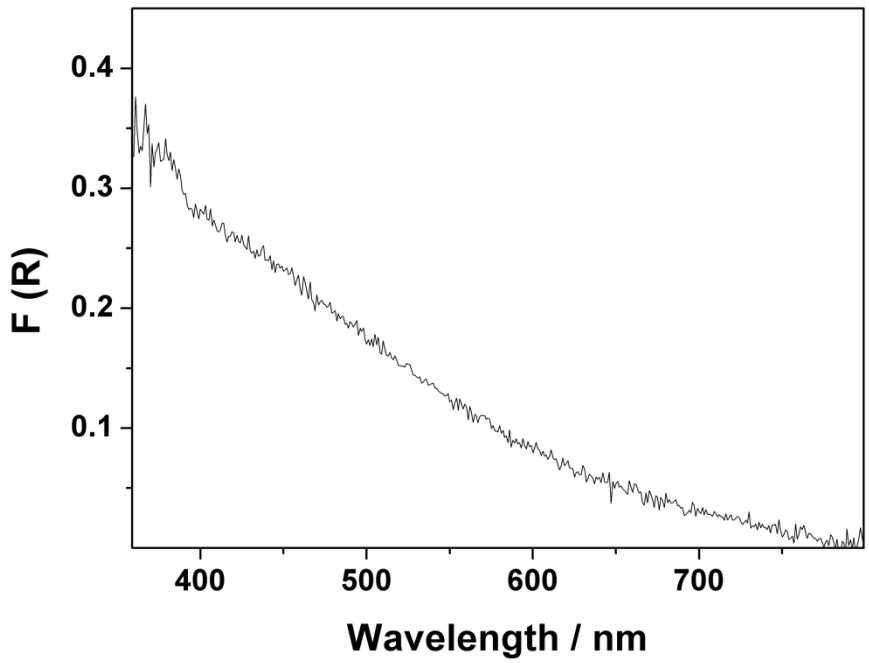

Figure 3.S3. UV-Vis-DR spectrum (Kubelka-Munk mode) of the SEP clay.

Tables

Table 3.S1. CIELAB color coordinates for FL1/SEP and PFL3/SEP hybrid materials.

Samples	Condition	**L***	**a***	**b***
FL1/SEP	Fresh	76.9271	13.5882	18.8697
	pH 10	80.6730	9.9535	20.8192
	105 °C	76.1717	15.0878	19.6579
	120 °C	74.4944	15.4514	19.6908
PFL3/SEP	Fresh	62.0158	7.1031	-11.8908
	pH 10	68.5025	9.5429	-6.4145
	105 °C	63.9056	7.2337	-7.2530
	120 °C	66.0127	6.6829	4.8840

References

Alkan, M., Demirbaş, Ö., Doğan, M., 2005. Electrokinetic properties of sepiolite suspensions in different electrolyte media. J. Colloid Interface Sci. 281, 240–248. https://doi.org/10.1016/j.jcis.2004.08.036

Arbeloa, F.L., Arbeloa, T.L., Arbeloa, I.L., 2002. Spectroscopy of Rhodamine 6G Adsorbed on Sepiolite Aqueous Suspensions. J. Colloid Interface Sci. 187, 105–112. https://doi.org/10.1006/jcis.1996.4672

Arnold, E., Branden, J., 2008. The first direct evidence for the production of Maya Blue: rediscovery of a technology. Antiquity 82, 151–164. https://doi.org/https://doi.org/10.1017/S0003598X00096514

Brigatti, M.F., Galan, E., Theng, B.K.G., 2006. Structures and Mineralogy of Clay Minerals, in: Chapter 2, Handbook of Clay Science, Developments in Clay Science.

pp. 19–86. https://doi.org/10.1016/S1572-4352(05)01002-0

Brouillard, R., Chassaing, S., Fougerousse, A., 2003. Why are grape/fresh wine anthocyanins so simple and why is it that red wine color lasts so long? Phytochemistry 64, 1179–1186. https://doi.org/10.1016/S0031-9422(03)00518-1

Casassa, L.F., Harbertson, J.F., 2014. Extraction, Evolution, and Sensory Impact of Phenolic Compounds During Red Wine Maceration. Annu. Rev. Food Sci. Technol. 5, 83–109. https://doi.org/10.1146/annurev-food-030713-092438

Çelik, M.S., 2004. Electrokinetic Behavior of Clay Surfaces, in: Clay Surfaces: Fundamentals and Applications. pp. 57–89. https://doi.org/10.1016/j.inoche.2007.06.005

Chiari, G., Giustetto, R., Druzik, J., Doehne, E., Ricchiardi, G., 2008. Pre-columbian nanotechnology: Reconciling the mysteries of the maya blue pigment. Appl. Phys. A Mater. Sci. Process. 90, 3–7. https://doi.org/10.1007/s00339-007-4287-z

Chiari, G., Giustetto, R., Ricchiardi, G., 2003. Crystal structure refinements of palygorskite and Maya Blue from molecular modelling and powder synchrotron diffraction. Eur. J. Mineral. 15, 21–33. https://doi.org/10.1127/0935-1221/2003/0015-0021

Doménech-Carbó, A., Doménech-Carbó, M.T., Valle-Algarra, F.M., Domine, M.E., Osete-Cortina, L., 2013. On the dehydroindigo contribution to Maya Blue. J. Mater. Sci. 48, 7171–7183. https://doi.org/10.1007/s10853-013-7534-z

Doménech, A., Doménech-Carbó, M.T., Edwards, H.G.M., 2011. On the interpretation of the Raman spectra of Maya Blue: A review on the literature data. J. Raman Spectrosc. 42, 86–96. https://doi.org/10.1002/jrs.2642

Fan, L., Zhang, Y., Zhang, J., Wang, A., 2014. Facile preparation of stable palygorskite/cationic red X-GRL@SiO_2 “Maya Red” pigments. RSC Adv. 4,

63485–63493. https://doi.org/10.1039/C4RA13739F

Figueiredo-González, M., Cancho-Grande, B., Simal-Gándara, J., Teixeira, N., Mateus, N., De Freitas, V., 2014. The phenolic chemistry and spectrochemistry of red sweet wine-making and oak-aging. Food Chem. 152, 522–530. https://doi.org/10.1016/J.FOODCHEM.2013.12.018

Freitas, A.A., Maçanita, A.A.L., Quina, F.H., 2013. Improved analysis of excited state proton transfer kinetics by the combination of standard and convolution methods. Photochem. Photobiol. Sci. 12, 902–10. https://doi.org/10.1039/c3pp25445c

Freitas, A.A., Silva, C.P., Silva, G.T.M., Maçanita, A.L., Quina, F.H., 2018. Ground- and Excited-State Acidity of Analogs of Red Wine Pyranoanthocyanins,. Photochem. Photobiol. 94, 1086–1091. https://doi.org/10.1111/php.12944

Freitas, A.A., Silva, C.P., Silva, G.T.M., Maçanita, A.L., Quina, F.H., 2017. From vine to wine: photophysics of a pyranoflavylium analog of red wine pyranoanthocyanins. Pure Appl. Chem. 89, 1761–1767. https://doi.org/10.1515/pac-2017-0411

Fulcrand, H., Dueñas, M., Salas, E., Cheynier, V., 2006. Phenolic reactions during winemaking and aging. Am. J. Enol. Vitic. 57, 289–297.

Galan, E., 1996. Properties and applications of palygorskite-sepiolite clays. Clay Miner. 31, 443–453.

Gilchrist, A., Nobbs, J., 1999. Colorimetry , Theory. Encycl. Spectrosc. Spectrom. Second Ed.

Gionis, V., Kacandes, G.H., Kastritis, I.D., Chryssikos, G.D., 2007. Combined near-infrared and x-ray diffraction investigation of the octahedral sheet composition of palygorskite. Clays Clay Miner. 55, 543–553. https://doi.org/10.1346/CCMN.2007.0550601

Giustetto, R., Levy, D., Chiari, G., 2006. Crystal structure refinement of Maya Blue

pigment prepared with deuterated indigo, using neutron powder diffraction. Eur. J. Mineral. 18, 629–640. https://doi.org/10.1127/0935-1221/2006/0018-0629

Giustetto, R., Levy, D., Wahyudi, O., Ricchiardi, G., Vitillo, J.G., 2011a. Crystal structure refinement of a sepiolite/indigo Maya Blue pigment using molecular modelling and synchrotron diffraction. Eur. J. Mineral. 23, 449–466. https://doi.org/10.1127/0935-1221/2011/0023-2105

Giustetto, R., Llabrés I Xamena, F.X., Ricchiardi, G., Bordiga, S., Damin, A., Gobetto, R., Chierotti, M.R., 2005. Maya blue: A computational and spectroscopic study. J. Phys. Chem. B 109, 19360–19368. https://doi.org/10.1021/jp048587h

Giustetto, R., Seenivasan, K., Bonino, F., Ricchiardi, G., Bordiga, S., Chierotti, M.R., Gobetto, R., 2011b. Host/guest interactions in a sepiolite-based maya blue pigment: A spectroscopic study. J. Phys. Chem. C 115, 16764–16776. https://doi.org/10.1021/jp203270c

Giustetto, R., Vitillo, J.G., Corazzari, I., Turci, F., 2014. Evolution and reversibility of host/guest interactions with temperature changes in a methyl red@palygorskite polyfunctional hybrid nanocomposite. J. Phys. Chem. C 118, 19322–19337. https://doi.org/10.1021/jp4091238

Giustetto, R., Wahyudi, O., 2011. Sorption of red dyes on palygorskite: Synthesis and stability of red/purple Mayan nanocomposites. Microporous Mesoporous Mater. 142, 221–235. https://doi.org/10.1016/j.micromeso.2010.12.004

Giustetto, R., Wahyudi, O., Corazzari, I., Turci, F., 2011. Chemical stability and dehydration behavior of a sepiolite/indigo Maya Blue pigment. Appl. Clay Sci. 52, 41–50. https://doi.org/10.1016/j.clay.2011.01.027

He, C., Makovicky, E., Osbæck, B., 1996. Thermal treatment and pozzolanic activity of sepiolite. Appl. Clay Sci. 10, 337–349. https://doi.org/10.1016/0169-

1317(95)00035-6

Held, B., Tang, H., Natarajan, P., Silva, C.P., Silva, V.O., Bohne, C., Quina, F.H., 2016. Cucurbit[7]uril inclusion complexation as a supramolecular strategy for color stabilization of anthocyanin model compounds. Photochem. Photobiol. Sci. 15, 752–757. https://doi.org/10.1039/C6PP00060F

Heras-Roger, J., Díaz-Romero, C., Darias-Martín, J., 2016. What Gives a Wine Its Strong Red Color? Main Correlations Affecting Copigmentation. J. Agric. Food Chem. 64, 6567–6574. https://doi.org/10.1021/acs.jafc.6b02221

Hubbard, B., Kuang, W., Moser, A., Facey, G.A., Detellier, C., 2003. Structural study of Maya Blue: Textural, thermal and solid-state multinuclear magnetic resonance characterization of the palygorskite-indigo and sepiolite-indigo adducts. Clays Clay Miner. 51, 318–326. https://doi.org/10.1346/CCMN.2003.0510308

Karataş, D., Tekin, A., Çelik, M.S., 2017. Density functional theory computation of organic compound penetration into sepiolite tunnels. Clays Clay Miner. 65, 1–13. https://doi.org/10.1346/CCMN.2016.064043

Kohno, Y., Kinoshita, R., Ikoma, S., Yoda, K., Shibata, M., Matsushima, R., Tomita, Y., Maeda, Y., Kobayashi, K., 2009. Stabilization of natural anthocyanin by intercalation into montmorillonite. Appl. Clay Sci. 42, 519–523. https://doi.org/10.1016/j.clay.2008.06.012

Kohno, Y., Shibata, Y., Oyaizu, N., Yoda, K., Shibata, M., Matsushima, R., 2008a. Stabilization of flavylium dye by incorporation into the pore of protonated zeolites. Microporous Mesoporous Mater. 114, 373–379. https://doi.org/10.1016/j.micromeso.2008.01.023

Kohno, Y., Tsubota, S., Shibata, Y., Nozawa, K., Yoda, K., Shibata, M., Matsushima, R., 2008b. Enhancement of the photostability of flavylium dye adsorbed on mesoporous

silicate. Microporous Mesoporous Mater. 116, 70–76. https://doi.org/10.1016/j.micromeso.2008.03.014

Li, H., Zhang, A., Wang, A., Mu, B., An, X., 2018. Cobalt blue hybrid pigment doped with magnesium derived from sepiolite. Appl. Clay Sci. 157, 111–120. https://doi.org/10.1016/j.clay.2018.02.032

Li, Z., Willms, C.A., Kniola, K., 2003. Removal of anionic contaminants using surfactant-modified palygorskite and sepiolite. Clays Clay Miner. 51, 445–451. https://doi.org/10.1346/CCMN.2003.0510411

Lima, E., Guzmán, A., Vera, M., Rivera, J.L., Fraissard, J., 2012. Aged natural and synthetic Maya Blue-like pigments: What difference does it make? J. Phys. Chem. C 116, 4556–4563. https://doi.org/10.1021/jp207602m

Madejová, J., Gates, W.P., Petit, S., 2017. IR Spectra of Clay Minerals, in: Chapter 5, Handbook of Clay Science, Developments in Clay Science. pp. 107–149. https://doi.org/10.1016/B978-0-08-100355-8.00005-9

Marquez, A., Serratosa, M.P., Merida, J., 2013. Pyranoanthocyanin Derived Pigments in Wine: Structure and Formation during Winemaking. J. Chem. 2013, 1–15. https://doi.org/10.1155/2013/713028

Martínez-Martínez, V., Corcóstegui, C., Bañuelos Prieto, J., Gartzia, L., Salleres, S., López Arbeloa, I., 2011. Distribution and orientation study of dyes intercalated into single sepiolite fibers. A confocal fluorescence microscopy approach. J. Mater. Chem. 21, 269–276. https://doi.org/10.1039/c0jm02211j

Oliveira, J., Mateus, N., de Freitas, V., 2014. Previous and recent advances in pyranoanthocyanins equilibria in aqueous solution. Dye. Pigment. 100, 190–200. https://doi.org/10.1016/J.DYEPIG.2013.09.009

Ovarlez, S., Giulieri, F., Chaze, A., Delamare, F., 2009. The Incorporation of Indigo

Molecules in Sepiolite Tunnels. Chem. - A Eur. J. 15, 11326–11332. https://doi.org/10.1002/chem.200901482

Ruiz-Hitzky, E., 2001. Molecular access to intracrystalline tunnels of sepiolite. J. Mater. Chem. 11, 86–91. https://doi.org/10.1039/b003197f

Sánchez Del Río, M., Martinetto, P., 2006. Synthesis and Acid Resistance of Maya Blue Pigment. Archaeometry 48, 115–130. https://doi.org/10.1111/j.1475-4754.2006.00246.x

Schwarz, M., Wabnitz, T.C., Winterhalter, P., 2003. Pathway Leading to the Formation of Anthocyanin−Vinylphenol Adducts and Related Pigments in Red Wines. J. Agric. Food Chem. 51, 3682–3687. https://doi.org/10.1021/JF0340963

Shariatmadari, H., Mermut, A.R., Benke, M.B., 1999. Sorption of selected cationic and neutral organic molecules on palygorskite and sepiolite. Clays Clay Miner. 47, 44–53. https://doi.org/10.1346/CCMN.1999.0470105

Siddique, F., Silva, C.P., Silva, G.T.M., Lischka, H., Quina, F.H., Aquino, A.J.A., 2019. The electronic transitions of analogs of red wine pyranoanthocyanin pigments. Photochem. Photobiol. Sci. 18, 45–53. https://doi.org/10.1039/C8PP00391B

Silva, C.P., Pioli, R.M., Liu, L., Zheng, S., Zhang, M., Silva, G.T.M., Carneiro, V.M.T., Quina, F.H., 2018. Improved Synthesis of Analogues of Red Wine Pyranoanthocyanin Pigments. ACS Omega 3, 954–960. https://doi.org/10.1021/acsomega.7b01955

Silva, G.T.M., Silva, C.P., Gehlen, M.H., Oake, J., Bohne, C., Quina, F.H., 2018. Organic/inorganic hybrid pigments from flavylium cations and palygorskite. Appl. Clay Sci. 162, 478–486. https://doi.org/10.1016/j.clay.2018.07.002

Silva, G.T.M., Thomas, S.S., Silva, C.P., Schlothauer, J.C., Baptista, M.S., Freitas, A.A., Bohne, C., Quina, F.H., 2019. Triplet Excited States and Singlet Oxygen Production

by Analogs of Red Wine Pyranoanthocyanins. Photochem. Photobiol. 95, 176–182. https://doi.org/10.1111/php.12973

Tang, K., Liu, T., Han, Y., Xu, Y., Li, J.M., 2017. The Importance of Monomeric Anthocyanins in the Definition of Wine Colour Properties. South African J. Enol. Vitic. 38, 1–10. https://doi.org/10.21548/38-1-661

Tian, G., Wang, W., Wang, D., Wang, Q., Wang, A., 2017. Novel environment friendly inorganic red pigments based on attapulgite. Powder Technol. 315, 60–67. https://doi.org/10.1016/j.powtec.2017.03.044

Tilocca, A., Fois, E., 2009. The color and stability of maya blue: TDDFT calculations. J. Phys. Chem. C 113, 8683–8687. https://doi.org/10.1021/jp810945a

Tomasini, E.P., Román, E.S., Braslavsky, S.E., 2009. Validation of fluorescence quantum yields for light-scattering powdered samples by laser-induced optoacoustic spectroscopy. Langmuir 25, 5861–5868. https://doi.org/10.1021/la803492k

Tsiantos, C., Tsampodimou, M., Kacandes, G.H., Sánchez Del Río, M., Gionis, V., Chryssikos, G.D., 2012. Vibrational investigation of indigo-palygorskite association(s) in synthetic Maya blue. J. Mater. Sci. 47, 3415–3428. https://doi.org/10.1007/s10853-011-6189-x

Tunç, S., Duman, O., Uysal, R., 2008. Electrokinetic and Rheological Behaviors of Sepiolite Suspensions in the Presence of Poly(acrylic acid sodium salt)s, Polyacrylamides, and Poly(ethylene glycol)s of Different Molecular Weights. J. Appl. Polym. Sci. 109, 1850–1860. https://doi.org/10.1002/app.28245

Vogt, C., Lauterjung, J., Fischer, R.X., 2002. Investigation of the Clay Fraction (<2 µm) of the Clay Minerals Society Reference Clays. Clays Clay Miner. 50, 388–400.

Wang, M.K., Tseng, P.C., Chang, S.S., Ray, D.T., Shau, Y.H., Shen, Y.W., Chen, R.C., Chiang, P.N., 2009. Origin and mineralogy of sepiolite and palygorskite from the

tuluanshan formation, eastern taiwan. Clays Clay Miner. 57, 521–530. https://doi.org/10.1346/CCMN.2009.0570502

Wang, Q., Mu, B., Wang, W., Wang, A., Tian, G., 2016a. Cost-efficient, vivid and stable red hybrid pigments derived from naturally available sepiolite and halloysite. Ceram. Int. 43, 1862–1869. https://doi.org/10.1016/j.ceramint.2016.10.145

Wang, Q., Mu, B., Zhang, Y., Zhang, J., Wang, A., 2016b. Palygorskite-based hybrid fluorescent pigment: Preparation, spectroscopic characterization and environmental stability. Microporous Mesoporous Mater. 224, 107–115. https://doi.org/10.1016/j.micromeso.2015.11.034

Weir, M.R., Kuang, W., Facey, G.A., Detellier, C., 2002. Solid-state nuclear magnetic resonance study of sepiolite and partially dehydrated sepiolite. Clays Clay Miner. 50, 240–247. https://doi.org/10.1346/000986002760832838

Wu, S., Cui, H., Wang, C., Hao, F., Liu, P., Xiong, W., 2018. In situ self-assembled preparation of the hybrid nanopigment from raw sepiolite with excellent stability and optical performance. Appl. Clay Sci. 163, 1–9. https://doi.org/10.1016/j.clay.2018.07.009

Wu, S., Duan, Z., Hao, F., Xiong, S., Xiong, W., Lv, Y., Liu, P., Luo, H., 2017. Preparation of acid-activated sepiolite/Rhodamine B@SiO2 hybrid fluorescent pigments with high stability. Dye. Pigment. 137, 395–402. https://doi.org/10.1016/J.DYEPIG.2016.10.030

Wu, S., Huang, J., Cui, H., Ye, T., Hao, F., Xiong, W., Liu, P., Luo, H., 2019. Preparation of organic–inorganic hybrid methylene blue polymerized organosilane/sepiolite pigments with superhydrophobic and self-cleaning properties. Text. Res. J. https://doi.org/10.1177/0040517519829924

Zhang, Y., Dong, J., Sun, H., Yu, B., Zhu, Z., Zhang, J., Wang, A., 2016a. Solvatochromic

Coatings with Self-Cleaning Property from Palygorskite@Polysiloxane/Crystal Violet Lactone. ACS Appl. Mater. Interfaces 8, 27346–27352. https://doi.org/10.1021/acsami.6b09252

Zhang, Y., Fan, L., Chen, H., Zhang, J., Zhang, Y., Wang, A., 2015a. Learning from ancient Maya: Preparation of stable palygorskite/methylene blue@SiO2 Maya Blue-like pigment. Microporous Mesoporous Mater. 211, 124–133. https://doi.org/10.1016/j.micromeso.2015.03.002

Zhang, Y., Wang, W., Mu, B., Wang, Q., Wang, A., 2015. Effect of grinding time on fabricating a stable methylene blue/palygorskite hybrid nanocomposite. Powder Technol. 280, 173–179. https://doi.org/10.1016/j.powtec.2015.04.046

Zhang, Y., Zhang, J., Wang, A., 2016b. From Maya blue to biomimetic pigments: durable biomimetic pigments with self-cleaning property. J. Mater. Chem. A 4, 901–907. https://doi.org/10.1039/C5TA09300G

Zhang, Y., Zhang, J., Wang, A., 2015b. Facile preparation of stable palygorskite/methyl violet@SiO2 “Maya Violet” pigment. J. Colloid Interface Sci. 457, 254–263. https://doi.org/10.1016/j.jcis.2015.07.030

CHAPTER 4

Final remarks

Comparing the results from both the Chapter 2 and Chapter 3, we can consider a range of relevant points.

The dye loading on the clay directly affects the color and fluorescence properties. Thus, the greater the amount of adsorbed dye, the more intense the color of the hybrid pigment, but the less fluorescent, and *vice versa*. Therefore, as substrates, both palygorskite and sepiolite have unique characteristics for these hybrid pigments, since their adsorption capacities are distinct. Palygorskite is suitable to form hybrid pigments with more intense and attractive colors, however less fluorescent, unlike sepiolite. Accordingly, in this aspect, palygorskite has an advantage over sepiolite, since it would be expected that a smaller amount of flavylium cations adsorbed on palygorskite would also generate more fluorescent hybrid pigments (vide Figure 2.3, in Chapter 2).

The size of the tunnels and grooves of the fibrous clays is of paramount importance for the stability of these dye molecules. As shown for the flavylium cation FL1, although palygorskite promoted improved pH-dependent color stability of FL1, sepiolite has been shown to be more efficient. In addition, the larger channels of sepiolite permitted us to extend the study of hybrid material formation to pyranoflavylium cations.

The results obtained here definitively point to flavylium cations and pyranoflavylium cations as promising chromophores and fibrous clays as promising substrates for the development of novel highly fluorescent hybrid pigments with attractive colors and marked chemical and thermal stability. Therefore, these results should inspire

the development of new stable fluorescent hybrid flavylium or pyranoflavylium cation / fibrous clay pigments that retain their fluorescent properties and color.

It is also important to emphasize that, besides developing novel hybrid flavylium cation / fibrous clay materials in this work, we have achieved advances in the stabilization of these dye molecules with regard mainly to their pH-dependent equilibrium and thermal treatment. In addition, the present work represents the first systematic study of the properties of hybrid materials prepared from pyranoflavylium cations.

Curriculum Vitae

Name:

Gustavo Thalmer de Medeiros Silva

Email address:

thalmer@usp.br

gtms_js@hotmail.com

Description / Practice areas

Gustavo Thalmer graduated in Chemistry from the Universidade do Estado do Rio Grande do Norte (Brazil). He did his Master's degree in Chemistry at the Universidade Federal do Rio Grande do Norte (Brazil). He is currently a PhD student in the graduate program in Chemistry of the Institute of Chemistry of the Universidade de São Paulo (Brazil) under the supervision of Prof. Frank Quina. His areas of research have focused on physical chemistry of adsorption at interfaces, colloids, materials chemistry, photophysics and photochemistry.

Education

2014	Ph.D. in Sciences with qualification in Chemistry (in progress).
	Universidade de São Paulo, USP, Brasil.
2012 - 2014	Master's degree in Chemistry.
	Universidade Federal do Rio Grande do Norte, UFRN, Brazil.
2012 - 2014	Specialization in the Chemistry of Petroleum.
	Universidade Federal do Rio Grande do Norte, UFRN, Brazil.
2008 - 2012	Undergraduate in Chemistry.
	Universidade do Estado do Rio Grande do Norte, UERN, Brazil.

Teaching Experience

2016 Monitor, 3ª Escola de Coloides e Superfícies, São Paulo, Brasil.

Graduate teaching assistant, Institute of Chemistry, Universidade de São Paulo:

2015 Experimental Physical Chemistry.

2015 Physical Chemistry for Pharmacy.

2014 Physical Chemistry for Pharmacy.

Research Experience

My background in research has focused mainly on the areas of colloids, materials science, photochemistry and photophysics.

- My undergraduate research was based on formation of complexes formed between oppositely charged polyelectrolytes.
- In my Master's degree, I worked with surfactants and micelles, studying the physical chemistry of adsorption at interfaces and the physical chemistry of micelle formation.
- During the PhD, I worked on the development of hybrid materials based on clays and synthetic analogues of anthocyanin and pyranoanthocyanin dyes, gaining experience with several photophysical techniques, under the guidance of Prof. Frank H. Quina.

Awards

2016 Travel Award from the Institute of Chemistry, Universidade de São Paulo.

Publications

Articles in Scientific Journals

1) Silva, G. T. M.; Silva, K. M.; Silva, C. P.; Rodrigues, A. C. B.; Oake, J.; Gehlen, M. H.; Bohne, C.; Quina, F. H.; Highly fluorescent hybrid pigments from anthocyanin- and red wine pyranoanthocyanin-analogs adsorbed on sepiolite clay. Accepted in: Photochemical and Photobiological Sciences, v. xx, p. xx-xx, 2019. DOI: https://doi.org/10.1039/C9PP00141G

2) Li, X.; Siddique, F.; Silva, G. T. M.; Quina, F. H.; Lischka, H.; Aquino, A. J. A.; Quantum Chemical Evidence for the Origin of the Red/Blue Colors of *Hydrangea macrophylla* Sepals. Accepted in: New Journal of Chemistry, v. xx, p. xx-xx, 2019. DOI: https://doi.org/10.1039/C9NJ00237E

3) Silva, C. P.; Silva, G. T. M.; Costa, T. S.; Carneiro, V. M. T.; Siddique, F.; Aquino, A. J. A.; Freitas, A. A.; Clark, J. A.; Espinoza, E. M.; Vullev, V. I.; Quina, F. H.; Chromophores Inspired by the Colors of Fruit, Flowers and Wine. Accepted in: Pure and Applied Chemistry, v. xx, p. xx-xx, 2019. DOI: https://doi.org/10.1515/pac-2019-0226

4) He, J.; Li, X.; Silva, G. T. M.; Quina, F. H.; Aquino, A. J. A.; Quantum Chemical Investigation of the Intramolecular Copigmentation Complex of an Acylated Anthocyanin. Journal of the Brazilian Chemical Society, v. 30, p. 492-498, 2019. DOI: http://dx.doi.org/10.21577/0103-5053.20180233.

5) Siddique, F.; Silva, C. P.; Silva, G. T. M.; Lischka, H.; Quina, F. H.; Aquino, A. J. A.; The Electronic Transitions of Analogs of Red Wine Pyranoanthocyanins Pigments. Photochemical and Photobiological Sciences, v. 18, p. 45-53, 2019. DOI: https://doi.org/10.1039/c8pp00391b

6) Silva, G. T. M.; Thomas, S. S.; Silva, C. P.; Schlothauer, J. C.; Baptista, M. S.; Freitas, A. A.; Bohne C.; Quina, F. H.; Triplet Excited States and Singlet Oxygen Production by Analogs of Red Wine Pyranoanthocyanins. Photochemistry and Photobiology, v. 95, p. 176-182, 2019. DOI: https://doi.org/10.1111/php.12973

7) Silva, G. T. M.; Silva, C. P.; Gehlen, M. H.; Oake, J.; Bohne C.; Quina, F. H.; Organic/inorganic hybrid pigments from flavylium cations and palygorskite. Applied Clay Science, v. 162, p. 478-486, 2018. DOI: https://doi.org/10.1016/j.clay.2018.07.002

8) Freitas, A. A.; Silva, C. P.; Silva, G. T. M.; Maçanita, A. L.; Quina, F. H.; Ground and Excited State Acidity of Analogs of Red Wine Pyranoanthocyanins. Photochemistry and Photobiology, v. 94, p. 1086-1091, 2018. DOI: https://doi.org/10.1111/php.12944

9) Silva, C. P.; Pioli, R. M.; Liu, L.; Zheng, S.; Zhang, M.; Silva, G. T. M.; Carneiro, V. M. T.; Quina, F. H.; Improved Synthesis of Analogues of Red Wine

Pyranoanthocyanin Pigments. ACS Omega, v. 3, p. 954-960, 2018. DOI: 10.1021/acsomega.7b01955

10) Freitas, A. A.; Silva, C. P.; Silva, G. T. M.; Maçanita, A. L.; Quina, F. H.; From vine to wine: photophysics of a pyranoflavylium analog of red wine pyranoanthocyanins. Pure and Applied Chemistry, v. 89, p. 1761-1767, 2017. DOI: https://doi.org/10.1515/pac-2017-0411

11) De Lima, C. R. M.; de Morais, W. A.; Silva, G. T. M.; Nunes, J. S.; Wanderley Neto, A. O.; Pereira, M. R.; Fonseca, J. L. C.; Preparation and characterization of dispersions based on chitosan and poly(styrene sulfonate). Colloid and Polymer Science, v. 295, p. 1071-1078, 2017. DOI: https://doi.org/10.1007/s00396-017-4099-4

12) De Lima, C. R. M.; de Souza, P. R. S.; Stopilha, R. T.; de Morais, W. A.; Silva, G. T. M.; Nunes, J. S.; Wanderley neto, A. O.; Pereira, M. R.; Fonseca, J. L. C.; Formation and Structure of Chitosan-Poly (Sodium Methacrylate) Complex Nanoparticles. Journal of Dispersion Science and Technology, v. 39, p. 83-91, 2017. DOI: https://doi.org/10.1080/01932691.2017.1296772

13) De Morais, W.A.; Silva, G.T.M.; Nunes, J.S.; Wanderley Neto, A.O.; Pereira, M.R.; Fonseca, J.L.C.; Interpolyelectrolyte complex formation: From lyophilic to lyophobic colloids. Colloids and Surfaces. A, Physicochemical and Engineering Aspects, v. 498, p. 112-120, 2016. DOI: https://doi.org/10.1016/j.colsurfa.2016.03.052.